

VOLUME 8

NUMBER 2

2015

ISSN 2218-7979

International Journal of  
**Biology**  
and **Chemistry**



Al-Farabi Kazakh National University

International Journal of Biology and Chemistry is published twice a year by al-Farabi Kazakh National University, al-Farabi ave., 71, 050040, Almaty, the Republic of Kazakhstan  
website: <http://ijbch.kaznu.kz/>

Any inquiry for subscriptions should be sent to:  
Prof. Mukhambetkali Burkitbayev, al-Farabi Kazakh National University  
al-Farabi ave., 71, 050040, Almaty, the Republic of Kazakhstan  
e-mail: [Mukhambetkali Burkitbayev@kaznu.kz](mailto:Mukhambetkali.Burkitbayev@kaznu.kz)

## **EDITORIAL**

The most significant achievements in the field of natural sciences are reached in joint collaboration, where important roles are taken by biology and chemistry. Therefore publication of a Journal, displaying results of current studies in the field of biology and chemistry, facilitates highlighting of theoretical and practical issues and distribution of scientific discoveries.

One of the basic goals of the Journal is to promote the extensive exchange of information between the scientists from all over the world. We welcome publishing original papers and materials of Biological and Chemical Conferences, held in different countries (after the process of their subsequent selection).

Creation of special International Journal of Biology and Chemistry is of great importance, because a great amount of scientists might publish their articles and it will help to widen the geography of future collaboration. We will be glad to publish also the papers of the scientists from the other continents.

The Journal aims to publish the results of the experimental and theoretical studies in the field of biology, biotechnology, chemistry and chemical technology. Among the emphasized subjects are: modern issues of technologies for organic synthesis; scientific basis of the production of physiologically active preparations; modern issues of technologies for processing of raw materials, production of new materials and technologies; study on chemical and physical properties and structure of oil and coal; theoretical and practical issues in processing of hydrocarbons; modern achievements in the field of nanotechnology; results of studies in the fields of biology, biotechnology, genetics, nanotechnology, etc.

We hope to receive papers from a number of Scientific Centers, which are involved in the application of the scientific principles of biology, biotechnology, chemistry and chemical technology on practice and carrying out research on the subject, whether it relates to the production of new materials, technology and ecological issues.

Abdulzhanova M.A. \*, Savitskaya I.S., Kistaubayeva A.S., Zhabakova A.B.

Department of Biotechnology, Faculty of Biology and Biotechnology,  
Al-Farabi Kazakh National University, Almaty, Kazakhstan  
\*e-mail: Malika\_81\_@mail.ru

### **Impact of feed additives SUBACIL-1 and SUBACIL-2 on productivity of chicken-broilers**

**Abstract:** One of the most important problems of probiotics production is the development of non-waste technologies, in particular, usage of microbial cultures fugate. In conventional technology, it must be disposed of after the intensive heat treatment in drains. The fugate does not contain bacteria, but rather products of their metabolism and biosynthesis, which may have therapeutic, preventive and growth-stimulating effects. The above mentioned fact shows the relevance of the development of non-waste technology of feed probiotics of the genus *Bacillus* and their metabolites. In al-Farabi Kazakh National University, at Biotechnology Department of Faculty of Biology and Biotechnology were obtained experimental samples of probiotic feed additives – SUBACIL. SUBACIL-1 is lyophilized biomass of *Bacillus subtilis* P-2 containing  $9 \times 10^{12}$  spores in 1g. SUBACIL-2 is a combined feed probiotic comprising metabolites of *B.subtilis* P-2 immobilized on sunflower meal with addition of soya flour hydrolyzate. In this study was investigated the impact of feed additives SUBACIL-1 and SUBACIL-2 for growing of broiler chickens, in accordance with the following factors: changes of body weight, average daily gain and safety of the birds. The addition SUBACIL-1 of feeding for broilers increases the productivity of poultry meat by 11%, SUBACIL-2 – 9%. The use of new additives during the growing period is accompanied by the increase in average daily gain. When using of SUBACIL-1 daily gain is by 9.7% more than that of control group and 2.4% while using of SUBACIL-2. The introduction of these additives allows gaining 90% (SUBACIL-1) and 85% (SUBACIL-2) preservation of livestock. The greatest efficiency index was 214.94.

**Key words:** feed additive, *Bacillus subtilis* P-2, fugate, SUBACIL.

#### **Introduction**

At the moment prevention of gastrointestinal diseases of poultry is an essential event in the organization of any profitable poultry farms. The traditional usage of antibiotics and chemicals for correction and treatment of gastrointestinal diseases leads to accumulation of drug-resistant strains of intestinal infections in the poultry production [1-3].

The most appropriate alternatives to feed antibiotics are considered sporogenous probiotics with approved results and comparable economic efficiency and, moreover, which pose no danger to humans and environment. Today's trend in their development is the use of bacteria of genus *Bacillus*.

Bacteria of genus *Bacillus* have high antimicrobial activity and a high level of production of enzymes [4-6]. In this regard, it seems promising to do research aimed at the development of probiotics – enzymatic microbial feed additives that enhance the

nutritional value and the digestibility of the feed and thus increase the productivity index.

Another major problem of probiotics production is the use of fugate of microbial cultures. In conventional technology, it must be disposed off [7]. The filtrate is a byproduct of production of bacterial preparations or concentrates [8-10]. The fugates as a rule do not contain the bacteria, but there are products of their metabolism and biosynthesis, which may have therapeutically and preventive and growth-stimulating effect. The above mentioned facts show the relevance of the development of non-waste technology of feed probiotics of genus *Bacillus* and their metabolites.

#### **Materials and methods**

**Object of study.** Culture and fugate of strain *Bacillus subtilis* P-2; probiotic feed additives SUBACIL-1 and SUBACIL-2.

### Methods of research.

In al-Farabi Kazakh National University, at Biotechnology Department of Faculty of Biology and Biotechnology were obtained experimental samples of probiotic feed additives – SUBACIL. SUBACIL-1 is lyophilized biomass of *Bacillus subtilis* P-2 containing  $9 \times 10^{12}$  spores in 1g. SUBACIL-2 is a combined feed probiotic comprising metabolites of *Bacillus subtilis* P-2 immobilized on sunflower meal with addition of soya flour hydrolyzate.

The experiments were performed on broiler chickens cross «Smena-7» (day 1 to 41; in the pilot house). The experimental groups (control and test) broiler chickens were formed at day-old, according to the scheme on the basis of the experience of peers on 20 goals each. Each chicken was assigned an individual number of labeled wing rings. The chicks of all groups were kept on the outdoor by sections. Conditions of growing, the parameters of the microclimate, the front of feeding and watering, lighting mode, and the stocking density of chickens of all groups were similar.

Test parameters:

1. Body weight of chickens. In order to control the dynamics of age changes of live weight of chickens, and the average daily gain and the relative homogeneity conducted individual weighing of all livestock on a weekly basis at the same time the day before feeding was conducted.

According to the individual values was defined the uniformity of poultry in live weight (calculated average live weight of all livestock was determined by the number of individuals as a percentage of all livestock in the group with body weight within  $\pm 10\%$  of the average of all livestock) (Formula 1).

$$K_o = \frac{(n_1 - n_2) \times 100}{n_1} \quad (1)$$

where,  $K_o$  – uniformity coefficient (%);  $n_1$  – the number of observations (number of goals);  $n_2$  – the number of cases, individual values deviate by more than  $\pm 10\%$  of the arithmetic mean.

2. The rate of growth of chickens (average daily gain). The rate is determined by the absolute weight gain of chickens, calculated according to the Formula 2:

$$U = U_1 - U_2 \quad (2)$$

where,  $U_1$  – mass at the beginning of the growing period, g;  $U_2$  – mass at the end of cultivation, g.

The average daily weight gain of chickens was calculated by Formula 3:

$$U/t = U_1/t_1 - U_2/t_2 \quad (3)$$

where,  $U/t$  – the average absolute increase,  $g \times d^{-1}$ ;  $t_1$  – the age at the beginning of the growing period, days;  $t_2$  – the age at the end of the growing period, days.

3. Preservation of broilers,%. It was calculated on the base on the daily account of the number of dead chickens. Preservation of livestock carried out on a daily basis, taking into account the causes of mortality. The cost of feed for the rearing period by taking into account a given feed and balances for the period.

4. Consumption of feed, kg per 1 kg of growth.

5. Performance Index of broiler growing by Formula 4:

$$PIBG = (Body\ weight \times Preservation) / (Period\ of\ growing \times Consumption\ of\ feed) \div 10 \quad (4)$$

Experimental data was processed using the application «Statistics for Windows, v 5.0» and «BIO-STAT», «Microsoft Excel for Windows 2007», spreadsheet Excel 7.0. Calculates an average value, the meridian, standard deviation, standard error of the mean and others.

### Results and their discussion

Probiotic feed additives SUBACIL – 1 and SUBACIL – 2 have a positive impact on microbiocenosis, stimulating the growth of lactobacilli and cellulose-fermenting bacteria in the intestines of broiler chickens on the background of the elimination of opportunistic and pathogenic enterobacteria. Application of SUBACIL -1 in experimental *Salmonella* infection increases the level of intestinal colonization resistance, as evidenced by the 85% of reduction of cases of isolation of pathogen from the material enrolled for study of.

During the study the impact of feed additives SUBACIL-1 and SUBACIL-2 for growing broiler chickens was examined, on the following factors: changes in body weight, average daily gain and the preservation of the Poultry.

The work was carried out on broiler chickens of 'Smena-7' cross. Technological parameters of feeding and keeping chickens corresponded to generally accepted recommendations in this area. Experimental and control groups included 20 broiler chickens.

**Table 1** – Scheme the search experience

Group	Number of chickens	Dose	Subjects factors
Control	20	-	The basic diet; Probiotics have not been used
Experiment 1	20	1 g to 30 L per water	Basic diet; SUBACIL-1
Experiment 2	20	1 g to 1 kg per dry food	Basic diet; SUBACIL -2
Experiment 3	20	1 g to 1 kg per dry food	Basic diet; Probiotic drug «Biosporin»
Experiment 4	20	5 ml to 10 L per water during five days	Basic diet; Antibiotic «Enroksil 10%»

Each experiment lasted for technological growth cycle (41 days).

The main indicator of the meat efficiency of poultry is dynamics of live weight during technological period of growing. Live weight is the main index according of which the amount of meat of poultry of any age is

determined [11]. Live weight is established by weighing. Broiler chickens were weighed in the morning, prior to feeding. The control determination of mass was performed weekly. As a result of the conducted investigations, the positive effect of feedings on intensity of chickens growth was established (Table 2).

**Table 2** – Changes of live weight of broiler chickens during the growth process

Age of broilers, days	Live weight, g				
	Control group	SUBACIL-1	SUBACIL-2	Biosporin	Enroksil 10%
1	36.0±0.2	36.0±0.3	36.0±0.3	36.0±0.4	36.0±0.3
7	125.5±4.0	128.7±32.8	131.4±19.6	128.5±23.7	121.5±22.8
14	288.9±6.5	289.5±21.4	302.7±29.5	288.9±7.5	278.5±23.3
21	589.8±43.0	603.3±11.4	627.6±20.8	597.6±22.3	591.3±14.5
28	901.8±41.7	923.0±16.0	941.2±34.0	899.5±11.5	901.4±14.4
35	1270.3±53.6	1342.7±21.2	1356.0±41.2	1268.0±44.2	1281.7±23.8
41	1705.3±7.2	1880.6±87.9	1850.8±89.9	1799.7±86.1	1712.6±76.4

The received data showed that chickens of the experimental group with introduction of feeding SUBACIL-1 were distinguished by high rate of growth compared to chickens of control group.

For the period from the 1st to the 7th day of the experiment the increase of the average live weight of chickens in the experimental group compared to the control group were more by 2.4%. From the 7th to the 14th day of the experiment the average weight of chickens in the experimental group increased by 0.3%. The third week of the experiment allowed the increase all the average weight of broilers by 2.3%. Further, from the 21st to the 28th day of 2.4%. In the next period (28 – 35 days) – 5.7%. In the final period (35–41 days) – 10.7%.

Thus, the maximum gain of live mass of chickens, receiving feed additive SUBACIL-1 relatively to

the control ones was in the final weeks of cultivation (10.7%).

For probiotic additive SUBACIL-2 the maximum live weight gain is 8.5% for Biosporin – 5.5% and antibiotic «Enroksil 10%» – 0.4%.

According to the obtained results it can be concluded that the probiotic preparations have a positive effect on live weight gain. The most effective preparation is SUBACIL-1. «Enroksil 10%» almost has no effect on live weight gain, as evidenced by the results (0.4%).

It is important indicator of the effectiveness of feed additives is the average daily gain of broiler chickens. Table 3 shows the calculation data of growth speed of chickens in experimental control groups.

**Table 3** – Dynamics of average daily gain of broiler chickens

Age of broilers, days	Average daily gain, g				
	Control group	SUBACIL-1	SUBACIL-2	Biosporin	Enroksil 10%
1-7	17.5±0.5	15.2±0.4	14.2±0.5	13.6±0.6	13.8±0.4
7-14	28.9±0.5	28.6±0.5	23.6±0.6	22.5±0.2	21.5±0.3
14-21	49.9±0.4	49.8±0.4	44.9±0.3	46.8±0.1	45.1±0.4
21-28	51.2±0.6	47.8±0.3	47.4±0.8	48.1±0.8	44.5±0.5
28-35	57.0±2.03	60.1±2.2	54.4±2.2	57.2±2.0	54.3±2.1
35-41	76.5±1.4	88.2±1.7	81.3±1.4	84.6±1.4	72.7±1.8
1-41	41.5±1.6	45.0±1.4	42.1±1.9	41.1±1.4	41.0±1.1

According to the table the dynamics of growth speed of chickens was corresponded to the increase of their mass. Over the whole period of the experiment (from the 1st to the 41st day) the growth speed of broiler chickens received SUBACIL-1 by 9.7% exceeded the indicators of the control group, SUBACIL-2 – 2.4%, Biosporin – 1.8%.

Preservation was determined by everyday counting of dead chickens. Data on the preservation of broiler chickens for the experimental period are shown in Table 4.

Chickens preservation receiving only food and water is 70%. Analyzing the obtained results, in general we can say that, within the technological cycle, the preservation of broilers after applying the test preparations was 90% (SUBACIL-1) and 85% (SUBACIL-2). In comparison groups using Biosporin and «Enroksil 10%» resulted in increased preservation till 80% and 75% respectively.

According to the obtained data an index of efficiency of growing of broiler chickens was calculated.

**Table 4** – Preservation of broiler chickens per experimental period

Index	Control group		SUBACIL-1		SUBACIL-2		Biosporin		Enroksil 10%		
	Heads	%	Heads	%	Heads	%	Heads	%	Heads	%	
Safety in weeks	1	19	95	19	95	20	100	20	100	20	100
	2	19	95	19	95	19	95	20	100	19	95
	3	18	90	19	95	19	95	19	95	19	95
	4	17	90	19	95	19	95	18	90	18	90
	5	17	85	18	90	18	90	17	85	17	85
	6	16	85	18	90	18	90	16	80	16	80
	7	14	70	18	90	17	85	16	80	15	75

**Table 5** – An index of efficiency of growing of broilers

Options	Live weight, g	Safety, %	Term cultivation, days	Consumption of feed on 1 kg of growth, kg	Performance Index
Control	1705.3±87.2	70	41	1.96	159.13
SUBACIL-1	1880.6±87.9	90	41	1.92	214.94
SUBACIL-2	1850.8±89.9	85	41	1.88	204.00
Biosporin	1799.7±86.1	80	41	1.95	180.01
Enroksil 10%	1712.6±76.4	75	41	1.98	168.71

The highest index of efficiency in the group, receiving the feed additive SUBACIL-1, is 214.94.

Thus, the addition of SUBACIL-1 in feed for broilers increases the meat productivity of poultry by 11%, SUBACIL-2 by 9%. Using the new additives during the whole growing period is accompanied by the increase of average daily gain. When using SUBACIL-1, an average daily gain by 9.7% or more than in the control group and by 2.4% when using SUBACIL-2. The introduction of these additives allows achieving 90% (SUBACIL-1) and 85% (SUBACIL-2) of preservation of livestock.

### Conclusions

The addition of SUBACIL-1 increases productivity of poultry meat by 11%, SUBACIL-2 by 9%. The use of new additives during the whole growing period is accompanied by the increase of average daily gains. When using SUBACIL-1 average daily gain by 9.7% more than in the control group and by 2.4% when using SUBACIL-2. The introduction of these additives allows achieving 90% (SUBACIL-1) and 85% (SUBACIL-2) of preservation of livestock. The greatest efficiency index was 214.94.

### References

1. Ricca E., Henriques A.O. and Cutting S.M., Eds EU regulations on bacillary probiotics for animal feeds In: *Bacterial Spore Formers: Probiotics and Emerging Applications* // Horizon Bioscience. – Norfolk, 2004. – P. 221–227.
2. Hume, M.E. Historic perspective: Prebiotics, probiotics, and other alternatives to antibiotics // *Poult. Sci.* – 2011. – Vol.90. – P. 2663–2669.
3. Smirnov V.V., Podgorskij V.S., Kovalenko N.K. Probiotiki na osnove zhivyh kul'tur mikroorganizmov // *Mikrobiol. zhurn.* – 2002. – T. 64. – №4. – S. 27-34.
4. Tohtiev A. G. Effektivnost' vozdeystviya probioticheskogo preparata na osnove soevogo moloka v sochetanii s dobavkami pektinovyh veshchestv na produktivnost' i myasnye kachestva cyplyat-brojlerov // *Avtoref. dis. kand. s-h. nauk.* – Vladikavkaz, 2005. – S. 25.
5. Osipova I. G., Sorokulova I. B. Bezopasnost' sporovyh probiotikov: sovremennye aspekty // *Probiotiki, prebiotiki, sinbiotiki i funktsional'nye produkty pitaniya. Fundamental'nye i klinicheskie aspekty: Tezis. Mezhd. Kongres.* – SPb. – 2007. – S. 59.
6. Osadchaya A. I., Kudryavcev V. A., Safronova JL A. i dr. Vliyanie istochnikov pitaniya na sintez ehkzopolisaharidov i aminokislot shtammami *Bacillus subtilis* // *Mikrotil. zhurn. (Kiev).* – 2009. – № 5. – S. 56-63.
7. Smirnov V.V., Sorokulova I.B., Pinchuk I.V. Bakterii roda *Bacillus* – perspektivnyj istochnik biologicheski aktivnyh veshchestv // *Mikrobiol. zhurn.* – 2001. – T. 63, № 1. – S.72-77.
8. Ochoa-Solano J., Olmos-Soto The functional property of *Bacillus* for animal feeds // *Food Microbiol.* – 2006. – Vol. 23. – P.519-525.
9. Bondarenko V. M. Metabolitnye probiotiki: mekhanizmy terapevticheskogo ehffekta pri mikroehkologicheskikh narusheniyah // *Consilium medicum.* – 2005. – № 1. – S. 36-45.
10. Rajput, I.R. and W.F. Li. Potential role of probiotics in mechanism of intestinal immunity // *Pak. Vet. J.* – 2012. – Vol. 32. – P. 303–308.
11. Klose V. Characterization of bacteria of the intestinal chicken microenvironment // *Book of abstracts XXI World's poultry congress.* – 2004. – P. 731.



Atabayeva S.D.\* , Asrandina S.Sh., Alybaeva R.A., Shoinbekova S.A.

Al-Farabi Kazakh National University, Almaty, Kazakhstan

\*e-mail: sauleat@yandex.ru

### **Intracellular localization, accumulation and distribution of heavy metals in plants**

**Abstract:** Heavy metals uptake, distribution and accumulation processes in plants are very important for their impact on physiological and biochemical processes and, consequently, on plant growth and development. The distribution of heavy metals in plant parts and cell organelles are discussed. There are detoxification mechanisms in cell compartments, like binding with cell wall, with organic acids in vacuoles, complexes with phytochelatins and etc. What proportion of given metal ions would be the in free form, and what – bound with organic molecules; it depends from pH of the environment and chemical properties of element. The stability of metals complexes decreases in the case of deviation pH of environment from neutral: at low pH there is a competition of protons with metal ions for binding sites in molecules, at high pH – by the reason of the competition of hydroxyl groups with ligand.

**Key words:** intracellular localization, heavy metals, distribution, accumulation.

#### **Main body**

Plant roots contain the greatest amount of heavy metals [1, 2]. Less heavy metal accumulate in stems and leaves, and even less – in the grain. Concentration of heavy metals in the grain and aboveground organs is mainly due to «the effect of detention» in their roots, which are more tolerant as compared to sensitive plant species. An effective mechanism for retarding the heavy metals exists in the roots. Comparison of heavy metals contents in soils and plant parts showed that the dependence of content in plants by soil concentration increases in the following order:  $Cd > Zn > Cu > Pb > Cr$  for monocots and depends on the mobility of metal in the soil. For dicots, this pattern is less pronounced [3].

The character distribution of heavy metals in cell organelles plays an important role in protective mechanism in plants [4-8]. The absorption of metal ions by the root system from the soil and nutrient solution is carried out in various ways, on which the likelihood of intake of ions directly into the cytoplasm of cells and the rate of movement of the tissues and organs of plants depends. The character of metal accumulation in organs of plants depends on the plant species and a metal nature (Table 1).

Zinc at high concentration (25 mg/kg) was accumulated in significant amounts in the aerial parts of wheat and beans. The protective function of the roots towards Cd was more expressed than for Zn, which is not accumulated in the roots, and moved in the stems

and leaves. This is probably due to unequal role of these elements in the plant metabolism. Translocation rate of cadmium and lead to the aboveground part as compared to Zn was much lower. Most of the Pb is retained in the root system. Localization of the metal in parts of the plant is dependent on its mobility. According to the researchers, Pb in plants of lupine was contained mostly in the tips of the roots, less – in the basal part, and hypocotyls. Most Pb detected in cortical parenchyma in comparison with central cylinder. This fact was explained by Pb lower mobility as compared to other metals.

Patterns of distribution of Pb, Cd and Zn in the tissues of the root are not well understood. The apical root sections on metal content may vary from basal. Many authors have noted that at high concentrations of metals in the environment of the basal part of the roots accumulate significantly more Pb, Cd and Zn, than apical one, especially in resistant populations. Other authors suggest that most of the metal accumulates in meristematic parts of the roots [3].

Different plant species have unequal protective opportunities, as evidenced by their tolerance to different heavy metals. According to one hypothesis, the main role in the development of resistance belongs to the binding of metal cell walls in the roots. Study of the intracellular localization of heavy metals found that they bind to the cell membrane and accumulate in the vacuoles. The relatively high concentration in the cell walls of Pb and Cd detected in a number of species. According to another hypothesis, their role

is a compartmentalization and metal accumulation in vacuoles of root cells. Cell walls of monocotyledonous and dicotyledonous plants differed in content of pectin and hemicelluloses, thereby manifest differences in their ability to bind cations. The bond strength of certain metal ions with the components of the cell wall varies. It correlates with different values of stability constants (Log K) metal complexes with functional groups of carbohydrates. For Pb, it is equal to 6.4, for Cd – 4.9. Therefore, Pb binds

more strongly with cellular membranes than Cd, and slowly moves along the apoplast. The affinity of other metals to polygalacturonic acid decreases in the following order: Pb > Cr > Cu > Ca > Zn. It was not studied the binding of Pb and Cd apoplast proteins. In barley leaf apoplast Cd increased the content of these proteins. However, the role of these proteins is uncertain. Under the influence of heavy metals can be enhanced suberin and callose deposition, reducing the absorption of metals [3].

**Table 1** – Intercellular localization of Cd and Pb in plants (I.V. Seregin, V.B. Ivanov, 2001)

Plant species, Metal, tissue	Cell wall	Vacuole	Golgi apparatus	Endoplasmic reticulum	Nucleus	Research method
<i>Zea mays</i> (Cd)						
Differentiated cells (Cd – $2 \times 10^{-1}$ mMol; $3 \times 10^{-3}$ mMol)		+			+	The X-ray microanalysis
Mature cortex and stele cells	+	+				Electronic microscopy
Rhizodermis	+					Histochemistry
Endodermis	+					
Pericycle	+/-					
Xylem parenchyma	+					
<i>Rhynchospora squarrosa</i> (Pb – 4.8 mMol)		+	+		+	Electronic microscopy
<i>Lemna minor</i> (Pb – $3 \times 10^{-3}$ mMol)					+	
The outer layer of root cap	+					Electronic microscopy
The other cell layers of root caps	+		+	+		Histochemistry
Epidermis			+	+		
Cortex	+		+	+		
The basal part of the root	+	+				
<i>Allium cepa</i> (Pb- $7.5 \times 10^{-3}$ mMol)	+	+	+			Autoradiography
<i>Zea mays</i> (Pb – $8 \times 10^{-1}$ mMol; $7.5 \times 10^{-3}$ mMol)	+	+	+			Electronic microscopy X-ray microanalysis
<i>Glycine soya</i> (Pb)	+	+	+			
<i>Lupinus luteum</i> (Pb – $4.3 \times 10^{-2}$ mMol)						Electronic microscopy
The cortex parenchyma	+		+	+		Histochemistry
Stele	+/-		+/-	+/-		Electronic microscopy
<i>Pisum sativum</i> (Pb)	+	+	+			Electronic microscopy
<i>Raphanus sativus</i> (Pb – 5 mMol)	+		+			Electronic microscopy

Heavy metals were also detected in the intercellular space, dictyosome, endoplasmic reticulum, nuclear membrane. In the cytoplasm ions can bind to biomolecules. In this case, the chelate is derived from a cell or accumulated therein (mostly in the vacuoles). Accumulation of toxic ions into vacuoles in the form of inactive compounds is more typical for plant tolerance to heavy metals. Fraction remaining in the cytosol as free ions or soluble complexes is moving simplistically from the root to the stem and then – to the leaves of plants by charged sites of xylem or carried away by the transpiration stream of water.

Cd accumulated in the shell in less than inside the cell. It can bind to intracellular lysosome like granules largest amount of the metal is in the cytoplasm. It is known that the usual response to the Cd is the induction of synthesis of low molecular weight, cysteine-rich proteins – metallothioneins, phytochelatins [5, 9-15].

Bond Cd with organic ligands is much stronger than other metals. At high concentrations of Cd-phytochelatins complexes are localized in the vacuoles. At low concentrations 86-100% of Cd found in the cytoplasm in *Datura innoxia* (Rauser, 1987). Under these conditions, there is no need to isolate the cells of Cd in the vacuoles. At high concentrations Cd binds with organic acids, and low – with glutathione in the cytosol [11-13, 16].

Cadmium is found in the cytoplasm and nucleus vacuoles bentgrass and roots of corn, and also indicates the presence of Cd in the cell wall of roots of maize. Other studies have detected a high concentration of Cd, associated with phosphorus and calcium in the sea fern *Azolla filiculoides* L. [17]. Most of them have been identified in the cell wall of the xylem vascular bundles. It is shown that the Cd concentration decreases with increasing content of Se, Al, K, Ca, P. The aerial parts and roots of wheat subjected to the effect of Cu, the metal was found in the cell wall and vacuoles. In the presence of Cu in the growth medium, the ratio of the metal content in the cell walls and vacuoles increased in favor of the latter [17, 18].

Copper was found in the matrix of the cell walls of *Enteromorpha compressa* [19]. The study of Pb effect on *Lemna minor* L. it has been found that Pb is present in the vacuoles, vesicles and the cell wall. At high concentrations of Pb found in symplast. Changing the ratios of content of Pb in vacuoles and cell walls after a 6- and 12-hour of exposure in favor of the latter indicates a redistribution of the metal cell walls [20]. It was found that in *Thlaspi*

*caerulescens* L., subjected to the effect of Zn, the metal is concentrated in the epidermal cells and vacuoles [21]. At low concentrations the greatest amounts of Zn was found in the vacuole. Perhaps tonoplast of epidermal cells of leaves of *T. caerulescens* has a higher ability to transport Zn in the vacuole than mesophilic cells. The ability to isolate in *T. caerulescens* Zn in epidermal vacuole is an important aspect in this type of hypertolerance to heavy metals. The preferential localization of Zn in the epidermis, apparently contributes to the protection of mesophyll cells from damage and maintains the functions of mesophyll cells at a high concentration of Zn in the leaves. *Arabidopsis halleri* L. is pseudometallophyte, i.e. it is growing in contaminated and uncontaminated soils. It is hyperaccumulators of Zn, as well as Cd. Recent studies using electron microscopy demonstrated the cellular distribution of Zn in the tissues *A. halleri*, grown in a hydroponic environment. Zinc in the plant leaves mainly found in the base of trichomes – hairs, present on the surface of plant leaves, and mesophyll cells [22, 23].

Thus, the character distribution of heavy metals in cell organelles plays an important role in protective mechanism in plants. The above data show that not all ions uptake by plants actively influence at its metabolism, so as a definite part of metals can bind with organic acids and low-molecular proteins and concentrate in an metabolically low-active compartments. Part of toxic ions turns out of firmly bound with reactive-capable portions on the surface cell wall and in the apoplast, and are penetrating across the plasmalemma – with intracellular biomolecules. It is also important to take into account, that the multiply charged ions form more stable complexes, than the singly charged, possessing lesser charge density.

Thus, the heavy metals are mainly concentrated in the roots of plants, which limits their movement in the generative organs. A common feature of interstitial and intracellular distribution is the concentration of large amounts of metals in the surface structures and protecting cells from the toxic effect of metals. Concentration of heavy metals occurs by binding them into soluble compounds having a different nature. Despite the significant accumulation of heavy metals in a metabolically inactive cell compartments (vacuoles and cell walls), some of the metals enters the cytoplasm and exerts multiple toxic effects, and this may be due to both direct effect of metals and reducing the activity of some of the processes as a result of violation of others.

## References

1. Ayari F., Hamdi H., Jedidi ., Gharbi N., Kosai R. Heavy metal distribution in soil and plant in municipal solid waste compost amended plots // *Int. J. Environ. Sci. Tech.* – 2010. – 7 (3). – P. 465-472.
2. Tangahu B.V., Abdullah S.R.S., Basri H., Idris M., Anuar N., Mukhlisin M. Review on heavy metals (As, Pb, and Hg) uptake by plants through phytoremediation // *International Journal of Chemical Engineering.* – 2011. – Article ID 939161, 31 p. doi:10.1155/2011/939161
3. Seregin I.V., Ivanov V.B. *Physiologicheskie aspekti toxicheskogo deistvia rfdmia i svinca na visshie rastenia* // *Russian Plant Physiology.* – 2001. – T. 48. – S. 606-630.
4. Kvesitaze G.I., Hatisashvili G.A., Sadunishvili T.A., Evstigneeva Z.G. *Metabolism antropogennyh toksikantov v vysshih rasteniah.* – M.: Nauka, 2015. – 197 p.
5. Maksimović I., Kastori R., Krstić L., Luković J. Steady presence of cadmium and nickel affects root anatomy, accumulation and distribution of essential ions in maize seedlings // *Biol. Plant.* – 2007. – Vol. 51. – P. 589-592.
6. Seregin I.V., Kozhevnikova A.D. Roles of root and shoot tissues in transport and accumulation of cadmium, lead, nickel, and strontium // *Russ. J. of Plant Physiol.* – 2008. – Vol. 55. – P. 1–22.
7. Lux A., Martinka M., Vaculik M., White P.J. Root responses to cadmium in the rhizosphere: a review. – *J. Exp. Bot.* – 2011. – Vol. 62 – P. 21–37.
8. Gallegoa S.M., Penaa L.B., Barciaa R.A., Azpilicuetaa C.E., Iannonea M.F., Rosalesa E.P., Zawoznika M.S., Gropkaa M.D., Benavidesa M.P. Unraveling cadmium toxicity and tolerance in plants: Insight into regulatory mechanisms. – *Env. Exp. Bot.* – 2012. – Vol. 83. – P. 33–46.
9. White M.C., Decker A.H., Chaney R.L. Metal complexation in xylem fluid. I. Chemical composition of tomato and soybean stem exudate // *Plant Physiol.* – 1981. – Vol. 67. – P. 292-300.
10. Seregin I.V., Ivanov V.B. *Geohimicheskie metali. Izuchenie rasprostraneniya kadmiya i svinca v rasteniyah* // *Fiziol. rast.* – 1997. – T. 44, № 6. – S. 915-921.
11. Baker, A.J.M., McGrath S.P., Sidoli C.M.D., Reeves R.D. The possibility of in situ heavy metal decontamination of polluted soils using crops of metal-accumulating crops // *Resources, Conservation Recycling.* – 1994. – No. 11. – P. 41-49.
12. Neumann D., Zur Nieden U. How does *Armeria maritima* tolerate high heavy metal concentrations? // *Plant Physiol.* – 1995. – Vol. 146, № 5-6. – P. 704-717.
13. Ebbs S., Lau J., Ahner B. Phytochelatin synthesis is not responsible for Cd tolerance in the Zn/Cd hyperaccumulator *Thlaspi caerulescens* // *Planta.* – 2002. – Vol. 214. – P. 635-640.
14. Hose E., Clarkson D.T., Steudle E. The exodermis: a variable apoplastic barrier // *J. Exp. Bot.* – 2001. – Vol. 52. – P. 2245-2264.
15. Vogel-Lange R., Wagner G.J. Subcellular localization of cadmium and cadmium binding peptides in tobacco leaves // *Plant Physiol.* – 1996. – Vol. 92. – P. 1086-1093.
16. Yadav K. Heavy metals toxicity in plants: an overview on the role of glutathione and phytochelatins in heavy metal stress tolerance of plants // *South African Journal of Botany.* – 2010. – Vol. 76. – P. 167–179.
17. Shao, H.B., Chu, L.Y., Lu, Z.H., Kang, C.M. Primary antioxidant free radical scavenging and redox signaling pathways in higher plant cells // *International Journal of Biological Science,* 2008. – Vol. 4. – P. 8–14.
18. Sela M., Tel-Or E., Fritz E., Hutterman N. Localization and toxic effects of cadmium, copper and uranium in *Azolla* // *Plant Physiol.* – 1998. – Vol. 88. – P. 30-36.
19. A. Manara A. Plant responses to heavy metal toxicity. In: A. Furini (ed.), *Plants and heavy metals.* – Springer Briefs in Biometals, 2012. – P. 27-53. doi: 10.1007/978-94-007-4441-7\_2
20. Reed R., Darring S. Physiological response of ship-fouling and non-fouling isolates of *Enteromorpha compressa* to copper // *Heavy Metals Environ. – Intern. Conf. Heidelberg. Edinburg,* 1983. – Vol. 69. – P. 322-325.
21. Samardakiewicz S., Wozny B. The distribution of lead in duckweed (*Lemna minor* L.) root tip // *Plant and Soil.* – 2000. – Vol. 226. – P. 107-111.
22. Kupper H., Zhao F.J., McGrath S. Cellular compartmentation of zinc in leaves of the hyperaccumulator *Thlaspi caerulescens* // *Plant Physiol.* – 1999. – Vol. 119. – P. 305 – 312.
23. Dahmani-Muller H, Van-Oort F, Gelie B, Balabane M. Strategies of heavy metal uptake by three plant species growing near a metal smelter // *Environ Pollut.* – 2000. – Vol. 109. – P. 231-238.

UDC 577.114

Bishimbayeva N.K.<sup>\*1</sup>, Sartbayeva I.A.<sup>1</sup>, Murtazina A.S.<sup>1</sup>, Gunter E.A.<sup>2</sup>

<sup>1</sup>The Institute of Plant Biology and Biotechnology, Almaty, Kazakhstan

<sup>2</sup>The Institute of Physiology of Komi, Syktyvkar, Russia

\*e-mail: gen\_jan@mail.ru

## Chemical composition of polysaccharides from wheat cell culture

**Abstract:** Polysaccharides were extracted from wheat suspension culture and cultivated cells. Gas-liquid chromatography of wheat suspension culture allowed identifying the composition of polysaccharides that were found to contain arabinose, xylose, galactose, glucose, and a little amount of mannose and rhamnose. In dried cultivated cells the polysaccharide structure consisted mainly from arabinose, xylose, and galactose. It was found that the percentage of the amount of monosaccharides was positively correlated with the concentration of 2,4-D at the suspension media.

**Key words:** plant polysaccharides, chemical composition, wheat cell culture

### Introduction

Plant polysaccharides are famous for their important technical and physiologic traits. Currently, polysaccharides attract researchers with their high biological activity in regulating the growth, development and protection processes and are of a great interest in the search for and the production of new biologically active compounds [1, 2, 3].

Like a native plant, cell culture is capable for synthesis of a wide range of polysaccharides such as pectin, arabinogalactan, galactans, arabinans, xyloglucans, etc. [4, 5]. Studies of plant polysaccharides conducted mainly on various organs of the intact plants [6]. The polysaccharides derived from cell cultures of plant organs and plant cell lines, are much less become the objects of studies and are of a particular research interest.

Plant cell cultures serves as a convenient model system for studying the structure and biosynthesis of polysaccharides. Cell cultures have several advantages over the traditional raw materials: no organismic control, absence of dependency from the weather conditions, the ability to influence trophic, hormonal and physical factors, the possibility of streamlining and standardizing processes, the homogeneity of the system, the ability to identify the genes responsible for the synthesis of biologically active substances [7].

Our earlier investigations have shown that the ability to maintain embryogenic potential of the long-term cultivated embryogenic tissues of wheat and barley accompanied by the appearance of extracellular

polysaccharides [8]. In addition, we have determined high level of biological activity of polysaccharides obtained from embryogenic suspension culture [9]. The purpose of this study is to determine chemical composition of polysaccharides obtained from wheat suspension culture and dried cultivated cells.

### Materials and methods

The study object was an embryogenic suspension cell culture of wheat (*Triticum aestivum*). Suspension culture was grown in the Murashige and Scoog [10] liquid nutritious media with the addition of 1.0 and 5.0 mg/l of 2,4-D. The suspension liquid was filtered from suspension culture and was evaporated on rotary evaporator under 45-50°C. Extracellular polysaccharides from suspension liquid were extracted according to Gunter [11]. Polysaccharides inside the cells were extracted by water (I fraction) and by solution of ammonium oxalate (II fraction) from suspension cells. After that, solutions containing polysaccharides were evaporated and dried. The percentage output of monosaccharide composition was estimated on and compared with their initial dry biomass.

Protein composition in polysaccharide fractions was estimated by Louri methodology [12]. Overall polysaccharides presence and quantity was determined by phenol – sulfuric acid method by Dubious [13]. Spectrometric investigation was undertaken on the Ultraspec 3000 equipment. Monomers composition of polysaccharides was detected by Hewlett-

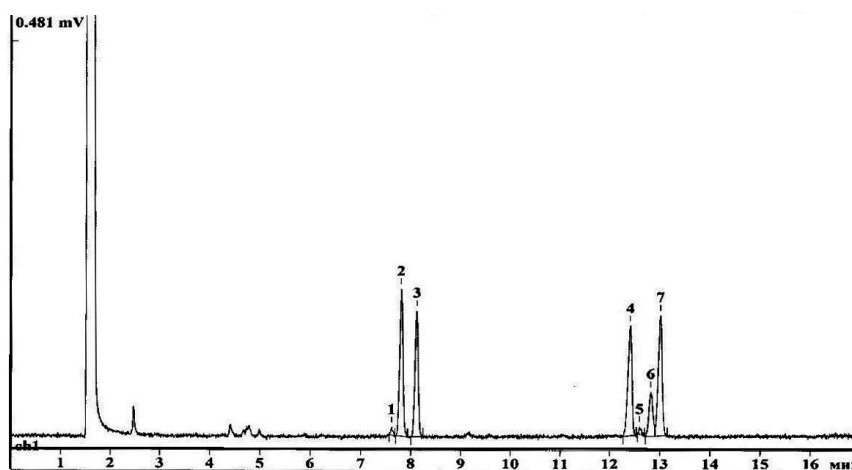
Packard 4890A gaz-liquid chromatography with plasma-ionization detector.

### Results and their discussion

Polysaccharides were extracted from wheat liquid suspensions and wheat cells. Extracellular polysaccharide containing liquid suspension was purified from low molecular weight compounds and other unnecessary compounds by dialysis. Obtained polysac-

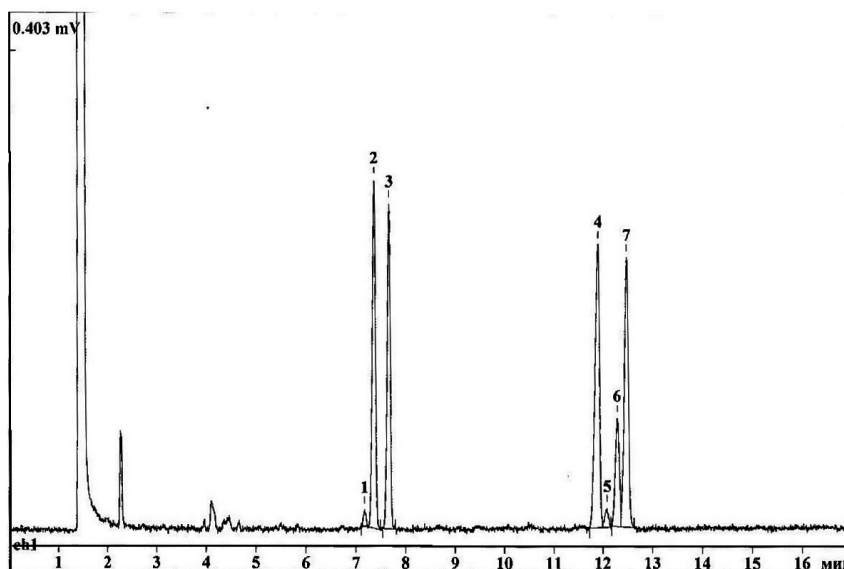
charide samples were tested by phenol-sulfuric acid method [13].

Monosaccharide composition of extracellular polysaccharides from wheat liquid suspension was detected by gas liquid chromatography (GLC). GLC allowed to identify that the quantity of monosaccharides obtained from media with 5.0 mg/l 2,4-D is considerably higher than those that growth on media with 1.0 mg/l 2,4-D (Figure 1 a, b). However, the chromatographic profiles of both concentrations were similar.



1 – rhamnose, 2 – arabinose, 3- xylose, 4 – inositol, 5 – mannose, 6 – glucose, 7 – galactose

**Figure 1 (a)** – Analysis of monosaccharide composition of polysaccharides from 1,0 mg/ml 2, 4 D media, using GLC

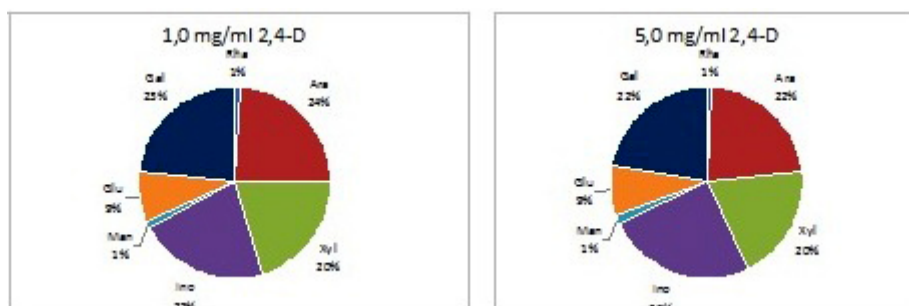


1 – rhamnose, 2 – arabinose, 3- xylose, 4 – inositol, 5 – mannose, 6 – glucose, 7 – galactose

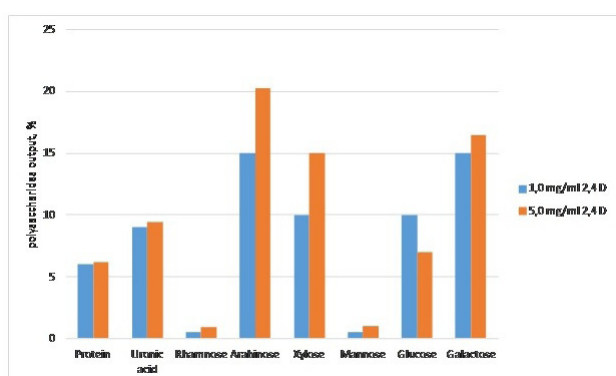
**Figure 1 (b)** – Analysis of monosaccharide composition of polysaccharides from 5.0 mg/ml 2,4 D media, using GLC

Analysis of chromatographic profile for monosaccharide composition of polysaccharides obtained from wheat liquid suspension revealed that the quantity of arabinose, xylose, galactose, and glucose

monosaccharides were considerably higher than the quantity of ramnose and mannose. Figure 2 presents percentage of each monosaccharide in polysaccharides obtained from suspension culture.



**Figure 2** – Percentage ratio of monosaccharides in polysaccharides obtained from suspension culture grown on different 2,4 D concentrations



1 – proteins, 2 – uronic acids, 3 – ramnose, 4 – arabinose, 5 – xylose, 6 – mannose, 7 – glucose, 8 – galactose

**Figure 3** – Monosaccharide composition of extracellular polysaccharides from wheat liquid suspension (%)

It was determined that the quantity of all monosaccharides of extracellular polysaccharides obtained from suspension culture grown on Murashige and Schoog media containing 5.0mg/l 2,4-D is considerably higher than those grown on media with 1,0mg/l 2,4-D, except glucose. There were no significant difference in the quantity of uronic acid (9.16%, 9.64%) and proteins (5.85%, 6.08%) between polysaccharide samples of 1.0 mg/l and 5.0 mg/l 2,4-D concentrations (Figure 3).

In order to characterize biosynthetic activity of cultivated cells, wheat cell suspension culture grown on Murashige and Skoog media was filtered and two fractions of polysaccharides were obtained. The first fraction (I fraction) was obtained from dried cells

water extract, whilst the second fraction (II fraction) was extracted by the solution of ammonium oxalate.

The analysis of the first fraction of cell polysaccharides revealed the increase of polysaccharides, protein, and uronic acid quantity with the escalation of 2,4-D enzyme concentration in culture media (Table 1). The quantity of the same compounds in the second fraction was found to have a similar dependence pattern with 2,4-D concentration increase, especially significant increase was found in uronic acid percentage (Table 1).

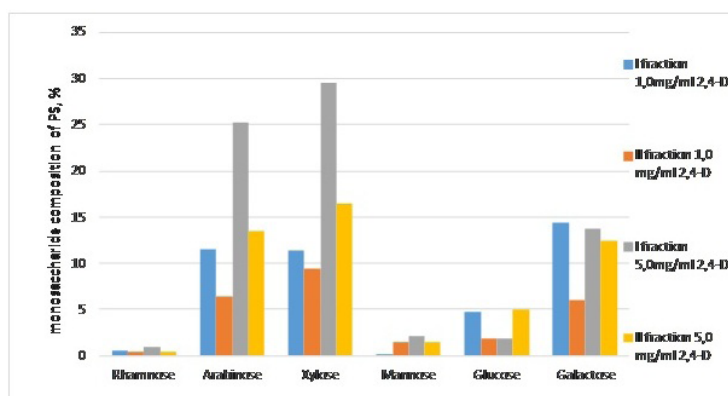
**Table 1** – The percentage of polysaccharides, protein and uronic acid in extract from dried wheat cells

Fractions	2,4-D concentration in media, mg/l	Polysaccharides,%	Protein,%	Uronic acid,%
I	1.0	0.93	4.06	14.72
	5.0	1.95	5.98	17.00
II	1.0	0.59	5.02	27.77
	5.0	0.77	6.45	66.40

Analysis of monosaccharide composition the I and II fractions obtained from wheat dried cultivated cells revealed that the quantity of arabinose, xylose, galactose were considerably higher rather than the quantity of neutral monosaccharides ramnose and mannose (Figure 4). It is important to point out that

the percentage of monosaccharides were higher in fraction I, which means that extraction method for the first fraction was more effective than the second one for both 2,4 D concentrations. Also, it was determined that, similar to polysaccharides from suspension culture, percentage of monosaccharides from dried callus cells showed the same dependency pat-

tern from the 2,4 D concentration increase. In other words, the percentage of monosaccharides increases with the escalation of 2,4-D in media. Thus, the quantity of arabinose, xylose and galactose (except galactose fraction I) is two times higher in polysaccharides from callus cells grown on 5.0 mg/ml 2,4 D, compared to 1.0 mg/ml 2,4 D (Figure 4).



**Figure 4** – Monosaccharide composition of extracellular polysaccharides from wheat dried cultivated cells

The study has shown that extracellular polysaccharides obtained from wheat liquid suspension culture consist of arabinogalactans, arabinoxylans, and xyloglucans. Polysaccharides extracted from wheat dried cultivated cells were found to contain of arabinogalactans and arabinoxylans. These findings correspond to earlier scientific investigation results on arabinogalactans [14] and xyloglucans [15] obtained from plant culturing *in vitro* described in literature. In addition, wide range of data in literature suggests that arabinogalactans and xyloglucans are capable to provide high biological activity. Considering earlier positive results of bioassays conducted in our laboratory [9], we assume that the high biological activity of substances obtained and extracted from liquid suspensions and dried cultivated cells explained by presence of these polysaccharides. Therefore, investigation of high biological activity of identified polysaccharides is the issue for our future research.

## References

1. Waggner H., Stuppner H., Schafer W., Zenk M. Immunologically active polysaccharides of *Echinacea* cell culture // *Phytochemistry*, 1988. – Vol. 27. – P. 119-126.
2. Roesler J., Emmensuffer A., Steinmiller C., Luetting B., Wagner H., Lohman-Matthes M.L. Ap-

plication of purified polysaccharides from cell cultures of the plant *Echinacea purpurea* to test subjects mediated activation of the phagocyte system // *Int.J.Immunopharmac*, 1991. – Vol. 13. – P. 931-941.

3. Ovodov U.S. Polysaccharides of flowering plants: structure and physiological activity // *Bioorganic chemistry*, 1998. – Vol. 24. – P. 483-501.

4. Goubet F., Morgan C., Synthesis of Cell Wall Galactans from Flex (*Linum usitatissimum* L.) Suspension-cultures Cells // *Plant and Cell Physiology*, 1994. – Vol. 35. – No. 5. – P. 729-727.

5. Gunter E.A., Popeyko O.V., Ovodov Yu.S., Modification of polysaccharides from callus culture of *Silene vulgaris* M. using carbohydrases *in vitro* // *Biochemistry*, 2007. – Vol. 72. – No. 9. – P. 1008-1015.

6. Olennikov D.N., Kashenko N.I. Polysaccharides. Modern state of research: experimental-scientific study // *Chemistry of natural raw materials*. 2014. – No. 1. – P. 5-26.

7. Gunter E.A. Pectin compounds of plant cellular cultures. Thesis. Syktyvkar, 2012.

8. Bishimbayeva N.K., Denebayeva M.G., Amirova A.K., Rakhimova E.V. Features of histological structure of friable embryogenic callus of barley // *Proceedings of the National Academy of Sciences of the Republic of Kazakhstan: Series biological and medical*, 2001. – No. 1-2. – P. 7-14.



9. Bishimbayeva N.K., Amirov A.K., Mur-tazina A.S., McDougall G.J., Rakhimbayev I.R. Biological activity of extracellular polysaccharides in suspension culture cells of wheat // *Physiological, biochemical and genetic and breeding plant research in Kazakhstan / Collection of articles*, 2010 – P. 103-111.
10. Bishimbaeyva N.K. *Cytophysiologic basics of long-term regeneration biotechnology in tissue culture of cereals / Synopsis for the doctor of biological sciences defense*, Almaty, 2007, 38 p.
11. Murashige T., Scoog F.A. revised medium for rapid growth and bioassays with tobacco tissue cultures // *Physiol.Plant*, 1962. Vol. 13. – P. 473-497.
12. Gunter E.A. Non-traditional plant's cell cultures as polysaccharides producers // *Chemistry and computer modeling. Butler messages*, 2001. – Vol. 5. – P. 11-12.
13. Lowry O.H., Rosebrough N.J., Farr A.L., Randall R.J. Protein measurement with the folin phenol reagent // *J. Biol. Chem.*, 1951. – Vol. 193. – P. 265-275.
14. Dubious M., Gilles K. A., Hamilton J.K., Rebers P.A., Smith F. Colorimetric method for determination of sugars and related substances // *Anal. Chem.*, 1956. – Vol. 28. – P. 350-356.
15. Arjon J. van Hengel, Zewdie Tadesse, Peter Immerzeel, Henk Schols, Ab van Kammen, Sacco C. de Vries. N-acetylglucoseamine and Glucosamine-Containing Arabinogalactan proteins Control Somatic Embryogenesis // *Plant Physiol.*, 2001. – Vol. 125. – P. 1880-1890.
16. McDougall G. J., Fry S.C. Structure-activity relationships for xyloglucan oligosaccharides with antiauxin activity // *Plant Physiol*, 1989. – Vol. 89. – P. 883

Kazybekova S.K.<sup>1</sup>, Bishimbaeyva N.K.<sup>1\*</sup>, Murtazina A.S.<sup>1</sup>,  
Tazhibayeva S.M.<sup>2</sup>, Miller R.<sup>3</sup>

<sup>1</sup>The Institute of Plant Biology and Biotechnology, Almaty, Kazakhstan

<sup>2</sup>Al-Farabi Kazakh National University, Almaty Kazakhstan

<sup>3</sup>Max Planck Institute of colloids and interfaces, Germany, Potsdam

\*e-mail: gen\_jan@mail.ru

### Physico-chemical properties of physiologically active polysaccharides from wheat tissue culture

**Abstract:** Polysaccharides (PS) from wheat cell culture were isolated by liquid-liquid extraction. The molecular mass distribution was determined by gel-permeation chromatography (GPC) using dual detectors for the simultaneous detection. It was supposed that PS sample from wheat cell culture has molecular weight of 1632 Da. The physico-chemical properties of PS such as solubility in different solvents, surface activity,  $\xi$ -potential, the pH value, polydispersity (PDI) were determined. The PS sample was soluble in water and insoluble in ethanol, acetone and chloroform.  $\xi$ -potential of PS was evaluated in order to determine its charge at different pH value from 3 to 9. As a result, the  $\xi$  values for the PS solution were negative throughout the pH range studied, varying from -2.85 mV (pH 3.0) to -21.1 (pH 9). Using tensiometry method, surface tension of the PS at the liquid/air interface was investigated. At 0.05% concentration interfacial tension decreases slowly and reaches an equilibrium value after ~ 8-8.5 hours. The pH was equal to 5.6±0.05. For a PS solution of 0.001% at pH 5.5 PDI was equal to 0.595.

**Key words:** polysaccharide, surface activity, average molecular weight

#### Introduction

All cell wall polysaccharides except cellulose are water-soluble compounds; their anchorage in the cell wall exists by use of different types of bonds [1]. The main monosaccharides that are part of the cell wall are: glucose, galactose, mannose, rhamnose and fucose, which contain six carbon atoms, as well as arabinose and xylose containing five carbon atoms. Common component of plant cell wall polysaccharides are uronic acids – modified sugars that have not closed in the ring – CH<sub>2</sub>OH group is replaced by a carboxyl group – COOH. Most frequent uronic acids are presented by galacturonic acid, which is a derivative of galactose [2].

One of the main physico-chemical parameters characterizing a macromolecule – whether it is naturally occurring or synthetically produced – is its «molecular weight» [3].

Determination of the molecular weight of water-soluble polysaccharides is usually carried out by gel-permeation chromatography (GPC), which effectively allocates the molecules based on their hydrodynamic volume. GPC is used in carbohydrate research to determine molecular weight distributions of polysaccharides. The columns are calibrated us-

ing commercially available standards which are commonly dextrans or pullulans [5].

GPC of polysaccharides is often based on size exclusion mechanism: physical exclusion of molecules that are unable to penetrate the pore structure of the resin. Sample molecules with a size greater than the pore diameter of the support matrix cannot enter the pores. They are excluded and eluted rapidly from the column in the void volume. Molecules with a size smaller than the pore diameter enter the pores and elute differentially in volumes that are in size between the void volume and the void volume plus pore volume [6].

Alternative approaches to determine the molecular weight is the analysis of light scattering and viscometer [7].

Polysaccharides consisting of one type of sugar unit uniformly linked in linear chains are usually water insoluble even when the molecules have a low molecular weight with degrees of polymerization (DP) 20-30. Insolubility results from the fit of molecules and their preference for partial crystallization. An exception to the rule is in (1→6)-linked homoglycans, which because of the extra degrees of freedom provided by the rotation about the C-5 to C-6 bonds gives higher solution entropy values. Homoglycans

with two types of sugar linkages or heteroglycans composed of two types of sugars are more soluble than purely homogeneous polymers. Ionized linear homoglycans are soluble but like all soluble linear polymers easily form gels because of segmental association which sometimes may be in a double helix formation. As these junction zones develop a stronger tertiary structure, gel hardness increases [8].

Zeta Potential analysis is a technique for determining the surface charge of particles in solution (colloids) [9].  $\zeta$ -potential has values that typically range from +100 mV to -100 mV. The magnitude of the zeta potential is predictive of the colloidal stability. Particles with zeta potential values greater than +25 mV or less than -25 mV typically have high degrees of stability. Dispersions with a low zeta potential value will eventually aggregate due to Van Der Waal inter-particle attractions [10].

Substances that capable to decrease the surface tension of the system ( $dy/dc < 0$ ) are referred to as surface active substances (SAS), or surfactants [11]. It follows from the Gibbs equation that the adsorption of such compounds is positive, i.e. their concentration within the surface layer is higher than that in the bulk. For example, at air-water and water-hydrocarbon interfaces the surface active compounds are the ones containing hydrocarbon (non-polar) chain and a polar group (-OH, -COOH, -NH<sub>2</sub> etc.) in their structure. Such an asymmetric (diphilic) structure of surfactant molecules accounts for their similarity to the nature of both contacting phases: a well-hydrated polar group has the strong affinity towards the aqueous phase, while the hydrocarbon chain has the affinity towards the non-polar phase [12].

The aim of present work was to reveal physicochemical properties of extracellular polysaccharides (PS) isolated from wheat cell suspension culture, including determination of molecular weight, surface activity and zeta potential of total PS fraction.

## Materials and methods

The molecular mass distribution was determined using size exclusion system at the Max Planck Institute of Colloids and Interfaces (Potsdam, Germany). The chromatograph was equipped with a reflective index (RI) detector (GE, Sweden) operating at 265 nm and two column in series, packed with Suprema 30 and Suprema 3000 (both from GE, Sweden). The range for Suprema 30 column is from 100-30000 Da, whereas Suprema 3000 column is suitable for range from 1000-3 000 000 Da. The analysis of molecular mass was carried out by this method [13]. In or-

der to determine the molecular weight the polysaccharides samples were analyzed by gel-permeation chromatography (GPC) using dual detectors for the simultaneous detection. The system was calibrated with pullulan standards. A mixture of standard pullulans with different molecular weights (342, 1460, 5600-710 kDa) were dissolved in 0.1 N NaNO<sub>3</sub> and applied on the same size exclusion Suprema 30 and Suprema 3000 columns and the same chromatography condition for the samples. After that, 7 mg of polysaccharide fraction was dissolved in 35 ml 0.1 N NaNO<sub>3</sub> solution at a flow rate of 1.000 ml/min and then filtrated through 0.22  $\mu$

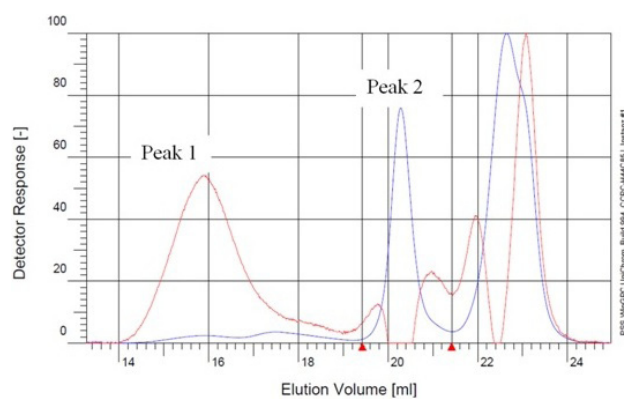


Figure 1 – The dependence of detector response on the elution volume

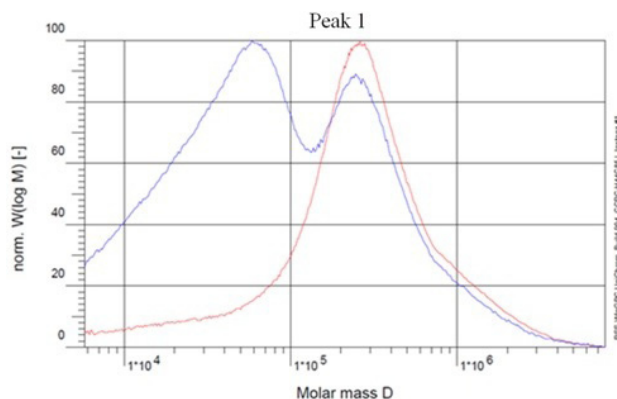
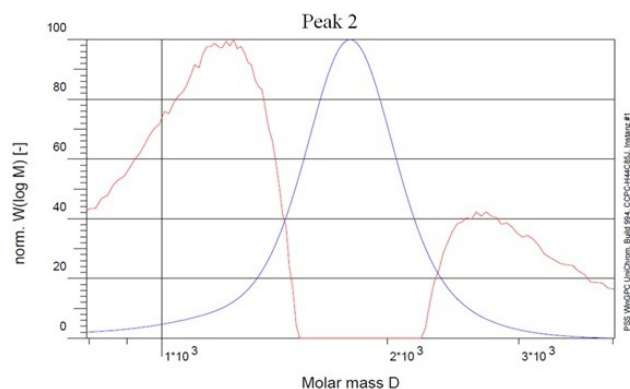


Figure 2 – The chromatogram of UV signal of PS sample

According to the literature review, proteoglycans consist of a core protein with one or more covalently attached glycosaminoglycan (GAG) chains. So, UV signal corresponding to the high molecular weight (430400 Da) can be explained by the structure of proteoglycan. If we reckoned in that polysaccharides can be detected only by RI detector

we can suppose that our PS sample has molecular weight of 1632 Da.

**Determination of PS solubility and pH of PS solutions.** The polysaccharide was soluble in water and insoluble in ethanol, acetone and chloroform. The PS sample was dissolved in distilled water in concentration of 1% (w/v) and measurements of pH value were conducted in three replications. As a result, it was found that pH of PS solutions was equal to  $5.6 \pm 0.05$ .

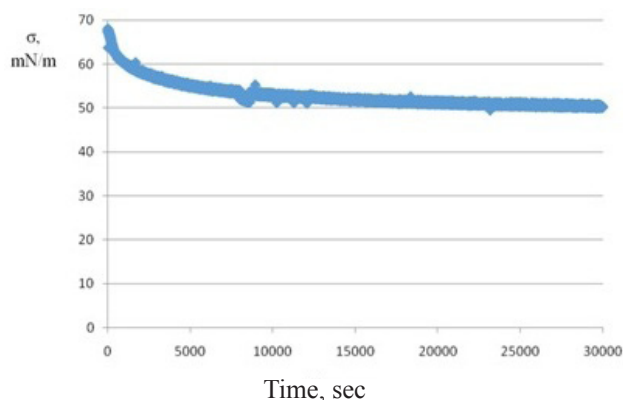


**Figure 3** – The chromatogram of RI signal of PS sample

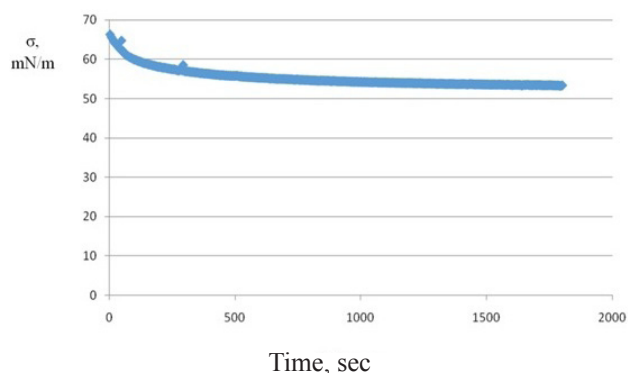
**Determination of surface activity.** The ability of the molecules of surfactants adsorb at interfaces is well known due to their amphiphilic structure. As a result of this process, the adsorption layers are formed, which in the equilibrium condition can be characterized by surface tension isotherms.

To clarify the characteristics of the formation of interfacial adsorption layers of PS solutions kinetic dependencies of the interfacial tension decrease at the time have been studied (Figure 4, 5). Figure 4 shows that the interfacial tension of the PS at 0.05% concentration decreases slowly and reaches an equilibrium value after ~ 8-8.5 hours. Duration of the interfacial tension decrease was due to the slow diffusion of the macromolecular coil to the surface, as well as conformational rearrangement of statistical balls' macromolecules on the surface of the active segment, which is reflected in the values of the relaxation time.

For the 1% solution the surface tension should be lower than for 0.05%. We have the opposite, which can be explained only by a certain multi-component composition of the substance, and consequently a completely different composition of the interfacial layer (Figure 5).



**Figure 4** – Surface tension ( $\sigma$ , mN/m) as a function of time (s) for 0.05% PS solution as measured by dynamic drop volume method.

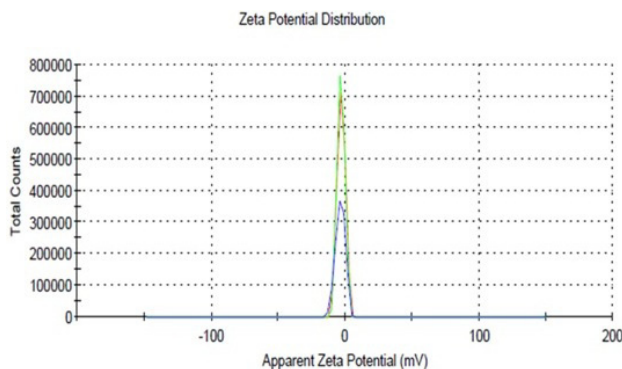


**Figure 5** – Surface tension ( $\sigma$ , mN/m) as a function of time (s) for 1% PS solution as measured by dynamic drop volume method

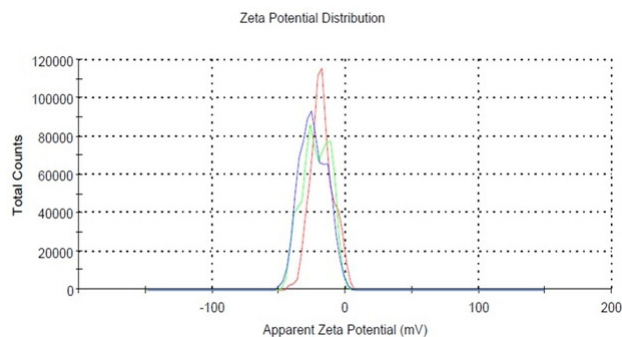
According to the results obtained by tensiometry method, it was established that investigated cell culture polysaccharides have the features of surface-active substances (SAS), which characterized by capability to decrease the surface tension of solutions.

**$\xi$ -potential and dynamic light scattering.** Electrostatic forces are usually the major driving force for the interaction of charged biopolymers in aqueous solutions, and so it was important to determine the electrical characteristics of the biopolymers used in this work.  $\xi$ -potential of PS was evaluated in order to determine the charge of their molecules at different pH value – from 3 to 9. The electronegativity of the solution increased with increasing pH from – 2, 85 mV (pH 3.0) to –21.1 (pH 9), respectively. At pH 3  $\xi$ -potential value of PS was equal to  $-2.85 \pm 0.27$

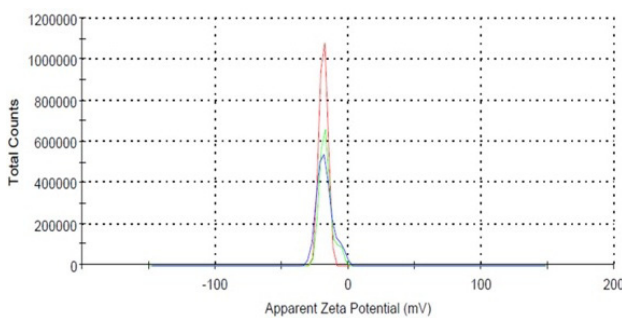
mV (Figure 6), thus showing that polysaccharide isolated from wheat is a practically neutral polysaccharide. The polysaccharides may be constituted either by polycations or by polyanions, depending on their functional group, and may also be neutral, which is the case of different types of polysaccharides with a higher content of mannose and galactose units. In neutral medium at pH 5.5 it was established that  $\xi$ -potential has higher negative value of  $-18.8 \pm 2.05$  (Figure 7). At pH 9 the value of  $\xi$ -potential corresponded to the  $-21.7 \pm 0.55$  (Figure 8).



**Figure 6** – Determination of  $\xi$ -potential at pH 3 value

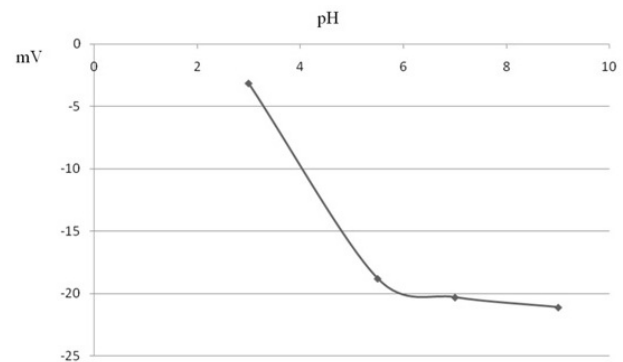


**Figure 7** – Determination of  $\xi$ -potential at pH 5.5 value



**Figure 8** – Determination of  $\xi$ -potential at pH 9 value

The pH dependence of the zeta potential ( $\xi$ ) for the PS solution is shown in Figure 9. The  $\xi$  values for the PS solution were negative throughout the pH range studied, varying from  $-2.85$  mV (pH 3.0) to  $-21.1$  mV (pH 9). The increase of negative  $\xi$  values that occurred by the increase of pH values can be attributed to the ionization of the carboxylic moieties ( $-\text{COOH}$ ) giving rise to carboxylate groups ( $-\text{COO}^-$ ), while the decrease of negative  $\xi$  values at pH=3 value are due to the protonation of the amino moieties ( $-\text{NH}_2$ ) giving rise to ammonium groups ( $-\text{NH}_3^+$ ).

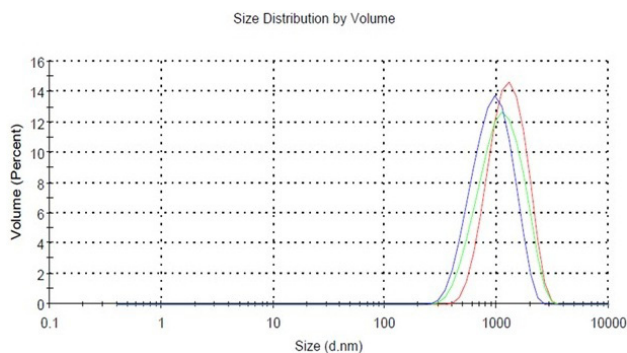


**Figure 9** – Dependence of zeta potential (mV) of the PS solution with concentration of 0.001% on pH values ranging from 3 to 9

$\xi$ -potential values are also related to the stability of solutions. As a general rule, absolute values of  $\xi$ -potential above 60 mV indicate an excellent stability, from 60 to 30 mV are physically stable, from 30 mV to 5 mV are at the limit of stability and below 5 mV are not stable and there are aggregates can be formed. According to this general rule, the results obtained with at different pH show that PS solutions are stable.

The information obtained by  $\xi$ -potential and Dynamic Light Scattering (DLS) are crucial to indicate the occurrence of stable functional nanostructures. Polydispersion index (PDI), obtained by DLS is a measure of the size distribution width (Figure 10)

When polydispersity equals zero, the sample is monodisperse. Values of PDI close to or above 0.5 represent heterogeneous solutions in relation to the particle size and are characteristic of samples outside the standards. The term «particle» represents the molecule of polysaccharide, which stay disperses into diluted solution. For a PS solution of 0.001% at pH 5.5, Z-average and PDI were 926.8 and 0.595, respectively. It was established that PS sample is polydisperse.



**Figure 10** – The size distribution by volume

In conclusion, physico-chemical properties of extracellular polysaccharides from wheat cell culture have been determined for the first time: molecular weight, solubility in different solvents, the pH value, surface activity,  $\xi$ -potential, polydispersity (PDI).

It was revealed that total fraction of PS consists of high molecular weight proteoglycan (430400 Da) and low molecular weight glycan (1632 Da).

Investigated PS are soluble in water, insoluble in ethanol, acetone and chloroform; pH of 1% solutions is equal to  $5.6 \pm 0.05$ .

Parameters of PS surface tension as well as dependency from concentrations of PS solution have been determined. Obtained results suggest that PS are high-molecular non-ionogenic compounds. It was shown that investigated PS have the characteristics of surface active substances.

Established dependence of  $\xi$ - potential from pH allow to assume the neutral nature of investigated polymers. Obtained results from dynamic light scattering (DLS) show the polydispersity of investigated PS.

## References

1. Gorshkova T.A., Wyatt S.E., Salnikov V.V. Cell-wall polysaccharides of developing flax plants // *Plant Physiol*, 1996. – Vol. 110. – P. 721-729.
2. Wu A.M. Complex Carbohydrates in Microbial and Viral infections and vaccine design // *The Molecular Immunology of Complex Carbohydrates*, 1997. – Vol. 2. – P. 173-176.
3. Gillis R.B., Adams G.G., Wolf B., Berry M., Besong T.D., Corfield A. et al. Molecular weight distribution analysis by ultracentrifugation: adaptation of a new approach for mucins // *Carbohydrate Polymers*, 2013. – Vol. 93. – P. 178-183.
4. Harding S.E., Abdelhameed A.S., Morris G.A. Molecular weight distribution, evaluation of

polysaccharides and glycoconjugates using analytical ultracentrifugation // *Macromolecular Bioscience*, 2010. – Vol.10. – P. 714-720.

5. Jingjing Yang, Fan Yang, Huimin Yang, Guiyun Wang. Water-soluble polysaccharide isolated with alkali from the stem of *Physalis alkekengi* L.: Structural characterization and immunologic enhancement in DNA vaccine // *Carbohydrate Polymers*, 2015. – Vol.121. – P.248-253

6. Kawahara K., Ohta K., Miyamoto H., Nakamura S. Preparation and solution properties of pululan fractions as standard samples for water-soluble polymers // *Carbohydrate Polymers*, 1984. – Vol.4. – P.335-356.

7. Freitas R.A., Martin S., Santos G.L., Valenga F., Buckeridge M.S., Reicher F. Physico-chemical properties of seed xyloglucans from different sources // *Carbohydrate Polymers*, 2005. – Vol.60. – P. 507-514.

8. Bi F., Mahmood S.J., Arman M., Taj N., Iqbal S. Physicochemical characterization and ionic studies of sodium alginate from *Sargassum terrarium* (brown algae) // *Physics and Chemistry of Liquids*, 2007, Vol. 45. – P.453-461.

9. Mikshina P.V., Idratullin B.Z., Petrova A.A., Shashkov A.S., Zuev Y.F., Gorshkova T.A. Physico-chemical properties of complex rhamnogalacturonan I from gelatinous cell walls of flax fibers // *Carbohydrate Polymers*, 2015. – Vol.117. – P.853-861.

10. Carneiro-da-Cunha M.G., Cerqueira M.A., Bartolomeu W.S. Souza, Teixeira J.A., António A. Vicente Influence of concentration, ionic strength and pH on zeta potential and mean hydrodynamic diameter of edible polysaccharide solutions envisaged for multilayered films production // *Carbohydrate Polymers*, 2011. – Vol. 85. – P.522-528.

11. Hernández-Marín N.Y., Lobato-Calleros C., Vernon-Carter E.J. Stability and rheology of water-in-oil-in-water multiple emulsions made with protein-polysaccharide soluble complexes // *Journal of Food Engineering*, 2013. – Vol.119. – P.181-187.

12. Murray B.S. Rheological properties of protein films // *Current Opinion in Colloid and Interface Science*, 2011. – Vol.16. – P.27-35.

13. Sluiter A., Hames B., Ruiz R., Scarlata C., Sluiter J., Templeton D. Determination of structural carbohydrates and lignin in biomass // *Analytical Journal*, 2005. – Vol.17. – P.123-125.

14. Romero A., Beaumal V., David-Briand E., Cordobes F., Guerrero A., Anton M., Interfacial and oil/water emulsions characterization of potato protein isolates // *Journal of Agricultural and Food Chemistry*, 2011. – Vol. 59. – No. 17. – P. 9466-9474.

UDC 631.879.2

Kanaev A.T., Esirkepova Zh.\* , Amanbayeva U.

Al-Farabi Kazakh National University, Almaty, Kazakhstan

\*e-mail: zh.yessirkep@gmail.com

### **Properties of a chemical agents study of the Bayaldyr tailing dams lead – zinc oresspoil dump**

**Abstract:** With the development of mining and metallurgical industries on a soil surface there is a constant accumulation of technogenic waste from processing of minerals. These include tailing, sludges, slags and other substandard varieties of mineral resources. These elements of human origin can reach high local concentrations, in some cases up to toxic or scatter over large aqueous spaces or air currents. Thus the aim of the current research was to study the properties of a chemical agents of the Bayaldyr tailing dams lead – zinc oresspoil dump.

**Key words:** chemical agents, dump, technogenic waste, study.

#### **Introduction**

With the development of mining and metallurgical industries on a soil surface there is a constant accumulation of technogenic waste from processing of minerals. These include tailing, sludges, slags and other substandard varieties of mineral resources. The bulk of this waste comes from waste dumps, landfills which occupy vast areas (in the volume of world dumps of more than 2000 km<sup>3</sup>) and a negative impact on the environment. These elements are of human origin can achieve high local concentrations, in some cases up to toxic or scattered over large aqueous spaces or air currents. Such deposit may include lead-zinc mine combine «Achpolimetall» with its Bayaldyr tailing dams waste tailings. Combine «Achpolimetall» was founded in 1955 on the basis of Mirgalimsay village for Achisay polymetallic deposit development [1-3].

After a while the village was transformed into a city of regional subordination Kentau in the Southern Kazakhstan region. Located at the foot of the Karatau, 30 km north-east of the city of Turkestan (Figure 1).

#### **Materials and methods**

**Objects.** To study the chemical composition of the solid sample tailing dump Bayaldyr tailings were taken away from the pumping station (point No. 1), north-eastern direction (point No. 2), the south-east side (point No. 3) and north-west side (point No. 4) (Figure 2).

**Sampling methods.** Samples of tailings were taken in May 2014. When sampling sought to ensure that the chemical composition of bulk materials Bayaldyr tailings correctly reflects the composition of the analyzed object.

Sampling granular materials used shovels with rims that have gone in in the portion of the material is taken from one place. We tried not to select a sample in small portions, repeating several times a selection of one and the same place. The width of the shovel was four times greater than the width of large pieces. Too big shovel did not apply, since they are hard to gain equal portions from different places. The amount of portion was depended on the pieces size the larger pieces of the material, the greater the portion of the bleed. For the value of the portion of the particulate material ranged from 0.2 to 0.5 kg. Samples were collected in special boxes a la carte. These boxes are filled a spade portion up to a point.

**Method of analysis.** Chemical analysis of the composition and the number of elements were performed on a gas chromatograph «model 3700» with detectors, flame ionization, thermal conductivity, electron capture, intended for mass analysis of organic and inorganic gaseous and liquid compounds.

#### **Results and their discussion**

Climatic conditions over the whole territory of the South Kazakhstan region are sharply continental [4].

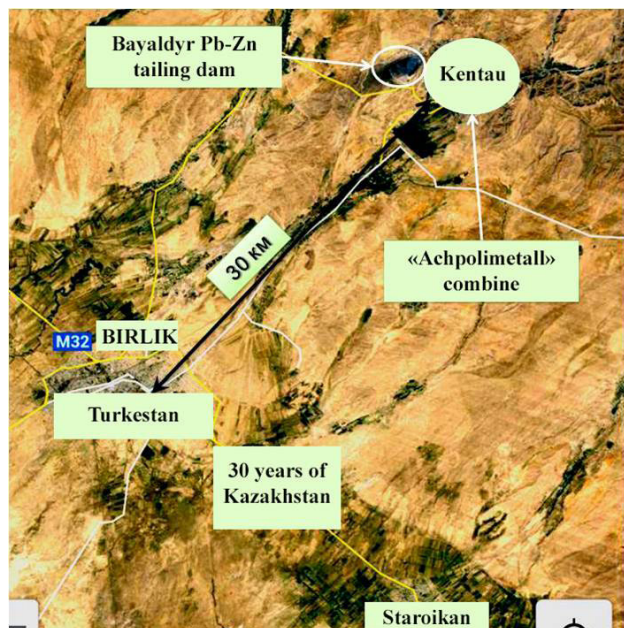
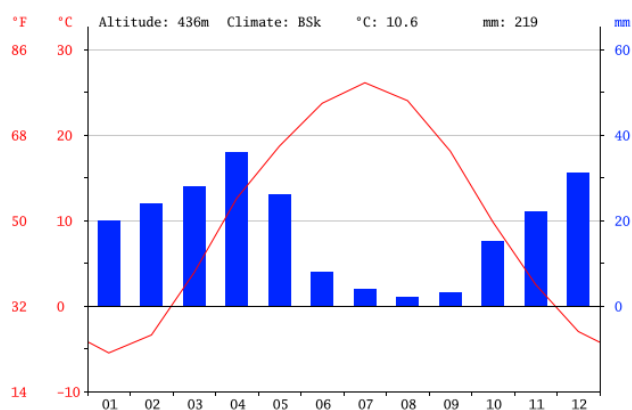


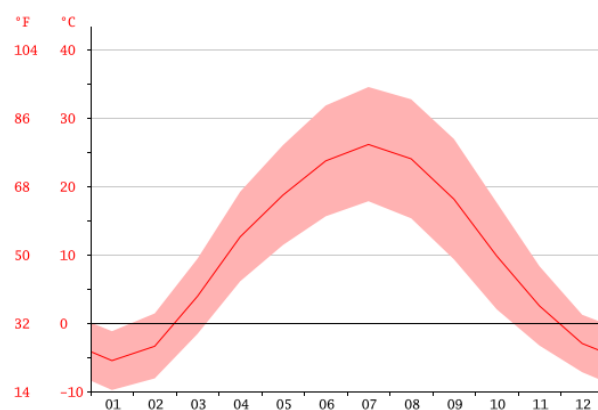
Figure 1 – Geographical location of «Achpolimetal» combine (Kentau).



Figure 2 – The sampling points for chemical analysis (May, 2014)



The driest month is August with 2 mm of precipitation. Most of the precipitation falls in April, an average of 36 mm.



The warmest month of the year – July, with an average temperature of 26.1°C. The average temperature in January – -5.5°C. This is the lowest average temperature for the year.

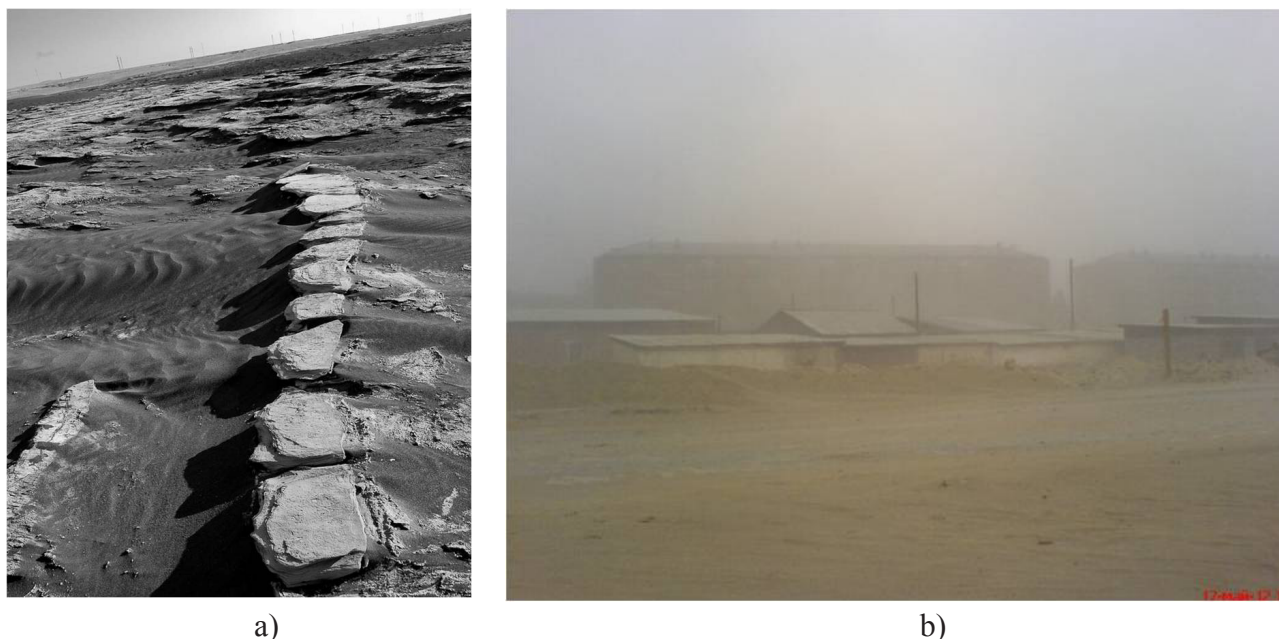
Figure 3 – Climatic conditions of the South Kazakhstan region

Winters are warm and mild with air temperature of -8°C. Spring is characterized by bright, vivid colors. Summer is usually hot and dry. In July the temperature surpasses the mark of 40 °C. Autumn is long and mild (Figure 3).

Refinement tailings of lead-zinc ores in Bayaldyr tailing dump of Kentau concentrating mill are about 170 million tons, which contain copper, zinc, cadmium, manganese, lead, nickel, cobalt, iron, strontium, and other nonferrous and precious metals.

Lead – zinc ores are extracted from the mines «Mirgalimsay» and «Deep» and enriched in the concentrating mill. After the flotation tailings were stored in Bayaldyr tailing dump. The surface of the tailings are not reinforced by any of the currently available methods of stabilization or reclamation. Consequently, it is exposed to wind and water erosion and the effects of physical – chemical and biological factors and leads to air pollution by dust and solid particles with high concentrations of heavy metals (Figure 4).





a)

b)

**Figure 4** – Surface appearance of Bayaldyr tailing dump (a) and clouds of toxic dust of Bayaldyr tailing dump (b). (May, 2014)

Waste processing contains inclusions to 20 reagents, including 12 particularly toxic substances – heavy metals, copper, lead, zinc. Earlier Bayaldyr tailing dump contained in the so-called wet concentration – the entire storage area (333 hectares) is constantly filled with water. Thanks to it toxins didn't disappear from the tailing dump, constantly being on a place in the form of the solid moistened slags. With the liquidation of the mine tailing dump has stopped being moisten. Now, clouds of toxic dust rises on Bayaldyr tailing dump with the slightest breeze, which cover up with sand not only Kentau and Turkestan, but a dozen villages.

We have studied the geo-ecological status and chemical composition of the refinement tailings of Bayaldyr tailing dump of «Deep» and «Myrgalym-say» lead and zinc ore deposit.

In the study of mineral and chemical composition of tailings was considered necessary to determine their quality, their content of useful components and harmful impurities [5, 6].

The chemical composition of samples taken from the surface dam of Bayaldyr tailing is dump shown on Figure 5. Chemical analysis of tailings that the dominant elements in the samples selected in the area of the pumping station are copper (108 mg/kg), cobalt (92.5 mg/kg) and nickel (65.6 mg/kg), while zinc, manganese, cadmium, lead, iron and strontium are present in small quantities.

However, the amount of copper, nickel and cobalt are contained in a large amount. This is probably due to the views of flotation reagents used. Thus, as a depressant and sulphidizer floatable ore added in a large amount of these elements sulfide reagents.

At one time, in Kentau concentrator lead-zinc ore floated froth flotation, whereby through the particle mixture with water passed small air bubbles, particles of certain minerals are collected at the interface «air-liquid» adhere to the air bubbles and was carried with them surface composed of a three-phase foam (with the addition of a foaming agent which regulates foam stability). The foam was further concentrated. As the liquid is water.

Lead-zinc ore of Kentau combine enriched by the scheme of direct selective flotation. Feature reagent regime is applied using a mixture of ethyl xanthogenate in a ratio of 2:1, as well as combinations of sodium sulfide and ammonium sulphate minerals to sulphidization oxidized. In order to reduce lead content in the pyrite concentrate to the lead flotation pulp is mixed with lime at pH 9.0 ... 9.5, and then reducing the pH value to 8.3 ... 8.8. A mixture of sodium sulfide and zinc sulfate is using for depression sphalerite. Lead concentrate produced at the enrichment of sulfide ores contain 74 ... 75% of the lead when removing the 93 ... 95% of lead: zinc concentrates containing 52 ... 53% zinc extraction at 92 ... 94%.

Thus we consider that low levels of lead and zinc tailings in a natural, because it is connected by a major amount of lead and zinc goes to concentrate on the process of ore flotation.

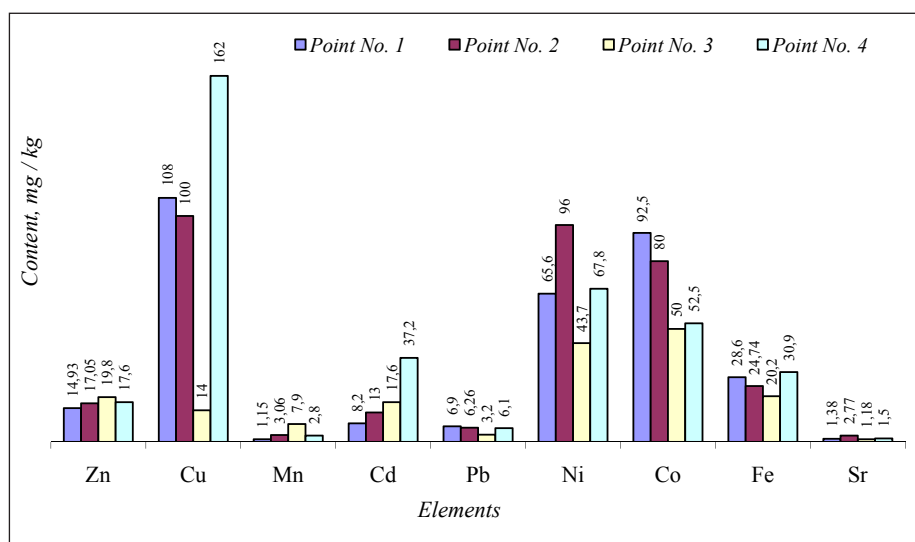
Tailings are the terock particles, resulting from the mechanical processing of ores (crushing, grinding, classification, flotation). Solid phase tailings slurry is a mixture of mine ralparticles of different sizes – from 3 mm to submicron.

The material composition of the tailings particles Bayaldyr and their densitydependson the mineral composition of the rocks. Size distribution of the particles with a size of 0.01 mm have a shape similar to a sphere. Since the composition of tailings in large quantities mostly contain flotation re-

agents. In this regard it necessary to elaborate on their characteristics.

Potassium butyl xanthate hate intended for use as a collector reagent in the beneficiation of ores by flotation and in the hydrometallurgical industry [7].

It is a powder from light gray to yellowish-green color and odor, is highly soluble in water. In the presence of moisture decomposes, especially at temperatures above 30°C. Harmful by inhalation (weakness, headache, dizziness, shortness of breath, palpitations, chest pain, nausea, vomiting, cyanosis of the skin and mucous membranes), in contact with skin (redness, swelling) and eyes (pain in the eyes). Works through the uninjured skin. In case of hit and mucous renders an irritant action on skin.



Note: Point No. 1 – injection pump station pipe, point No. 2 – the southeastern part, point No. 3 – north-eastern part, point No. 4 – north-western part

**Figure 5** – The chemical composition of samples taken from the surface dam of Bayaldyr tailing dump

**Table 1** – Physical and chemical properties of butyl xanthate

Indicator name	Standard for STO 00204168-003-2009		
	High grade	First grade	Second grade
Appearance	Powder from light gray to yellow-green		
Mass fraction of main substance,%, not less	91.5	90.0	87.0
Mass fraction of free potassium hydroxide (KOH),%, not more	0.1	0.2	0.2
Mass fraction of volatile substances,%, no more	2	3	5

Note: Indicator 3 is determined only at the request of the consumer

Prolonged contact celebrated drug reaction and appearance of eczema, dermatitis. If you get inside the predominantly affects the central nervous system that is associated with the release of carbon disulfide and its toxic effects.

In the course of the flotation of «Mirgalimsay» and «Deep» lead-zinc oxide ores deposits sodium sulfide, as component flotation, used as sulphidizer. Sodium sulfide inhalation causes consequences in the form of cough, chest tightness, runny nose, watery eyes and dangerous to other mucous membranes, causes damage to the eyelids, conjunctiva, and iris of the eye. The sharp effect on unprotected skin high concentration of sodium sulfide can cause a chemical burn.

Also ammonium sulfate has used for the sulphidation of oxidized minerals as flotation reagents. Human has severe irritation and inflammation of the airways in case of Inhalation of ammonium sulphate. In that case, if the person used the ammonium sulfate into the causes irritation of the gastrointestinal tract, accompanied by nausea, vomiting and diarrhea. When ammonium sulphate contact with skin or eyes occurs irritation, redness, itching and pain.

As mentioned above, in the process of flotation concentrator KOOF-1c was used as a depressant of sphalerite zinc sulfate, which in high concentrations is toxic effect on the human body.

## References

- 1 Batrakova L.H., Egeubaev B.S., Edenbaev S.S. Complex processing of mineral raw materials of Kazakhstan (state, problems, solutions), Almaty, 2003. – 390 p.
- 2 Ussov A.F. Prospects of technologies for disintegration of rocks and ores. Proceedings of the Academy of Sciences, Power engineering, 2001, No.1. – P. 54-62.
- 3 Levine R.M. The mineral industry of Kazakhstan, 1992. P. 309-315.
- 4 RSE «Kazhydromet» Annual bulletin of climate change monitoring in Kazakhstan, 2012. – P. 8-15.
- 5 Zhang Xiu-Wu, Yang Lin-Sheng, Li Yong-Hua, Li Hai-Rong, Wang Wu-Yi, Ge Quan-Sheng. Estimation of lead and zinc emissions from mineral exploitation based on characteristics of lead/zinc deposits in China. Trans. Nonferrous Met. Soc. China, 2011, Vol. 21. – P. 2513-2519.
- 6 Top ten toxic pollution problems. Lead pollution from mining and ore processing. Available at: [http://www.worstpolluted.org/projects\\_reports/display/84](http://www.worstpolluted.org/projects_reports/display/84)
- 7 National Environmental Research Institute University of Aarhus. Denmark. Environmental Impact of the Lead-Zinc Mine at Mestersvig, East Greenland. NERI Research Note No. 241, 2008

UDC 553.3/4:573.6.

Kanaev A.T., Semenchenko G.V., Konysbayeva A.A.,  
Shilmanova A.A. Kanayeva Z.K.

Al-Farabi Kazakh National University, Almaty, Kazakhstan

\*e-mail: Ashimhan.Kanaev@kaznu.kz

### **Method of gold extraction from ores of bakyrchik deposit by percolation bioleaching**

**Abstract:** With a presumed steady decline of gold ore grade in mineral resources, mining applications enabling efficient metal extraction from low-grade ores are of increasing interest to the minerals industry. Microbial processes may provide one such solution since they can participate in the biogeochemical cycling of gold in many direct and indirect ways. This review examines current literature on the role of microorganisms in gold processing and recovery. The review covers aspects such as the biotechnical pre-treatment of gold ores and concentrates, microbially catalysed permeability enhancement of ore bodies, gold solubilisation through biooxidation and complexation with biogenic lixivants, and microbially mediated gold recovery and loss from leach liquors.

**Key words:** gold extraction, ores, deposit, bioleaching, review.

#### **Introduction**

The role of biological agents in the mining industry is currently limited to the use of microorganisms in bioleaching and bioremediation. However, there are a number of ways in which biotechnology will be used in the near future to aid the mining industry. This review focuses on the development of novel biotechnologies and the role they will play in gold exploration, processing and remediation. The development of these biotechnologies has been enabled by advances in our molecular-level understanding of the role microorganisms play in the solubilisation, dispersion and precipitation of gold, brought upon by the rapid development of molecular genetic techniques over the past decade. This fundamental knowledge is now being used to develop new methods for gold exploration, processing and remediation.

An understanding of the distribution of microbial species in soils overlying mineralization can be utilized to develop bioindicator systems that assist with gold exploration. An in-depth knowledge of how microorganisms interact with gold complexes is being used to develop biosensors, further supporting exploration. Processing technologies are being improved based upon advances in our understanding of the interactions between microorganisms, cyanide and gold. For instance, cyanide-producing microorganisms are being investigated for use in situ leaching of gold. In turn, the use of cyanide-utilizing microorgan-

isms for the degradation of cyanide is being explored. Combined the implementation of biotechnologies in the gold mining sector is set to revolutionize the industry, leading to the greener, more efficient extraction of gold [1, 2].

Chemical leaching and biooxidation stages were examined in a two-stage biooxidation process of an auriferous sulfide concentrate containing pyrrhotite, arsenopyrite and pyrite. Chemical leaching of the concentrate (slurry density at 200 g/L) by ferric sulfate biosolvent (initial concentration at 35.6 g/L), which was obtained by microbial oxidation of ferrous sulfate for 2 hours at 70°C at pH 1.4, was allowed to oxidize 20.4% of arsenopyrite and 52.1% of sulfur. The most effective biooxidation of chemically leached concentrate was observed at 45°C in the presence of yeast extract. Oxidation of the sulfide concentrate in a two-step process proceeded more efficiently than in one-step. In a two-step mode, gold extraction from the precipitate was 10% higher and the content of elemental sulfur was two times lower than in a one-step process [3].

Plant design parameters for gold extraction, leach residence time and cyanide consumption are generally determined from standard bench-scale bottle roll or agitation leach tests. The application of laboratory data to process design has essentially evolved from the testing of oxide or low cyanide-consuming ores. Such scale-up factors may not be appropriate for ores that deplete cyanide and oxygen since this interferes

with gold extraction kinetics. High cyanide-consuming ores also exacerbate the differences between the conditions applicable to small batch tests and large continuous operations. Testing a reactive high-sulfide South American ore deposit necessitated the re-evaluation of conventional bench-scale cyanidation procedures. Pulp density can be a major factor affecting the results for plant design purposes and should be treated as a test work variable. As with high clay-bearing ore, where pulp viscosity can hinder mass transfer, minimizing the influence of test equipment on gold extraction kinetics may require low pulp densities. This introduces interpretative complexity since cyanide consumption changes as a function of pulp density. Activated carbon also consumes cyanide, so its effect has to be accounted for in the case of carbon-in-leach (CIL) or carbon-in-pulp (CIP) plant flowsheets. Since cyanide is an expensive reagent, often a major component of plant operating costs, it is important that the scale-up of cyanide consumption from laboratory to plant be representative. The traditional method of reporting cyanide consumption in bench-scale testing is questioned since it takes credit for residual free cyanide in leach tails. The projected plant consumption may be better estimated by using the total cyanide addition in a laboratory test. We propose a test work protocol that categorizes the cyanide consumption into its components but requires more extensive testing to generate design data. The ultimate validation of scale-up factors used by project engineers requires rigorous bench-scale versus commercial plant comparative data. Such data are not readily available [4].

Rapid technological advancement and the relatively short life time of electronic goods have resulted in an alarming growth rate of electronic waste which often contains significant quantities of toxic and precious metals. Compared to conventional chemical recovery methods, bioleaching has been shown to be an environmentally friendly process for metal extraction. In this work, gold bioleaching from electronic scrap material (ESM) was examined using batch cultures of the bacterium *Chromobacterium violaceum* which produces cyanide as a secondary metabolite. Gold was bioleached via gold cyanide complexation. The ESM was pretreated using nitric acid to dissolve the base metals (mainly copper) in order to reduce competition for the cyanide ion from other metals present in ESM. ESM was added to the bacterial culture after it reached maximum cyanide production during early stationary phase. Leaching with spent medium using bacterial cell-free metabolites showed a higher gold recovery of 18%, compared to that of two-step bio-

leaching of 11% at 0.5% w/v pulp density of ESM. Gold bioleaching was further enhanced to 30% when the pH of the spent medium was increased to shift the equilibrium in favor of cyanide ions production. Spent medium bioleaching of pretreated ESM yield a higher gold recovery compared to two-step bioleaching at a pulp density of 0.5% w/v [5].

Some of refractory gold ores represent one of the difficult processable ores due to fine dissemination and interlocking of the gold grains with the associated sulphide minerals. This makes it impossible to recover precious metals from sulphide matrices by direct cyanide leaching even at high consumption of cyanide solution. Research to solve this problem is numerous. Application of bacteria shows that, some types of bacteria have great affect on sulphides bio-oxidation and consequently facilitate the leaching process. In this paper, leaching of Saudi gold ore, from Alhura area, containing sulphides before cyanidation is studied to recover gold from such ores applying bacteria. The process is investigated using stirred reactor bio-leaching rather than heap bioleaching. Using statistical analysis the main affecting variables under studied conditions were identified. The design results indicated that the dose of bacteria, retention time and nutrition  $K_2SO_4$  are the most significant parameters. The higher the bacterial dose and the bacterial nutrition, the better is the concentrate grade. Results show that the method is technically effective in gold recovery. A gold concentrate containing >100 g/t gold was obtained at optimum conditions, from an ore containing < 2 g/t gold i. e., 10 ml bacterial dose, 6 days retention time, and 6.5 kg/t  $K_2SO_4$  as bacteria nutrition [6].

The beneficiation of mineral substances through biotechnology forms the objective and basis of the present study of the pyrite bacterial leaching (bioleaching) process. The use of ferrous and sulfide oxidizing bacteria in bioleaching processes is a recent technique that has found industrial applications in copper, uranium, cobalt and gold extraction. To pursue its application and extend it to the upgrading of other ores, its technical and economic viability must be continually demonstrated and optimized through credible technological innovations in terms of scale-up and better control of biochemical activity. This is what this work aims to achieve by improving our knowledge of the intimate mechanisms governing the action of microorganisms during pyrite bacterial oxidative dissolution. The substrate used is formed of finely ground pyrite. The cultures (classical nutritive medium without ferrous iron) are batch-prepared and kept at a temperature of 35°C. agitated and aerated.

The bacterial population used comprises three species: *Thiobacillus ferrooxidans*, *Thiobacillus thiooxidans* and *Leptospirillum ferrooxidans*. Specific equipment was developed and adapted for the study, including the design of special pyrite electrodes and the use of electrochemical methods for corrosion and interface investigations. These tools served to identify and monitor the electrochemical reactions occurring during bioleaching, both in solution and on the surface of the pyrite electrodes. The work consisted in relating the observations of the changes in certain key electrochemical parameters to the presence of  $\text{Fe}^{2+}$  and  $\text{Fe}^{3+}$  ions in solution. The electrochemical behavior of pyrite during bioleaching was studied by continuous measurement of certain electrochemical parameters in different situations, both natural and induced. The overall chemical process of pyrite bioleaching was determined and subdivided into distinct elementary stages. The key factors of each elementary stage and their respective roles were identified. This made it possible, for each stage, to differentiate the electrochemical reactions occurring in solution and at the interfaces, which, when combined, lead to overall reactions that advance the bioleaching of pyrite. The results completely contradict the theory of direct dissolution of the pyrite by the bacteria and indicate that (i) the ferric ion hence remains the only powerful oxidant of pyrite during its bacterial leaching, (ii) the only role of the bacteria is (re)generation of ferric ions in solution, and (iii) the process of bacterial adhesion or contact or attack no longer has the same meaning as was hitherto attributed [7].

A quick, simple and reproducible method for the indirect determination of the population of the absorbed and suspended bacterias in the cultivation media is the Bradford's method. It has been used to evaluate the fraction of bacteria adhered to the mineral during the bioleaching process and the suspended fraction. It was observed that a significant fraction of the bacteria is adhered to the mineral surface. This proportion varies with the environmental conditions, mainly pH, the presence of ferric ions and the way to supply the mineral sulphide. It has also been observed that the fraction adhered to the solid shows a progressive loss of its oxidative activity. The results can help demonstrate that the sulphides leaching is due to the combination of the direct bacterial action on the sulphide mineral surface with the indirect leaching by the ferric ion produced by the bacteria into the solution [8].

The bacterial oxidation of sulfide ores can be exploited in the mining industry to leach and extract heavy metals from metal sulfide deposits. Conven-

tional methods for the extraction of precious metals from such complex sulfidic matrices are highly energy consuming and notorious for environmental pollution problems. Precious metals in the form of grains are very finely distributed and encapsulated in the sulfide matrices and direct cyanidation of the refractory sulfide ores usually gives unsatisfactory recovery of such metals. Bio-oxidation of a gold-bearing pyrite concentrate has been considered as an alternative process for the pretreatment of such a refractory ores prior to cyanidation. In this research, mixed cultures of *Thiobacillus ferrooxidans*, *Thiobacillus thiooxidans*, and *Leptospirillum ferrooxidans* strains of DSM culture collection were examined batchwise for their ability to oxidize iron portion of gold-bearing pyrite concentrate from Mouteh mine in Isfahan. Effects of initial levels (i.e. ratio of the bacterial cell numbers in the inoculum) and ore adaptation of mixed cultures of the above named bacterial species on bioleaching; of the sulfidic pyrite has been studied. Time course of changes in iron concentration was determined. Iron dissolution during bioleaching could be used as an index for release of gold, which has been intergrown in the sulfidic matrix. Mixed cultures of these strains of three bacterial species acted efficiently in leaching iron and the variables indicated above had positive influence on the rate of iron dissolution. In order to characterize kinetics of the bio-oxidation in terms of the logistic equation, the data obtained were fitted to this equation. A linear regression was performed on the data in their logarithmic form and logistic model parameters were calculated. The logistic equation was found to be a good fit to all of the data obtained in this study [9].

A proposal for a modified in situ leaching method for extracting gold from oxidized gold ores using a non-cyanide lixiviant is described. A non-cyanide lixiviant is suggested because of the obvious concerns posed by injecting cyanide-bearing solutions into the subsurface. Oxidized gold ores were chosen as a focus because earlier research on the use of sodium thiosulphatic as a lixiviant under anaerobic conditions indicated that the presence of pyrite led to rapid thiosulphatic breakdown. A reconnaissance research program involving ore characterization and hydrometallurgical test work on samples from four Australian ore deposits and preliminary reactive transport modeling studies was carried out. This work showed that lixiviant-oxidant combinations of sodium thiosulphatic and ferric EDTA and iodide and iodine are both capable of extracting high percentages of accessible gold from the selected samples in bottle roll tests under anaerobic conditions. The ore

characterization and reactive transport studies suggested that both physical and chemical methods of permeability enhancement may be required to lift bulk permeability and the availability of gold for dissolution to sufficiently high levels to obtain adequate gold recoveries. Assuming that such methods prove to be both necessary and economically viable, the mining method would no longer be regarded as simple in situ leaching. Therefore, the term «in-place leaching» has been adopted for the proposed gold extraction system [10].

The intensification of the thiosulphatic leaching of silver, gold and bismuth from sulfide concentrates using mechanical activation and mechanochemical pretreatment step was investigated. The physico-chemical changes in a complex sulfide concentrate (Casapalca, Peru) as a consequence of mechanochemical pretreatment had a pronounced influence on the subsequent silver extraction. The optimum results from mechanochemical pretreatment and subsequent leaching of the concentrate with ammonium thiosulphatic were achieved with 99% recovery of Ag after only 3 min of leaching. The leaching of gold from a mechanically activated complex sulfide concentrate (Banska Hodrusa, Slovakia) using ammonium thiosulphatic was studied as follows. Physico-chemical transformations in the concentrate due to mechanical activation have an influence on the rate of extraction and the recovery of gold. It was possible to achieve 99% Au recovery within 45 min for a sample mechanically activated. Mechanical activation proved to be an appropriate pretreatment for this concentrate before extraction of gold into thiosulphatic leaching solution. The selective leaching of bismuth from the lead concentrate (Atacocha, Peru) by using of sodium thiosulphatic and mechanical activation as the pretreatment step was examined as the last example. It is possible to achieve more than 90% recovery of bismuth in leachate even in three minutes for mechanically activated samples [11].

Heap leaching with thiosulphatic is only used in one location for the treatment of a refractory preg-robbing gold ore initially pre-treated with bio-oxidation. The chemistry of thiosulphatic leaching is complex. Further work is required to develop a better control of the system. A mild refractory gold ore containing pyrite and chalcopyrite was used in this study to investigate the use of thiosulphatic as an alternative heap leaching technology. Preliminary bottle rolls tests indicated that similar gold extraction was obtained with cyanide and thiosulphatic. In the column leach test, effects of thiosulphatic, copper and ammonia concentrations, and their ratio on both gold

extraction and reagent consumption, were assessed. The range of reagent concentration were: 0.1 – 1.0M  $(\text{NH}_4)_2\text{S}_2\text{O}_3$ , 0.03 – 0.10M  $\text{CuSO}_4 \cdot 5\text{H}_2\text{O}$ , 1.0 – 6.0M  $\text{NH}_4\text{OH}$ . The solid-liquid ratio was in the range of 0.83:1 to 5.1. Best results showed that 72% of gold was extracted in 50 days with 0.3M  $(\text{NH}_4)_2\text{S}_2\text{O}_3$ , 0.05M  $\text{CuSO}_4 \cdot 5\text{H}_2\text{O}$  and 6M  $\text{NH}_4\text{OH}$  or a combination of 1.0M  $(\text{NH}_4)_2\text{S}_2\text{O}_3$ , 0.03M  $\text{CuSO}_4 \cdot 5\text{H}_2\text{O}$  and 3M  $\text{NH}_4\text{OH}$ . The reagent consumption at solid/liquid ratio of 3.1 was 37 – 48.6 kg/t  $(\text{NH}_4)_2\text{S}_2\text{O}_3$  and 0 – 0.62 kg/t  $\text{CuSO}_4 \cdot 5\text{H}_2\text{O}$ . The results of thiosulphatic leaching were also compared with cyanide leaching [12].

The leaching of gold using alkaline amino acid-hydrogen peroxide solutions at low concentrations has been studied. The application of alkaline amino acid-hydrogen peroxide system may offer an alternative and environmentally benign process for gold leaching, particularly in the context of leaching low grade gold ores in an in-situ or in heap leach processes. In the presence of an oxidant or oxidants, it was found that amino acids can dissolve gold at alkaline condition at low and moderate temperature. Heating the leach solution between 40 and 60 degrees C was found to enhance the gold dissolution significantly in alkaline amino acid-peroxide solutions. It was also found that gold dissolution increases by increasing amino acid concentration, peroxide and pH. Amino acids acts synergistically to dissolve gold. Although glycine showed the highest gold dissolution as a single amino acid compared to histidine and alanine, histidine was found to enhance gold dissolution when used in equimolar amounts with glycine. The presence of  $\text{Cu}^{2+}$  ion enhances gold dissolution in the glycine-peroxide solutions. The process will propose an environmentally benign process for gold treatment in order to replace the use of cyanide in heap or in-situ leaching. In the presence of pyrite, the amount of gold leached was lower due to the peroxide consumption in sulphide oxidation [13].

Biobleaching is one of advanced technologies of processing of gold-consisting ores with such advantages as low-wasteness and ecological purity since gas and dust are not emitted into the atmosphere [14]. The technology of biobleaching is simple in application and highly effective, especially for processing of ores with low content of precious metals. It allows to save materials and energy and in the future can replace such ways of processing of mineral raw materials as roasting, autoclave leaching, metallurgical melting which pollute environment with poisonous gases and toxic chemicals. In practice of biobleaching there are used various microorganisms depending

on aims. Acidophile thionone bacteria from the sort *Acidithiobacillus ferrooxidans* are the most popular. In the USA 20% of production of copper is the share of its receiving from dumps of off-balance ores by means of the above bacteria. In China and Mexico there are skilled installations for bacterial leaching of copper concentrates. The assessment of the similar enterprises shows that at capital expenditure for building of installation about 900 thousand dollars prime cost of 1t of the received product makes less than 50 dollars, time of payback of installation – 18 months. That is, in a year after installation development the profit makes 375 thousand dollars [15].

The Pacific Ore Technology company at the enterprise «Radio Hill» (Australia) operates trial installation of compact bacterial leaching of copper-nickel ore, this technology, according to experts, can be applied to bacterial obduction of persistent gold-sulphide ores. Sulphidic minerals make about 15% of total amount of ore. Ores split up to a class of fineness minus 7,5 mm and are put on the waterproofing basis in stacks of 5 m high, with a lump of 1000 t. Process continues for about a year, so non-ferrous metals are extracted in concentrates for 70-90% [16].

It is known that leaching is transfer to solution (usually water) of one or several components of strong substance by means of water or organic solvent, it is frequent with the participation of gases of oxidizers or reducers [17].

The work purpose – research of regularities and the technological scheme of gold extraction from ores of Bakyrchik deposit, the East Kazakhstan region, by percolation bioleaching.

### Materials and methods

There are several some ways of leaching, in this experiment there was applied a percolation leaching by infiltration (percolation) of liquid reagent of solution through a motionless layer of solid material. The percolation way is imitation of a compact way of leaching. Generally percolation leaching is applied, for example, for processing gold-consisting porous structure with particles of 0.2-1.0 mm in special round sand of porous structure with particles of 0.2-1.0 mm in special round (height of 2-4 m, diameter of 12-14 m) and rectangular (length of 25 m, width of 15 m) tubs capacity on sand of 800 – 900 t; duration of full processing of one sand loading is 4-8 days. Percolation leaching is carried out by consecutive supply of solutions of cyanides alkaline alkaline-agrarian metals of the decreasing concentration from 0.1 – 0.2 to 0.03 – 0.05%.

In the administrative relation the Bakyrchik mining enterprise is located in the Zharminsky Area of East Kazakhstan region at distance of 90 km to the southwest from the regional center of Ust-Kamenogorsk. In close proximity to the enterprise on the southwest there is an Auezov working settlement, in 4 km to the West – the settlement of Shalobai (Figure 1). Transport system of the enterprise and settlements with the regional center and Semipalatinsk which is in 170 km<sup>2</sup> to the northwest.



**Figure 1** – Geographical location of Bakyrchik gold-arsenous deposits

### Results and their discussion

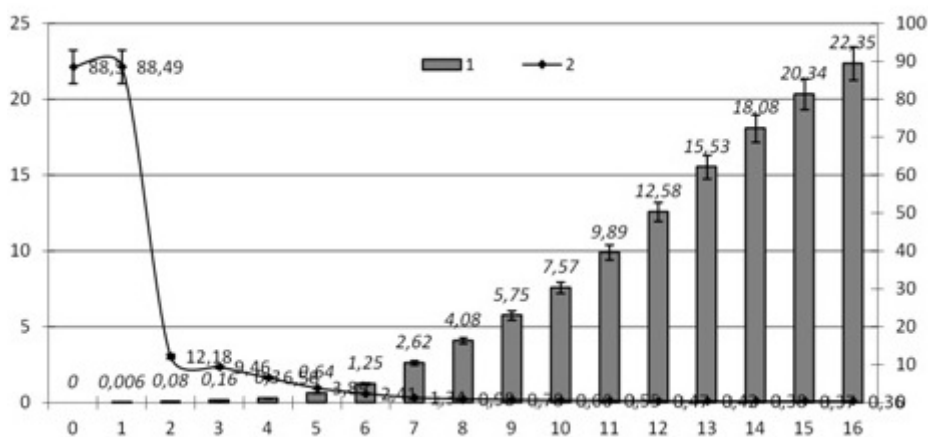
Gold leaching by solutions of cyanide of sodium was carried out in the following mode: at the 1 stage (to 20% of extraction of gold) concentration of cyanide of sodium is 0.6 g/dm<sup>3</sup>, density of an irrigation is 25 dm<sup>3</sup>/t of ore, without pauses in an irrigation; at the 2nd stage (20-40% of extraction of Au) concentration of NaCN is 0.4 g/dm<sup>3</sup>, density of an irrigation is 15 dm<sup>3</sup>/t of ore, a pause in an irrigation - 1 day; at the 3rd stage (extraction of gold 40%) concentration of NaCN is 0,2 g/dm<sup>3</sup>, density of an irrigation is 5 dm<sup>3</sup>/t of ore, a pause in an irrigation of 2 days, Figure 2. Stage-by-stage decrease in density of irrigation allows maintaining concentration of gold in solution at higher level, in this case 2 mg/dm<sup>3</sup>, pH of initial solution of cyanide of sodium in all cases was equal to 10.

After each irrigation the whole solution was removed from a leaching cycle, i.e. the ore irrigation in each cycle was carried out by fresh alkaline solution of cyanide of sodium. The gold-consisting solution removed from a turn was analyzed on the content of gold, residual cyanide, alkaline, the content of iron and non-ferrous metals was periodically defined: cobalt, nickel, zinc, copper.



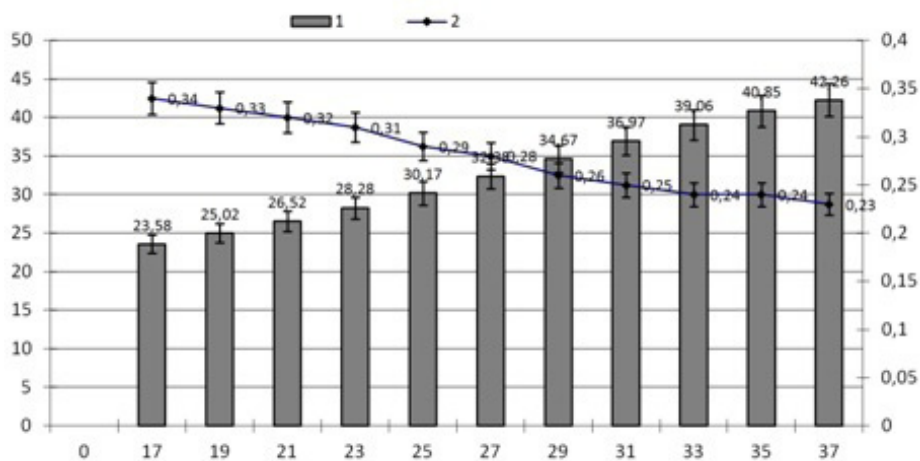
The general duration of leaching made 162 days, the maximum concentration of gold in solution is 5,63 mg/dm<sup>3</sup>. Extent of extraction of gold in solution for the entire period of leaching is 75,17%.

In process of increase in duration of leaching, on each of three stages concentration of gold increased in solution in the beginning, and then evenly decreased.



Note: Concentration of NaCN – 0.6 g/dm<sup>3</sup>, density of irrigation is 25 dm<sup>3</sup>/t of ore, without pauses in an irrigation. Abscissa: leaching duration, days.  
Ordinate: 1 – Au extraction,%; 2 – Expense of NaCN, Au t/kg.

**Figure 2** – Dynamics of gold extraction at percolation ore leaching of the Bakyrchik deposit. I – stage.



Note: Concentration of NaCN – 0.4 g/dm<sup>3</sup>, density of irrigation is 15 dm<sup>3</sup>/t of ore, pause -1 day. Abscissa: leaching duration, days.  
Ordinate: 1 – Au extraction,%; 2 – Expense of NaCN, Au t/kg.

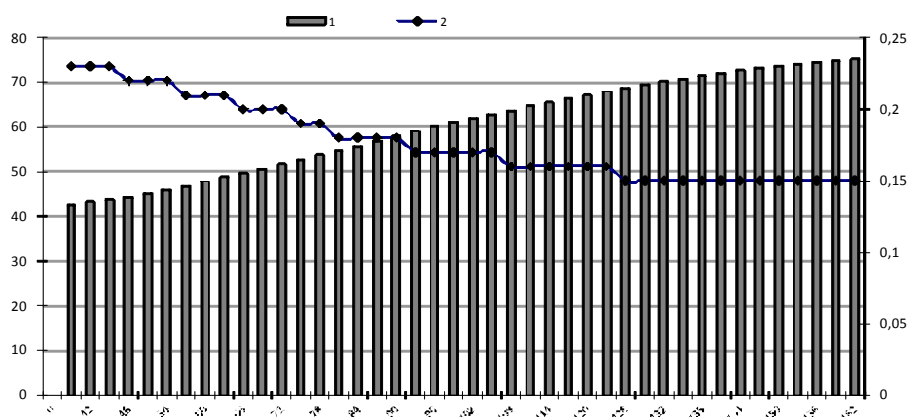
**Figure 3** – Dynamics of gold extraction at percolation ore leaching of the Bakyrchik deposit. II – stage.

Dynamics of gold extraction at percolation ore leaching of the Bakyrchik deposit. II – stage was given on Figure 3.

The average content of gold in solution at 1st stage of leaching (duration of 16 days) is 1.93 mg/dm<sup>3</sup>, at the 2nd stage (22 days) – 3,13 mg/dm<sup>3</sup>, at

the 3rd stage (124 days) – 4.08 mg/dm<sup>3</sup>, extraction of the 1 irrigation 1.40, 1.81, 0.78% respectively. For the entire period of leaching average concentration of gold in solution made 2.50 mg/dm<sup>3</sup>, extraction of the 1 irrigation – 1.09%. The most noticeable decrease of gold concentration was observed at the final stage of leaching. In the range from 65th to 69th irrigation, con-

centration of gold in solution decreased from 2.54 to 1.54 mg/dm<sup>3</sup>. For receiving the solutions (2mg/dm<sup>3</sup>), which were more concentrated on gold at the final stage of leaching it is recommended to periodically carry out an irrigation without removal of solutions. Dynamics of gold extraction at percolation ore leaching of the Bakyrchik deposit. III – stage, Figure 4.



Note: Concentration of NaCN – 0.2 g/dm<sup>3</sup>, density of irrigation is 15 dm<sup>3</sup>/t of ore, pause – 2 days. Abscissa: leaching duration, days.

Ordinate: 1 – Au extraction, %; 2 – Expense of NaCN, Au t/kg.

**Figure 4** – Dynamics of gold extraction at percolation ore leaching of the Bakyrchik deposit. III – stage

It is revealed that cyanation of gold-arsenic concentrates of Bakyrchik deposits after bacterial leaching leads to gold extraction increase, and the best results are received when procedures of thiosulphatic and sulphatic leaching are preceded by *A. ferrooxidans* culture processing.

## References

1. Kaksonen A.H. The role of microorganisms in gold processing and recovery: review // *Hydrometallurgy*. – 2014. – Vol.142. – P.70-83.
2. Zammit C.M. The future of biotechnology for gold exploration and processing // *Minerals Engineering*. – 2012. – Vol. 32. – P.45-53.
3. Murav'ev M.I. Investigation of stages of chemical leaching and biooxidation during the extraction of gold from sulfide concentrates// *Prikladnaia biokhimiia i mikrobiologiia*. – 2015. – Vol. 51. Issue 1. – P.65-72.
4. Brittan M. Estimating process design gold extraction, leach residence time and cyanide consumption for high cyanide-consuming gold ore //

*Minerals and Metallurgical Processing*. – 2015. – Vol. 32. Issue 2. – P. 111-120.

5. Natarajan G. Two-step Bioleaching and Spent Medium Leaching of Gold from Electronic Scrap Material using *Chromobacterium violaceum* // *Integration Of Scientific And Industrial Knowledge On Biohydrometallurgy*. – 2013. – Vol. 825. – P. 270-273.

6. Ahmed, H.A.M. Statistical Optimization of Gold Recovery from Difficult Leachable Sulphide Minerals Using Bacteria// *Materials Testing*. – 2012. – Vol. 54. Issue 5. – P. 351-357.

7. Cabral T. Mechanistic study of the pyrite-solution interface during the oxidative bacterial dissolution of pyrite FeS<sub>2</sub> by using electrochemical techniques // *International Journal of Mineral Processing*. – 2001. – Vol. 62. Issue 1-40. – P. 41-64.

8. Nestor D. Mechanisms of bioleaching of a refractory mineral of gold with *Thiobacillus ferrooxidans* // *International Journal of Mineral Processing*. – 2001. – Vol. 62. Issue 1-4. – P. 187-198.

9. Cheng D.H. Heap Bioleaching of Refractory Arsenic Gold Concentrates // *Asian Journal of Chemistry*. – 2013. – Vol. 25. Issue 5. – P. 2839-2844.

10. Roberts P.A. Ore characterization, hydrometallurgical and reactive transport studies for in-place leaching of oxidized gold deposits // *Minerals and Metallurgical Processing*. – 2010. Vol. 27. Issue 2. – P. 72-80.
11. Ibarra-Galvan V. Role of oxygen and ammonium ions in silver leaching with thiosulphatic-ammonia-cupric ions // *Rare Metals*. – 2014. – Vol. 33. Issue 2. – P. 225-229.
12. Yen W.T. Development in percolation leaching with ammonium thiosulphatic for gold extraction of a mild refractory ore // *EPD Congress*. – 1999. – P. 441-455.
13. Eksteen J.J. The leaching and adsorption of gold using low concentration amino acids and hydrogen peroxide: Effect of catalytic ions, sulphide minerals and amino acid type // *Minerals Engineering*. – 2015. – Vol. 70. – P. 36-42.
14. Kanayev A.T., Kanayeva Z.K., Mukhambetov N.M., Murataliyeva A.A., Kemelbayeva A.K., Mukhamedsadykova A. Geological and mineralogical features of ore of the Bakyrchik gold deposit // *KazNU Herald: ecological series*. – Almaty. – 2013. – No. 3 (39). – P. 59-64.
15. Kanayev A.T., Kanayeva Z.K., Mukhambetov N., Bidaybekov D. Microbic cenosis of gold arsenic Bakyrchik deposits // *Bulletin d'eurotalent-fidjip, Editions du jipto*. – 2014. – No. 5 – P. 40-44.
16. Kanayev A.T., Kanayeva Z.K., Mukhambetov N., Bidaybekov D. Textures and structures of a gold ore exposure- an arsenic deposit Bakyrchik // *Bulletin d'eurotalent-fidjip, Editions du jipto*. – 2014. – No. 5 – P. 45-49.
17. Kanayev A.T., Hamuda R.A., Kanayeva Z.K., Kamalov M.R. Microbiological bases of chemical and technological processes of deep gold extraction from concentrates of Bakyrchik deposit // *KA-ZNPU Messenger. Series ecological*. – 2009. – No. 2. – P.25-32.

UDC 582.26

Kakimova A.<sup>1</sup>, Kozhakhmetov S.<sup>1</sup>, Kazhybayev A.<sup>1</sup>, Mukasheva G.<sup>2</sup>,  
Saduakhassova S.<sup>1</sup>, Khassenbekova Zh.<sup>1</sup>, Urasova M.<sup>1</sup>, Kushugulova A.<sup>1</sup>, Nurgozhin T.<sup>1</sup>

<sup>1</sup>Human Microbiome Laboratory, Center for Life Sciences, Nazarbayev University

<sup>2</sup>Eurasian National University named after L.N. Gumilyev

\*e-mail: akbota.kakimova@gmail.com

## Insights into the role of the gut microbiome in metabolic syndrome

**Abstract:** Metabolic syndrome is a worldwide epidemic which is a combination of various metabolic disorders of organism. Nowadays biodiversity in gut microbiome and its impact on health is being studied very intensively. Gut microbiome has a main role as a reservoir of human genetics. Therefore its study is very topical. There are a lot of factual materials which indicate that gut undeniable influence on the immune system and intestinal barrier function, digestion, metabolism and systemic inflammation. It can be rightfully claimed that microbes «in dialogue» with the whole body by way of sending us signals, which have to be researched and identified in the future.

**Key words:** metabolic syndrome, metagenome, gut, microbiome, bacteria.

### Introduction

Nowadays one of the most prevalent public health problems in the world is metabolic syndrome. Metabolic syndrome is a combination of various metabolic disorders of organism and it is considered as worldwide epidemic. This syndrome contains group of risk interconnected factors that increases the risk for heart disease, atherosclerosis and other health problems, such as diabetes and stroke [1]. There are different definitions of the metabolic syndrome. His-

torically, professor Reaven was the first who used the term «syndrome X» on his investigations on different factors of organism which lead to diseases. Then the term was renamed into metabolic syndrome [2]. Worldwide Health Organization (WHO) proposed the following definition: Metabolic syndrome is multiplex risk factors which constitute of basic components of abdominal obesity, high triglyceride level of blood, less HDL cholesterol, great fasting glucose, arterial pressure, dyslipidemia, high or low density of lipoproteins, and high level of BP.

**Table 1: The new International Diabetes Federation (IDF) definition**

According to the new IDF definition, for a person to be defined as having the metabolic syndrome they must have:

**Central obesity** (defined as waist circumference\* with ethnicity specific values)

**plus any two of the following four factors:**

<b>Raised triglycerides</b>	≥ 150 mg/dL (1.7 mmol/L) or specific treatment for this lipid abnormality
<b>Reduced HDL cholesterol</b>	< 40 mg/dL (1.03 mmol/L) in males < 50 mg/dL (1.29 mmol/L) in females or specific treatment for this lipid abnormality
<b>Raised blood pressure</b>	systolic BP ≥ 130 or diastolic BP ≥ 85 mm Hg or treatment of previously diagnosed hypertension
<b>Raised fasting plasma glucose</b>	(FPG) ≥ 100 mg/dL (5.6 mmol/L), or previously diagnosed type 2 diabetes If above 5.6 mmol/L or 100 mg/dL, OGTT is strongly recommended but is not necessary to define presence of the syndrome.

\* If BMI is >30kg/m<sup>2</sup>, central obesity can be assumed and waist circumference does not need to be measured.

[3].

If three or more of the measurements attend, this means that metabolic syndrome occurs [4]. Having just one of these conditions doesn't mean metabolic syndrome. However, any of these conditions increase risk of serious disease. If more than one of these conditions occurs in combination, risk is even greater [3, 4]. However pathogenic mechanism and criteria for diagnosis of metabolic syndrome have not been fully investigated.

### **Epidemiology of metabolic syndrome**

It was thought that metabolic syndrome is mostly related to middle-aged and old people for a long time; especially it is disseminated between men. But recent studies have shown that young people tend to metabolic syndrome too.

According to the data of Worldwide Health Organization about 30% of populations in the world are overweight, 16.8% of them – women and 14.9% are men. The number of people with obesity increases progressively every 10 years by 10%. Likelihood of arterial hypertension is high for 50% between people with obesity than those with normal weight. According to the Framingham study, systolic blood pressure increases by 4.4 in men and 4.2 among women for every extra 4.5 kg weight. Several conducted investigations elucidate that body weight is direct proportional to total mortality. Obesity increases the risk of 2 type diabetes [5].

Over the past 15 years more than 20 epidemiological studies carried out on the prevalence of the metabolic syndrome. Large-scale meta-analysis has shown that in an adult population by 10% in China and 24% in the US are diagnosed with metabolic syndrome. Most studies have identified common patterns that play an important role in the development of metabolic syndrome, such as age, women's postmenopausal status, behavioral factors – sedentary lifestyles and the prevalence of carbohydrate diet, socioeconomic status. Research recently conducted in Russian on a random sample of the adult population have shown the data of 20.6% of persons aged 30-69 have metabolic syndrome; it occurs 2.4 times more frequently in females than between man; the more the age, the higher the number of patients with metabolic syndrome [6].

According to the data of Kuopio Ischemic Heart Disease Risk Factors Study the risk for coronary heart disease is higher for 2,9-4,2 times and death rate from ischemic heart disease for 2.6-3.0 times in patients with metabolic syndrome. In another prospective study ARIC (Atherosclerosis Risk in Com-

munities) we can notice the results have elucidated that patients with metabolic syndrome can tend to stroke 2 times more than the control group: the risk was 1.9 for men; for women – 1.52 [7].

Metabolic syndrome is a cluster of risk factors associated with prothrombotic, proinflammatory conditions, non-alcoholic fatty liver disease, and dysfunction of the reproductive system. The prevalence of metabolic syndrome depends on gender, age, ethnicity, as well as the use of diagnostic criteria, and varies over a wide range between male populations from 8% in India to 25% in the US, among women from 7% in France to 46% Iran. The study INTERHEART showed that metabolic syndrome related to 26% of adult population in the world.

In South Asia the prevalence of metabolic syndrome is 2.5 times higher than in Europe. Its frequency is very high among obese patients: metabolic syndrome is revealed in 49% of them. According to the opinion of some researchers, the metabolic syndrome is a consequence of urbanization, the increasing prevalence of obesity and sedentary lifestyles [8].

Metabolic syndrome is widespread in Asia. According to statistics, 17 million people die from stroke in China every year. 60% of patients with diabetes in Asia are Chinese citizens. In China If the index of weight is 30 kg/m<sup>3</sup> and higher, it means that people tend to obesity. According to this 64 million people suffer from metabolic syndrome. Children in China also prone to metabolic syndrome and 15% of children tend to obesity [9]. The studies conducted in Taiwan have determined that 9 boys from 100000 and 15 girls from 100000 have a diagnose of diabetes [10].

314 million people with metabolic syndrome are estimated in the world in 2001, as well as 400 million – in 2006. It's predicted that number of patients will increase up to a 500 million in 2025. Epidemiological studies conducted in different countries have shown that of metabolic syndrome occurs on average 10-40% of individuals depending on the population [11]. According to studies high prevalence of this syndrome is marked in Greece, the Netherlands and Finland. For example, in Greece, the figure is 41.8% (63.0% among men, 37% – women) by NCEP criteria and 43.4% according to the criteria IDF. Pilot studies conducted in Russia showed that 20.6% of persons aged 30-69 suffer from metabolic syndrome. According to the Federal State Institution «Endocrinology Research Center» syndrome was diagnosed in 66% of patients with obesity [12].

There are only a few studies on the prevalence and ethnic characteristics of the metabolic syndrome

in Kazakhstan. Shalharova carried out the epidemiological research in South Kazakhstan, and the results corresponded with European results [13].

### The role of the gut microbiome on development of metabolic syndrome

Nowadays biodiversity in gut microbiome and its impact on health is being studied very intensively. Gut microbiome has a main role as a reservoir of human genetics. Therefore its study is very topical. The human gut microbiome contained 1.5 kg of microorganisms, about 1000. The microflora performs a number of very important functions: differentiation of the intestinal epithelium, protection against pathogens and metabolic – involved in the processes of deposit in the liver and adipose tissue formed as a result of fermentation of energy substrates, which makes up 10% of the energy homeostasis. MetaHIT project's purpose is to create the «microbiome» – gene bank of microflora. «Microbiome» contains 3.3 million of coding sequences of nucleotides – it is 150 times larger than the human genome, and has been called 'our other genome».

The development of the metabolic syndrome is associated with systemic inflammation of lower grades. The role of the microflora in the origin of obesity can be explained by two aspects: 1. Additional extraction of energy from the indigestible part of food; 2. the maintenance of systemic inflammatory response due to the increased lipopolysaccharide of bacteria, in other word – endotoxemia. In addition, certain bacteria can inhibit the expression of the protein induced by starvation in the intestinal contents, which exhibits the properties of an inhibitor of lipoprotein lipase.

Active studies the role of gut microbiome on pathogenesis of the metabolic syndrome started with experiments on mice which demonstrate that obesity is associated with an increased content of microbial groups *Firmicutes* and reduced levels of *Bacteroides* [14]. Many studies indicate that people with obesity and 2 type diabetes are characterized by changes in the composition of intestinal microflora, in particular the reduction of species that are actively produce the butyrate – *Roseburia intestinalis* and *Faecalibacterium prausnitzii*. Apparently butyrate has an anti-diabetic effect. Low variability in the composition of microflora is considered as a possible predictor of obesity treatment absence by diet [15].

Behaviors of the microbiota on inflammatory bowel disease, allergic diseases are being studied extensively. Fecal microflora transplantation from healthy

donors is one of the newest and effective methods. This method has proven itself particularly in the treatment of recurrent infection of *Clostridium difficile*. The latest recommendations of the American College of Gastroenterology allow the transplantation of fecal microflora after the third recurrence of *Clostridium difficile* in case of failure of vancomycin [16].

There is a widespread interest in transplantation of microflora in other diseases too. It is believed that in some situations, this arrangement will avoid prescribing. Patients with metabolic syndrome showed increased sensitivity of peripheral tissues to insulin and an increase in species diversity of the microbiota, when fecal transplants from healthy donors [17, 18].

The limitations of the method of transplantation above are explained by insufficiently established procedures for screening donors and insufficient study of the method. There are a lot of factual materials which indicate that gut undeniable influence on the immune system and intestinal barrier function, digestion, metabolism and systemic inflammation. It can be rightfully claimed that microbes «in dialogue» with the whole body, and send us signals, which have to be researched and identified.

### Conclusion

There is a widespread interest in researching metabolic syndrome because it is a worldwide epidemic which is a combination of various metabolic disorders of organism. Interaction between gut microbiome and metabolic syndrome is very topical studies. There are a lot of factual materials which indicate that gut undeniable influence on the immune system and intestinal barrier function, digestion, metabolism and systemic inflammation. It can be rightfully claimed that microbes «in dialogue» with the whole body by way of sending us signals, which have to be researched and identified in the future. Studying Kazakhstani population with metabolic syndrome, researching their gut behavior will help scientists to identify new methods of treating the dangerous diseases such as an obesity, diabetes, atherosclerosis, coronary heart disease and so on.

### References

1. Grundy S.M., Brewer H.B. Jr., Cleeman J.I., Smith S.C. Jr., Lenfant C. Definition of metabolic syndrome: report of the National Heart, Lung, and Blood Institute/American Heart Association conference on scientific issues related to definition. *Arterioscler Thromb Vasc Biol* 2004. – 24: e13-e18.

2. Reaven GM: Banting lecture. Role of insulin resistance in human disease. *Diabetes* 1988. – 37: 1595-1607.
3. Kassi E., Pervanidou P., Kaltsas G., Chrousos G. Metabolic syndrome: definitions and controversies // *BMC Medicine*, 2011. – 9: 48.
4. <http://www.heart.org>
5. Ziramet P., Shaw J., Alberti G. Preventing type 2 diabetes and the dysmetabolic syndrome in the real world: a realistic view // *Diabetic medicine*, 2003. – 20(9): 693-702.
6. Mamedov M, Suslonova N, Lisenkova, Tokareva Z. Metabolic syndrome prevalence in Russia: Preliminary results of a cross-sectional population study. *Diab Vase Dis res*, 2007. – 4(1): 46-7.
7. <https://www2.uef.fi/ru/nutritionepidemiologists/kihd>
8. Grundy S.M., Cleeman J.I., Daniels S.R., Donato K.A., Eckel R.H., Franklin B.A., Gordon D.J., Krauss R.M., Savage P.J., Smith S.C., Spertus J.A., Costa F. Diagnosis and Management of the Metabolic Syndrome. *Circulation*, 2005. – 112: 35–52.
9. Gu D, Reynolds K, Wu X, Jing Chen, Duan X, Reynolds R, Whelton P, He J; InterASIA Collaborative Group. Prevalence of the metabolic syndrome and overweight among adults in China // *Lancet*, 2005. – 365: 1398-405.
10. Jung-Nan Wei, Fung-Chang Sung, Chau-Ching Lin, Ruey-Shiung Lin, Chuan-Chi Chiang, Lee-Ming Chuang. National surveillance for type 2 diabetes mellitus in Taiwanese children // *JAMA*, 2003. – 290: 1345-50.
11. Ervin R.B. Prevalence of Metabolic Syndrome Among Adults 20 Years of Age and Over, by Sex, Age, Race and Ethnicity, and Body Mass Index: United States, 2003–2006 // *National Health Statistics Reports*, 2009.
12. Meigs J.B. Epidemiology of metabolic syndrome // *Am. J Manag Care*, 2002. – 8(11): 283-292.
13. Shalharova Zh.S. *Metabolicheskyi sindrom: epidemiologiya, diagnostika, klinika i lechenie.* – Almaty, 2006.
14. Ley R.E., Bäckhed F., Turnbaugh P., Lozupone C.A., Knight R.D., Gordon J.I. Obesity alters gut microbial ecology // *Proc Natl Acad Sci USA*, 2005. – 102(31): 11070-5.
15. Everard A., Lazarevic V., Derrien M, Girard M., Muccioli G.G., Neyrinck A.M., Possemiers S., Holle AV., Francois P., Willem M. de Vos., Delzenne N., Schrenzel J., Cani P. Responses of gut microbiota and glucose and lipid metabolism to prebiotics in genetic obese and diet-induced leptin-resistant mice // *Diabetes*, 2011. – 60(11): 2775-86.
16. Surawicz C.M., Brandt L.J., Binion D.G., Ananthakrishnan A.N., Curry S.R., Gilligan P.H., McFarland L., Mellow M., Zuckerbraun B. Guidelines for diagnosis, treatment, and prevention of *Clostridium difficile* infections // *Am J Gastroenterol*, 2013. – 108(4): 478-98.
17. Bercik P., Denou E., Collins J., Jackson W., Lu J., Jury J., Deng Y., Blennerhassett P., Macri J., McCoy KD., Verdu EF., Collins SM. The intestinal microbiota affect central levels of brain-derived neurotrophic factor and behavior in mice // *Gastroenterology*, 2011. – 141(2): 599-609
18. Vrieze A., Van Nood E., Holleman F., Salo-järvi J., Kootte R.S., Bartelsman J.F., Dallinga-Thie GM., Ackermans MT., Serlie MJ., Oozer R., Derrien M., Druesne A., Van Hylckama Vlieg JE., Bloks WW., Groen AK., Heilig HG., Zoetendal EG., Stroes ES., de Vos WM., Hoekstra JB., Nieuwdorp M. Transfer of intestinal microbiota from lean donors increases insulin sensitivity in individuals with metabolic syndrome // *Gastroenterology*, 2012. 143(4): 913-6.

UDC 633.2.03(574.51)

Nazarbekova S.T.\* , Kuatbayev A.T., Childibayeva A.Zh.,  
Kurmanbayeva M.S., Mendygaliyev B.

Department of Biodiversity and Bioresources,  
Al-Farabi Kazakh National University, Almaty, Kazakhstan

\*e-mail: saltanat.nazarbekova@kaznu.kz

## Features of the vegetation cover of the natural fodder lands of southern Kazakhstan

**Abstract:** Results of the floristic analysis of a vegetation cover of southern pasturable lands (Zhambyl area, Chu area, Abay rural district) are being discussed. Key land soils and condition of vegetation, the floristic structure of fodder lands are defined. The distribution of species on major taxonomic groups considered. It was the analysis of familial range of flora. It was performed for the key area of pastures area which is located in the foothill-desert-steppe zone.

**Key words:** Republic of Kazakhstan, vegetation cover, key land, phytocenosis, soil, fodder lands

### Introduction

According to the Institution of world resources, pasturable lands in the Republic of Kazakhstan cover 188 million hectares or 70 percent of all area. General part of the degraded lands makes more than 48 million hectares or 26 percent from total area [1]. The extensive pasturable economy which has the insufficient level of equipment is the main reason for degradation of lands and, as a rule, is unstable. Dry years or long cold winters have a bad influence on a condition of cattle, in this regard development of stable fodder providing is necessary [2].

Change of forms of ownership in agriculture led to uneven and irregular use of pastures. The repasture and a contamination of pastures in territories near settlements led to degradation of soils and vegetation, and it, in turn, led to decrease in stocks of forages that as a result leads to decrease in a standard of living of the population. In this regard detailed researches of a current state of pastures, identification of their anthropogenous degradation level as a basis for planning of actions for restoration and rational use are relevant [3].

The purpose of our researches in the last decade consists in periodic control of a condition of vegetation and soils of a key land on the southern pasturable lands of Kazakhstan, and also studying of floristic structure and dynamics of productivity of fodder grounds.

### Materials and methods

In 2011 on pasturable lands of the area of our researches key land No. 19 was formed and, for more detailed characteristic of the prevailing vegetation associations and soils, PSEP No. 55, 56, 57 were formed as well. The land KU-19 is in 7 km to the northwest from the settlement of Abay near the bridge through Kuragata river on its left coast. The area of a key land made 1196 and, the scale of researches – 1:10 000; PSEP square – on 1 hectare everyone, the area of researches – 1:2000. Works are carried out with use of photoplans of scale 1:10 000.

During field researches on a key land 16 soil and botanical contours, are allocated for No. 55 PSEP – 8 contours, for No. 56 PSEP – 4 contours, for No. 57 PSEP – 6 contours, 6 soil cuts are put and described. From 5 main cuts (including from 3 cuts on PSEP) on the genetic horizons 19 tests on chemical and mechanical analyses are selected.

The land is located on the second above floodplain terrace of Shu river interfluvial area of Shu-Kuragata. Relief is accumulative and erosive, barely billowy, with the low uvala and hilly rises complicated by eolian processing. Valley of the river Kuragata has width up to 150 m and depth of erosive cutting of 2-3 m. The river flows from the South to the north along the western border of the land. The land was actively used in the past as the irrigated arable land under landings of mainly melon cultures. Along northern and



eastern borders there is a channel, along it, and also along the river there are numerous ditches. Now they are dry and also not used. In work of definition of the general distribution of species of flora we used literary data [4-5]. At allocation of vital forms of plants we used the most known biomorphological classifications of K. Raunkiya [6] and I.G. Serebryakova [7].

### Results and their discussion

The territory of the key land located on pasturable lands of the Abay rural district belongs to a foothill and desert and steppe zone, a subband of gray soils of the light northern. Mechanical structure of soils – sandy, sabulous, barely loamy and middling loamy. The main type of a relief – barely billowy plain, absolute height is 439-446 m. The vegetation cover is presented by the semidesertic

(desert and steppe) vegetation which is characterized by a wide circulation of desert semi-suffrutescent and low-shrubby elements of flora, and steppe – firm-bunch grasses. The floristic list on materials of field inspection makes 92 species relating to 25 families and 74 classes.

From vital forms perennials prevail: grassy perennials (47 species), among them long-term vegetative (saltmarsh-grass, a feather grass, *Aeluropus*) and short-term vegetative (ephemeroids- onions, a sedge, a desert-candle). 4 species), of bushes is *Calligonum leafless*, *Hulthemia persica*, multiramose tamarisk and *Lycium ruthenicum*; 2 species of semi-bushes – *Kohia prostrata* and *Ceratoides Krascheninnikovia*; low shrubs and semi-low shrubs, 1 type (*Convolvulus fruticosus* and *Artemisia terrae-albae*), a tree – 1 (*Elaeagnus oxycarpa*). 33 species are annual plants, biennials – 3 species (Table 1).

**Table 1** – Quantity of species in the main families

	Name of a family	Quantity of the registered types, in total	including							
			grassy perennials	Annual plants	biennials	bushes	Low bushes	Semi-bushes	Semi low bushes	tree
	species in total	92	47	33	3	4	1	2	1	1
	including the main families:									
1	<i>Gramineae</i> Juss.	21	14	7						
2	<i>Chenopodiaceae</i> Vent.	12	1	9				2		
3	<i>Compositae</i> Giseke.	11	7	3					1	
4	<i>Cruciferae</i> Juss.	8	2	6						
5	<i>Leguminosae</i> Juss.	8	8							
6	<i>Polygonaceae</i> Lindl.	4	1	2		1				
7	<i>Liliaceae</i> Juss.	3	3							
8	<i>Umbelliferae</i> Juss.	3	2	1						
9	<i>Labiatae</i> Juss.	3	2	1						

15 species in vegetation community are dominants. By quantity of species in families prevail *Gramineae*- 21 species (22.8%), then 12 species from the *Chenopodiaceae* family (13.0%), in the family *Compositae* 11 species (11.9%), *Cruciferae* and *Leguminosae* families – 8 species each, *Polygonaceae*

family – 4 species, *Liliaceae*, *Umbelliferae* and *Labiatae* families-3 species each. Other families have 1-2 species. The ecological analysis of flora of the research land shows a wide expansion of xerophytes, xerohalophytes and mesohalophytes on the barely billowy plain, mesophytes along the Kuragata river.



**Figure 1** – Ephemeral camel thorn's modification

Everywhere in the territory of the key there are landcommunities of group of the torgayot (383 hectares) and the camel thorn pastures (352 hectares) (Figure 1).

The group of the torgayot pastures includes torgayot-ephemeral, saltwort-ephemeral-camel thorn communities. Camel thorn pastures are presented by camel thorn – ephemeral, camel thorn-azhrek-ephemeral communities with ephemeral-camel thorn, ephemeral and ephemeral-*Poterium* modifications. Soils – pit-and-mount fixed sand, gray soils are usual light northern, mead gray soil light northern slightly alkalized, slightly solonchak and middling solonchak and slightly loamy.

Dominants of communities – *Climacoptera oppositifolius* (torgayot) and camel thorn. In spring in herbage a large number ephemeral plants develop: meadow grass bulbous, cheat grass, desert alison, *Carex pachystylis*, *Eremopyrum triticeum*. In the summer ephemeral plants become dry and to their change comes numerous steppe xerophyte grasses: *Serratula dissecta*, *Heliotropium olgae* Bunge, *Lappula microcarpa*, *Allium caesium*, *Cousinia triflora* Schrenk. In autumn saltworts prevail: *Ceratocarpus arenarius* L., *Ceratocarpus utriculosus* Bluket, *Climacoptera lanatay*, *Camphorosma monspeliaca* L., and others. Aspect of herbage on the torgayot communities from bright green (spring) to lilac-brown with red impregnations (autumn). Aspect of the camel thorn communities from bright green to dark green with brown impregnations of the died-off ephemeral plants.

*Artemisia terrae-albae*-ephemeral communities are widespread in central and northern parts of a key land in contours 10.16. The area occupied by them is 141 hectares. They are dated for the increased plain elements and formed on mead gray-soil light northern slightly alkalized sandy soils. They form complexes with camel thorn ephemeral, ephemeral

camel thorn communities. It is singly among edificatorial vegetation to meet *Climacoptera lanata*, *Sal-sola paulsenii*, *Ceratoides Krascheninnikovia*, *Stipa lessingiana*. The described communities belong to lands of spring summer autumnal use for a pasture of sheep, goats and horses.

In the southern part of the land in a contour 2 there is a calligonum-ephemeral-*Poterium* modification. They are met in a complex with camel thorn ephemeral communities.

Dominant – *Calligonum leafless*. Subdominants – ephemeral plants: *Taeniatherum crinitum*, *Alison desert*. Other: *Agropyrum fragile*, *Goebelia pachycarpa*, *Alhagi*, *Eryngium planum*.

### Conclusion

Thus, in recent years in some contours there were considerable changes: so earlier in a contour six *Aeluropus* communities were widespread in a complex with *Climacoptera crassa* and absinthial ephemeral, now in a contour prevail saltwort-ephemeral-camel thorn communities in a complex with absinthial ephemeral camel thorn. In contours 8 and 15 instead of the *Artemisia terrae-albae* ephemeral communities modification of ephemeral-camel thorn and ephemeral-camel thorn-*Aeluropus* extended. Many fodder plants such as *Aeluropus*, *Artemisia terrae-albae* were forced out by annual saltworts and ephemeral plants which points to degradation of pastures. It is obvious that this consequence of a pasture of considerable quantity of cattle in the territory of the key land. Getting pastured from early spring to late autumn, and also moving to Kuragata river on a watering place they constantly bite and wear out plants and don't allow long-term herbs to grow. Change of climatic conditions has also great influence on efficiency of communities, in this regard the vegetation cover towards a xerophytisation significantly changed. But together with that, at the proper organization of pasture rotation system it is possible to restore vegetation and growth of perennial fodder plants.

### References

1. [http://tengrinews.kz/kazakhstan\\_news/okolo-50-millionov-gektarov-pastbisch-v-kazahstane-nahodyatsya-v-upadke-220604/](http://tengrinews.kz/kazakhstan_news/okolo-50-millionov-gektarov-pastbisch-v-kazahstane-nahodyatsya-v-upadke-220604/)
2. Muratova N.R., Bekmuhanedov N.E., Kauzov A.M., Malahov D., Islamgulova A.F., Dyagtereva O.Yu. Mapping of fodder grounds of the South

of Kazakhstan according to modern data of space shooting // Rural, forest and water management., 2013 – 312 p.

3. Rachkovskaya E.I., Volkova E.A., Hramciov V.N. Botanical geography of Kazakhstan and Central Asia (within a desert region). St. Petersburg, 2003. – 425 p.

4. Abdulina S.A. List of vascular plants of Kazakhstan. Almaty, 1999. – 187 p.

5. Flora Kazahstana. – Alma-Ata, AS KazSSR, 1956-1966. – Vol. 1-9.

6. Raunkiaer Ch. Om de danske Arter af Stellaria media-Gruppen. Botaniske Studier, J.H. Schultz Forlag, København, 1934, 1. hæfte (ed. C. Raunkiaer). – pp. 3-30

7. Serebryakov I.G. Ecological morphology of plants. Vital angiospermous and coniferous forms. – M.: 1962. – 378 p.

UDC 577.21

Niyazova R.<sup>1\*</sup>, Atambayeva Sh.<sup>1</sup>, Akimniyazova A.<sup>1</sup>, Pinsky I.<sup>1</sup>,  
Alybaeva A.<sup>1</sup>, Faye B.<sup>2</sup>, Ivashchenko A.<sup>1</sup>

<sup>1</sup>al-Farabi Kazakh National University, Almaty, Kazakhstan

<sup>2</sup>CIRAD, Montpellier, France

\*e-mail: raiguln@mail.ru

## Features of mir-466-3p binding sites in mRNA genes with different functions

**Abstract:** The importance of miRNA in cellular regulation is gaining momentum. We searched miRNA binding sites using the MirTarget program. We identified several miRNAs that have greater than 300 target genes in humans, with multiple binding sites per gene. We observed that miR-466-3p 1,463 binding sites with high affinity (with  $\Delta G/\Delta G_m$  values greater than or equal to 90%).

**Key words:** binding, sites, genes, functions.

### Introduction

Numerous microRNAs (miRNAs) that regulate the expression of several hundred genes by binding to their mRNAs have been identified [1-4]. These miRNAs play key roles in the regulation of many biological processes and changes in their concentrations are observed in various pathologies in humans and other animals [5-7]. Changes in miRNA concentrations can be a cause or a consequence of a disease.

### Materials and methods

The human gene mRNAs were taken from the GenBank (<http://www.ncbi.nlm.nih.gov>) using Lextractor002 script (<http://sites.google.com/site/malaheneee/software>). Human miR-466-3p was taken from the miRBase site (<http://mirbase.org>).

The target genes for the tested miRNA were revealed using the MirTarget program, which was developed in our laboratory. This program defines the following features of binding: a) the beginning of an miRNA binding with mRNAs; b) the localization of miRNA binding sites in the 5'-untranslated regions (5'UTRs), coding domain sequences (CDSs) and 3'-untranslated regions (3'UTRs) of the mRNAs; c) the free energy of hybridization ( $\Delta G$ , kJ/mole); and d) the schemes of nucleotide interactions between the miRNAs and the mRNAs. The ratio  $\Delta G/\Delta G_m$  (%) was counted for each site, where  $\Delta G_m$  equaled the free energy of a miRNA binding with its perfect complementary nucleotide sequence. The miRNA

binding sites located on the mRNAs had  $\Delta G/\Delta G_m$  ratios of 90% and more. We also note the position of the binding sites on the mRNA, beginning from the first nucleotide of the mRNA's 5'UTR. The MirTarget program computes the interactions between the nucleotides of miRNAs and those of target gene mRNAs. It found bonds between adenine (A) and uracil (U), guanine (G) and cytosine (C), and G and U, as well as between A and C via a hydrogen bond [8]. The distance between A and C was equal to the G-C, A-U, and G-U distances [9]. The numbers of hydrogen bonds in the G-C, A-U, G-U and A-C interactions were found to be 3, 2, 1 and 1, respectively. The free binding energies of these nucleotide pairs were accepted as the same values (3:2:1:1).

### Results and their discussion

One miRNA that has multiple binding sites is miR-466-3p, which has more than 300 target genes. Their mRNAs include a total of 1,463 binding sites, including from 1 to 18 sites in *RAPGEFL1* and *SYT2*, 25 in *PRKX*, and 38 sites in *DONSON* mRNA. The miRNA binding sites have  $\Delta G/\Delta G_m$  ratios of 90% or greater. This indicates a high degree of interaction between miRNAs and mRNAs. Multiple binding sites increase the probability that miRNAs interact with mRNAs, and as a consequence, the translation of such mRNAs is reduced.

The target genes of miR-466-3p serve various functions. Many are transcription factors and kinases, some are involved in the cell cycle, apoptosis, and other processes (Table «a»).

**Table «a»** – The characteristics of miR-466-3p binding in the 5'UTR of mRNA target genes

Gene	Start positions of binding sites, nt	$\Delta G$ , kJ/mole	Gene	Start positions of binding sites, nt	$\Delta G$ , kJ/mole
<i>BHLHE41</i>	89 (1)*	-106.1	<i>RUNDC3B</i>	172-160 (10)	-106.1÷-106.2
<i>CASQ2</i>	31 (1)	-106.1	<i>SPOP</i>	79 (1)	-106.2
<i>CD97</i>	140-138 (11)	-106.2÷108.3	<i>STAT6</i>	102-100 (5)	-106.2÷108.3
<i>CELF4</i>	299 (1)	-108.3	<i>TSHZ2</i>	22 (1)	-106.2
<i>CHRNA2</i>	9-23 (3)	-106.2÷108.3	<i>VWA3A</i>	17-23 (2)	-108.3÷110.4
<i>GRIA2</i>	52-68 (3)	-106.2	<i>XPO1</i>	499-507 (5)	-106.2
<i>KIAA0319</i>	265-291 (14)	-106.2	<i>ZNF331</i>	409-415 (4)	-106.2
<i>NOS1AP</i>	2099 (1)	-106.2			

Note. \*In brackets are number of binding sites

One of the objectives of this work was to identify the target genes of miR-466-3p, which may contribute to the development of several diseases. The mRNA of *ADAT2*, *ADCYAP1R1*, *BHLHE40*, *CDK6*, *FASLG*, *FGFR3*, *FLT1*, *MACC1*, *MAPKAPK2*, *MECOM*, *SPN*, *STAT6*, and *UGT8* genes, which are involved in the development of lung and breast cancer, are associated with miR-466-3p, indicating an increased probability that miR-466-3p influences these types of cancer. *ADRBK2*, *BHLHE40*, *CD36*, *EGR3*, *NDUFS2*, *NFAT5*, *NOS1*, *PLA2G7*, *SIPR2*, and *STAT6* genes are responsible for diseases of the cardiovascular system, and their mRNAs also interact with miR-466-3p. *CDK6* and *MECOM* genes are involved in cell cycle regulation and apoptosis, and their mRNA sequences contain targets for miR-466-3p. We identified the *BHLHE40* gene, which exhibits changes in expression in lung cancer, breast cancer, cardiovascular diseases, and circadian rhythm disorders. *BHLHE40* is a transcription factor that is expressed in various tissue types. It encodes a protein involved in the control of circadian rhythms, cell differentiation, proliferation, cell cycle, apoptosis, and the development of various diseases. Therefore, a change in the expression of this gene after binding with miR-466-3p can cause many diseases.

In addition to mir-466, we identified several miRNAs that have greater than 300 target genes in humans, with multiple binding sites per gene. We observed that miR-3960 has 2,563 mRNA binding sites with high affinity for 375 human genes. For example, miR-3960 has 565 binding sites in 5' UTRs and 515 sites in mRNA coding sequences (CDS). The mRNA regions that contain several miR-3960 binding sites have starting sites located through one, two, or three

nucleotides. The nucleotide sequences of the binding sites located in CDSs encode polyalanine or polyproline. We determined that most of the target genes for the miRNAs examined encode transcription factors. Specifically, miR-3960, miR-3620-5p, and miR-8072 bind with genes involved in cell cycle regulation and apoptosis. Hsa-miR-1322 has more than 2,000 binding sites in the mRNAs of 1,058 genes. This includes 1,889 binding sites in CDSs, 215 binding sites in 5' UTRs, and 160 binding sites in 3' UTRs. Between 2 and 28 binding sites were arranged sequentially with start positions overlapping with three nucleotides of the adjacent binding site. The nucleotide sequences of these sites in CDSs encode oligopeptides with the same and/or different amino acid sequences. We found that 33% of the target genes encoded transcription factors. The miR-1322 binding sites has arranged binding sites were arranged in the CDSs of the orthologous genes *MAMLD1*, *MAML2*, and *MAML3* genes. These sites encode a polyglutamine oligopeptide ranging from six 6 to 47 amino acids in length [1, 10].

We identified 266 target human genes for miR-574-5p and six target genes for miR-574-3p. The miR-574-5p binding sites were mainly located mainly in the 3' UTRs, and their number is equal to 1,429 in total. The miR-574-5p binding sites were located in the 3' UTRs of the mRNA sequences of 244 genes mRNAs, in the 5' UTRs of 20 genes mRNAs and in the CDSs of two genes mRNAs. The miR-574-5p binding sites in the CDS of *FGFRL1* and *REM2* genes mRNAs encode the oligopeptides HTHHTHS and DTDMDTDT in the relevant proteins. The beginning start sites of multiple miR-574-5p binding sites arranged located through two nucleotides and the number of binding sites in one region

ranged from 1 to 37. The target genes of miR-574-5p have been implicated in the development of breast and, lung cancer and other diseases. A significant substantial part portion of the target genes of miR-574-5p are transcription factors and kinases, which are involved in apoptosis and the cell cycle. The synthesis of miR-574-5p and miR-574-3p depends on the expression of the master's gene *FAM114A1* expression, which is the target for of 15 miRNAs. Changes in the expression of miR-574-5p and miR-574-3p are correlated with changes in the expression of their target genes, at which are associated with the development of many pathologies, including cardiovascular diseases and cancer [11].

Table «a» shows the characteristics of miR-466-3p binding sites in the 5' UTRs of 15 target genes mRNAs with the value of  $\Delta G/\Delta G_m$  values that were equal or greater than 90%. The number of miR-466-3p binding sites with mRNAs offer these genes varied from one 1 to 14 (Table «b», «c»), indicating the variation in the probability of an interaction between miR-466-3p interaction and target mRNAs, since the greater the length of the section of longer binding sites, is associated with a higher the probability of interaction. It is possible that the mRNA of the *KIAA0319* gene may contacts with two RISC complexes containing miR-466-3p, since the length of the site from nucleotides 265 to 314 nt, which contains multiple binding sites, is 50 nt.

**Table «b»** – The characteristics of miR-466-3p binding in the 3'UTR of mRNA target genes having 1-4 sites

Gene	Start positions of binding sites, nt	$\Delta G$ , kJ/mole	Gene	Start positions of binding sites, nt	$\Delta G$ , kJ/mole
<i>ADAMTS4</i>	3382 (1)	-110.4	<i>LSAMP</i>	2285 (1)	-106.2
<i>ADRB3</i>	2451 (1)	-110.4	<i>MAPKAPK2</i>	2587-2589 (2)	-106.2÷-108.3
<i>AKIRIN1</i>	1057 (1)	-106.2	<i>MECOM</i>	5099 (1)	-110.4
<i>AQP3</i>	1254-1477 (2)	-106.2	<i>MED24</i>	3606-3612 (4)	-106.2÷-108.3
<i>ARHGAP26</i>	8270 (1)	-106.2	<i>METTL16</i>	3581-3585 (4)	-106.2÷-108.3
<i>ARNT</i>	3104 (1)	-106.2	<i>MVB12B</i>	3440-3438 (2)	-106.2÷-108.3
<i>ATAD1</i>	1830 (1)	-106.2	<i>MYO16</i>	6426 (1)	-106.2
<i>ATG10</i>	1928 (1)	-108.3	<i>NACC2</i>	2484-5875 (2)	-106.1÷-108.3
<i>ATP6V0D1</i>	1201-1211 (3)	-106.1÷110.4	<i>NAVI</i>	9412-9418 (4)	-106.2
<i>ATXN7L3B</i>	3359 (1)	-108.3	<i>NCOA3</i>	5966-5974 (2)	-106.2÷-108.3
<i>BAHCC1</i>	8118 (1)	-108.3	<i>NET1</i>	2642 (1)	-106.2
<i>BHLHE40</i>	1687-1693 (4)	-106.2÷-108.3	<i>NFAT5</i>	8540-8548 (3)	-106.2÷-108.3
<i>BNC2</i>	3528-3534 (3)	-106.2	<i>NPAP1</i>	5206 (1)	-106.2
<i>BSN</i>	15555 (1)	-106.1	<i>NPTXR</i>	5706-5712 (3)	-106.2÷-108.3
<i>C16orf52</i>	1410-1416 (2)	-108.3÷-110.4	<i>NRID2</i>	3337 (1)	-110.4
<i>C19orf59</i>	816 (1)	-106.1	<i>OCLN</i>	3570-3572 (2)	-106.2÷-108.3
<i>C3orf72</i>	2537-2543 (2)	-108.3	<i>PARD3B</i>	4736 (1)	-110.4
<i>C9orf47</i>	1531 (1)	-106.2	<i>PDE7A</i>	2666 (1)	-106.2
<i>CACNA1B</i>	8725-8731 (4)	-106.2÷-108.3	<i>PHKA1</i>	5211-5213 (4)	-106.2÷-108.3
<i>CADM3</i>	2634-2646 (2)	-106.2	<i>PIK3R1</i>	6519-6523 (4)	-106.2÷-108.3
<i>CD19</i>	1861-1863 (2)	-106.2÷-108.3	<i>PLAG1</i>	4546 (1)	-106.2
<i>CD3EAP</i>	3086-3092 (4)	-106.2	<i>PLCXDI</i>	2548 (1)	-108.3
<i>CEP135</i>	5219-5221 (2)	-106.2÷-108.3	<i>PPARGCIA</i>	2806-2822 (2)	-106.2
<i>CEP85L</i>	3355 (1)	-106.2	<i>PPARGC1B</i>	9983 (1)	-106.2
<i>CISD2</i>	1146-1144 (4)	-106.2÷-108.3	<i>PPIC</i>	781-787 (4)	-106.2
<i>CLEC4D</i>	1001 (1)	-108.3	<i>PRR5L</i>	3504 (1)	-106.2
<i>CLN8</i>	2553-2555 (2)	-106.2	<i>PRSS23</i>	1454-1458 (3)	-106.2
<i>CLRN1</i>	1303-1309 (4)	-106.2÷-108.3	<i>PSD3</i>	4157-4161 (2)	-106.2÷-110.4

Continuation of Table «b»

Gene	Start positions of binding sites, nt	$\Delta G$ , kJ/mole	Gene	Start positions of binding sites, nt	$\Delta G$ , kJ/mole
<i>DDB1</i>	3990-3998 (3)	-106.2÷-108.3	<i>PTCH1</i>	6512-6520 (3)	-106.1
<i>DGKG</i>	3890 -3908 (4)	-106.1÷-106.2	<i>RNF121</i>	2208-2214 (3)	-106.2
<i>DOK6</i>	1761 (1)	-110.4	<i>RUNX1</i>	5455-5459 (2)	-106.2÷-110.4
<i>DPYSL5</i>	4857 (1)	-106.1	<i>SIPR2</i>	3189 (1)	-110.4
<i>DTNA</i>	5953 (1)	-106.2	<i>SBKI</i>	4530 (1)	-110.4
<i>DYNC1L1I</i>	1796 (2)	-106.2	<i>SEL1L3</i>	4370-4374 (3)	-106.2÷-108.3
<i>EGR3</i>	2026 (1)	-108.3	<i>SGPL1</i>	3972-3974 (2)	-106.2÷-108.3
<i>EPG5</i>	8002 (1)	-106.2	<i>SIK1</i>	2855-2857 (2)	-106.2
<i>EPHB3</i>	4065 (1)	-106.2	<i>SLC13A2</i>	2189 (1)	-106.2
<i>F11R</i>	4268 (1)	-106.2	<i>SLC16A9</i>	2962 (1)	-106.2
<i>FAM105B</i>	5211 (1)	-106.2	<i>SLCIA4</i>	4073 (1)	-108.3
<i>FAM178A</i>	4992-4996 (3)	-106.2÷-108.3	<i>SLC25A22</i>	2213 (1)	-106.2
<i>FAM46C</i>	5184 (1)	-106.1	<i>SLC35E3</i>	1905 (1)	-106.2
<i>FBXO9</i>	1718-1720 (2)	-106.2÷-112.5	<i>SLC6A6</i>	2306-2314 (2)	-106.2÷-110.4
<i>FGFR3</i>	2809 (1)	-110.4	<i>SLC7A11</i>	3438-3446 (3)	-106.2÷-108.3
<i>FHOD1</i>	3751-3759 (2)	-106.2	<i>SOGA3</i>	8790 (1)	-106.2
<i>FLVCR2</i>	3355 (1)	-106.2	<i>SPN</i>	4373-4387 (2)	-106.2÷-108.3
<i>FOXI2</i>	2790 (1)	-106.1	<i>SPOCK2</i>	1917 (1)	-108.3
<i>FRMD3</i>	3217	-108.3	<i>STARD8</i>	4681 (1)	-110.4
<i>FXYD6</i>	963-1138 (4)	-106.2÷-108.3	<i>STAT5B</i>	2717-2721 (3)	-106.2
<i>GADL1</i>	3346 (1)	-106.2	<i>STRBP</i>	6071-6073 (2)	-106.2
<i>GOLGA7B</i>	5601 (1)	-106.2	<i>STX1B</i>	1032-1180 (4)	-106.2÷-108.3
<i>GPX3</i>	1108 (1)	-106.2	<i>TFCP2</i>	3457-3610 (3)	-106.2
<i>GRID1</i>	5455 (1)	-106.2	<i>TM9SF3</i>	4448 (1)	-106.2
<i>GRIK4</i>	4357 (1)	-106.1	<i>TMC7</i>	4230 (1)	-106.2
<i>GSK3B</i>	4673 (1)	-106.2	<i>TMOD2</i>	8207 (1)	-108.3
<i>HIC2</i>	3104-3122 (2)	-106.2÷-108.3	<i>UGT8</i>	2500-2516 (3)	-106.2÷-108.3
<i>HIF1AN</i>	2037-2041 (2)	-108.3	<i>UNC80</i>	11147 (1)	-110.4
<i>HLF</i>	5348-1554 (3)	-106.2÷-110.4	<i>USH1G</i>	2580-2745 (3)	-106.2
<i>ICAM1</i>	2988 (1)	-106.2	<i>VPS13D</i>	14819-14821 (2)	-106.2
<i>IGFBP4</i>	1230-1234 (2)	-106.1	<i>WDR35</i>	6259 (1)	-106.2
<i>IMPG2</i>	5471 (1)	-114.6	<i>WDR37</i>	4026-4030 (3)	-106.2
<i>IRS1</i>	7318-7320 (2)	-106.2÷-108.3	<i>WDR5B</i>	2049 (1)	-106.2
<i>ITGAM</i>	3749 (1)	-106.1	<i>WDR72</i>	5941	-106.2
<i>KCTD11</i>	2640-2644 (3)	-106.2	<i>WSCD2</i>	4274-4276 (4)	-106.2÷-108.3
<i>KCTD16</i>	3932 (1)	-108.3	<i>ZBTB42</i>	3075-3077 (3)	-106.2÷-108.3
<i>KIAA0408</i>	5096 (1)	-106.2	<i>ZDHHC22</i>	1832-1836 (3)	-106.2
<i>KIAA1804</i>	5327 (1)	-108.3	<i>ZEB2</i>	6533 (1)	-106.2
<i>KIAA2022</i>	5693 (1)	-106.2	<i>ZNF33A</i>	3169 (1)	-108.3
<i>KIF13A</i>	6965 (1)	-106.2	<i>ZNF33B</i>	3103 (1)	-106.2
<i>KIF3C</i>	3122 (1)	-106.1	<i>ZNF346</i>	2186-2202 (2)	-108.3
<i>KLHL3</i>	2677-2679 (2)	-106.2	<i>ZNF428</i>	1214-1224 (2)	-106.2÷-108.3

Continuation of Table «b»

Gene	Start positions of binding sites, nt	$\Delta G$ , kJ/mole	Gene	Start positions of binding sites, nt	$\Delta G$ , kJ/mole
<i>KLHL42</i>	3780 (1)	-108.3	<i>ZNF483</i>	3636-3638 (3)	-106.2÷-108.3
<i>LFNG</i>	1270 (1)	-108.3	<i>ZNF562</i>	3963-3971 (3)	-106.2÷-110.4
<i>LILRB2</i>	2858-2864 (4)	-106.2÷-108.3	<i>ZNF618</i>	2835 (1)	-106.2
<i>LONRF1</i>	2685 (1)	-106.1			

**Table «c»** – The characteristics of miR-466-3p binding in the 3'UTR of mRNA target genes having five and more binding sites

Gene	Start positions of binding sites, nt	$\Delta G/\Delta G_m$ , kJ/mole	Gene	Start positions of binding sites, nt	$\Delta G/\Delta G_m$ , kJ/mole
<i>ABLIM1</i>	4472-4498 (14)	-106.2	<i>MLLT6</i>	4051-4075 (6)	-106.2÷-110.4
<i>ADAT2</i>	1950-1964 (8)	-106.2	<i>MMS22L</i>	5738-5754 (9)	-106.2
<i>ADCYAP1R1</i>	3841-3853 (7)	-106.2÷-108.3	<i>MYADM</i>	1982-1992 (6)	-106.2
<i>ADRBK2</i>	6676- 6696 (11)	-106.2	<i>MYSM1</i>	3512-3524 (7)	-106.2
<i>AFF1</i>	6829-6837 (5)	-106.2	<i>NDRG4</i>	3108-3116 (5)	-106.2÷-108.3
<i>AKAP11</i>	6559-6579 (11)	-106.2	<i>NDUFS2</i>	1917- 1925 (5)	-106.2÷-108.3
<i>ANKLE1</i>	2219-2255 (12)	-106.2	<i>NKTR</i>	5828-5838 (6)	-106.2
<i>ARHGAP12</i>	4800-4814 (8)	-106.2	<i>NOS1</i>	5560-5568 (5)	-106.2
<i>ATP9A</i>	3509-3523 (8)	-106.2	<i>OAS3</i>	6257-6267 (6)	-106.2
<i>BACH1</i>	4266 -4274 (8)	-106.2÷-110.4	<i>PAK6</i>	3163-3179 (9)	-106.2
<i>BACH2</i>	5578-5604 (14)	-106.2	<i>PARN</i>	2839-2861 (12)	-106.2
<i>BAZ2A</i>	6856-6868 (7)	-106.2	<i>PCBD2</i>	1805-1815 (6)	-106.2
<i>BGN</i>	1960-1980 (11)	-106.2	<i>PCK1</i>	2388-2414 (9)	-106.2÷-108.3
<i>C11orf75</i>	693-709 (9)	-106.2÷-108.3	<i>PDE1A</i>	2793-2805 (7)	-106.2÷-108.3
<i>C21orf91</i>	5113-5121 (5)	-106.2	<i>PDE3A</i>	4022-4040 (10)	-106.2
<i>C2orf91</i>	1577-1593 (7)	-106.2	<i>PEAK1</i>	7268-7290 (12)	-106.2÷-108.3
<i>CACFD1</i>	2283-2303 (9)	-106.2÷-108.3	<i>PIGS</i>	2585-2597 (7)	-106.2
<i>CACNG8</i>	6807-6817 (6)	-106.2	<i>PKNOX1</i>	1680-1688 (7)	-106.2÷-108.3
<i>CBX3</i>	1306-1314 (5)	-106.2÷-108.3	<i>PLA2G7</i>	1643-1651 (5)	-106.2÷-108.3
<i>CCDC9</i>	1815-1833 (10)	-106.2	<i>PLEKHA2</i>	1672-1684 (7)	-106.2
<i>CD2AP</i>	2829-2849 (11)	-106.2÷-108.3	<i>PRKX</i>	5366- 5390 (13)	-106.2
<i>CD36</i>	3530-3538 (5)	-106.2÷-108.3	<i>PTGES</i>	1664-1688 (13)	-106.2
<i>CDK6</i>	1907-1917 (8)	-106.2÷-108.3	<i>PTP4A2</i>	3572-3586 (8)	-106.2÷-108.3
<i>CHRDL1</i>	3452-3474 (12)	-106.2	<i>PTPN3</i>	7001-7039 (20)	-106.2
<i>CLASP1</i>	6695-6711 (9)	-106.2	<i>QSOX2</i>	3460- 3476 (9)	-106.2÷-108.3
<i>CNOT6</i>	5094-5104 (6)	-106.2÷-108.3	<i>RABGAP1</i>	4103-4105 (7)	-106.2÷-108.3
<i>DBT</i>	5929-5965 (19)	-106.2÷-108.3	<i>RAPGEFL1</i>	2305-2339 (18)	-106.2
<i>DMXL1</i>	9853-6922 (5)	-106.2÷-108.3	<i>RDX</i>	3321-3329 (5)	-106.2
<i>DONSON</i>	2372-2446 (38)	-106.2	<i>REEP3</i>	3836-3856 (12)	-106.2÷-108.3
<i>ELOF1</i>	429-455 (14)	-106.2	<i>RORA</i>	5293-5307 (8)	-106.2
<i>ETS1</i>	3887-3907 (11)	-106.2	<i>SAMD4A</i>	4191-4201 (6)	-106.2
<i>EVI2A</i>	2015-2027 (7)	-106.2	<i>SEPT3</i>	1319-1333 (8)	-106.2



Continuation of table «c»

Gene	Start positions of binding sites, nt	$\Delta G/\Delta G_m$ , kJ/mole	Gene	Start positions of binding sites, nt	$\Delta G/\Delta G_m$ , kJ/mole
<i>FAM120C</i>	4206-4222 (9)	-106.2	<i>SERBP1</i>	5153-5163 (6)	-106.2
<i>FAM126B</i>	3744-3764 (7)	-106.2÷-108.3	<i>SFN</i>	1189-1199 (6)	-106.2
<i>FAM180B</i>	928-940 (7)	-106.2	<i>SH3PXD2A</i>	8615-8623 (5)	-106.2
<i>FAM212B</i>	1317-3453 (7)	-106.2	<i>SLC1A5</i>	2651-2679 (10)	-106.2
<i>FAM216B</i>	1390-1398 (5)	-106.2	<i>SLC25A44</i>	1893-1913 (11)	-106.2
<i>FASLG</i>	1603-1613 (6)	-106.2÷-108.3	<i>SLC30A3</i>	1865-1905 (9)	-106.2
<i>FGF9</i>	1737-1745 (8)	-106.2÷-108.3	<i>SLFN5</i>	3046-3058 (7)	-106.2÷-108.3
<i>FLT1</i>	6910-6922 (8)	-106.2÷-108.3	<i>SMIM15</i>	2574-2584 (6)	-106.2
<i>FOXK1</i>	10612- 10628 (9)	-106.2÷-108.3	<i>SP1</i>	4146-4158 (7)	-106.2
<i>GGA2</i>	2081- 2103 (12)	-106.2	<i>ST8SLA1</i>	4536-4558 (12)	-106.2
<i>GID4</i>	2279 – 2291 (7)	-106.2÷-108.3	<i>SYNPO2L</i>	3586-3600 (8)	-106.2
<i>GLCC11</i>	3955- 3963 (5)	-106.2÷-108.3	<i>SYT1</i>	2739-2749 (6)	-106.2
<i>GNAI1</i>	2937-2945 (5)	-106.2	<i>SYT2</i>	1863-1907 (15)	-106.2÷-108.3
<i>GPR21</i>	1481- 1503 (12)	-106.2÷-108.3	<i>SYTL4</i>	2462-2480 (6)	-106.2÷-110.4
<i>GTPBP1</i>	2471-2485 (8)	-106.2	<i>TBX4</i>	1780-1798 (10)	-106.2÷-108.3
<i>HEMGN</i>	1841-1849 (6)	-106.2÷-108.3	<i>TIPRL</i>	2688-2702 (8)	-106.2÷-108.3
<i>HPS4</i>	3984-3998 (8)	-106.2	<i>TMEM132B</i>	5871-5879 (5)	-106.2
<i>IGF2R</i>	8446-8454 (5)	-106.2	<i>TMEM2</i>	6337-6345 (5)	-106.2
<i>JAK2</i>	5183-5199 (9)	-106.2	<i>TMEM30B</i>	2800-2812 (7)	-106.2
<i>KCNJ10</i>	3349-3375 (14)	-106.2	<i>TNFRSF21</i>	2497-2517 (7)	-106.2
<i>KCNJ12</i>	4656- 4670 (8)	-106.2÷-108.3	<i>TNIP3</i>	1604-1620 (9)	-106.2÷-108.3
<i>KCNK10</i>	5523-5547 (13)	-106.2÷-108.3	<i>UBN2</i>	10914-10924 (6)	-106.2
<i>KIAA2026</i>	6628-6644 (9)	-106.2	<i>UMPS</i>	4221-4241 (10)	-106.2
<i>KIFC1</i>	2488-2512 (13)	-106.2	<i>UNC5B</i>	4036-4046 (6)	-106.2
<i>LANCL3</i>	2972-2980 (5)	-106.2÷-108.3	<i>VAPB</i>	2523-2537 (8)	-106.2÷-108.3
<i>LSMI4A</i>	2048-2070 (10)	-106.2÷-108.3	<i>WDR3</i>	3560-3588 (11)	-106.2÷-110.4
<i>MACC1</i>	3950-3966 (10)	-106.2÷-108.3	<i>WT1</i>	2704-2714 (6)	-106.2
<i>MARCH5</i>	1863-1879 (9)	-106.2÷-108.3	<i>ZC3H12C</i>	6510-6528 (10)	-106.2
<i>MCTS1</i>	1294-1318 (7)	-106.2÷-108.3	<i>ZDHHC21</i>	7360-7374 (8)	-106.2
<i>MGAT5</i>	4307-4333 (14)	-106.2÷-108.3	<i>ZNF670</i>	1930-1940 (7)	-106.2÷-108.3
<i>MLLT4</i>	7131-7153 (12)	-106.2	<i>ZXDA</i>	3942-3952 (6)	-106.2÷-108.3

The binding characteristics of miR-466-3p in the 3'UTR of 147 target genes mRNAs with the value  $\Delta G/\Delta G_m$  equal or greater than 90% are shown in Table «b». The number of miR-466-3p binding sites on mRNAs of these genes varied from one to four, and indicates the different probability of miR-466-3p interaction with mRNAs, since the greater the length of the section of longer binding sites, is associated with a higher the probability of interaction. ZNF family transcription factors are among of target genes, and

they have less than four binding sites. Only *ZNF670* gene mRNA has seven binding sites (Table «c»). miR-466-3p target genes involved in many biological processes and, therefore, miR-466-3p may participate in the regulation and can cause diseases. Table «d» demonstrates some of these genes.

Table «c» demonstrates characteristics of miR-466-3p binding in the 3'UTR of target genes mRNAs, having five or more binding sites in the mRNA.

**Table «d»** – miR-466-3p target genes involved in many biological processes

Functional group	Genes
Transcription factors	<i>BACH1</i> , 4256-4274*, eight sites, -106.2÷-110.4**; <i>BHLHE40</i> , 1683-1693, four sites, -106.2÷-108.3; <i>EGR3</i> , 2026, one site, -108.3; <i>FOXI2</i> , 2790, one site, -106.2; <i>MECOM</i> , 5099, one site, -110.4; <i>RUNXI</i> , 5455-5459, two sites, -106.2÷-110.4; <i>ZNF618</i> , 2835, one site, -106.2.
Kinases	<i>ADRBK2</i> , 6676-6696, 11 SITES, -106.2; <i>AKAP11</i> , 6559-6579, 11 SITES, -106.2; <i>CDK6</i> , 1895-1919, EIGHT SITES, -106.2÷-108.3; <i>FLT1</i> , 6910-6936, EIGHT SITES, -106.2÷-108.3; <i>JAK2</i> , 5183-5199, NINE SITES, -106.2; <i>KIAA1804</i> , 5327, ONE SITE, -108.3; <i>MAPKAPK2</i> , 2587-2589, TWO SITES, -106.2÷-108.3; <i>PCK1</i> , 2388-2414, NINE SITES, -106.2÷-108.3; <i>PIK3RI</i> , 6519-6523, FOUR SITES, -106.2÷-108.3; <i>PRKX</i> , 1804-5390, 25 SITES, -106.2÷-108.3; <i>SBK1</i> , 4530, ONE SITE, -110.4.
Genes of cell cycle	<i>BACH1</i> ; <i>BHLHE40</i> ; <i>CBX3</i> , 1306-1314, five sites, -106.2÷-108.3; <i>CDK6</i> ; <i>DDBI</i> , 3990-4004, three sites, -106.2÷-108.3; <i>MECOM</i> ; <i>WDR3</i> , 3560-3588, 11 sites, -106.2÷-110.4; <i>MACC1</i> , 2979-3966, 10 sites, -106.2÷-108.3; <i>MAPKAPK2</i> ; <i>NDRG4</i> , 3108-3116, five sites, -106.2÷-108.3; <i>PIK3RI</i> .
Genes of apoptosis	<i>BACH1</i> ; <i>BHLHE40</i> ; <i>CD2AP</i> , 2829-2849, 11 SITES, -106.2÷-108.3; <i>CD36</i> , 3530-3538, FIVE SITES, -106.2÷-108.3; <i>CDK6</i> ; <i>CNOT6</i> , 5094-5104, SIX SITES, -106.2÷-108.3; <i>DDBI</i> ; <i>FASLG</i> , 1603-1613, SIX SITES, -106.2÷-108.3; <i>FGF9</i> , 1729-1753, EIGHT SITES, -106.2÷-108.3; <i>FLT1</i> ; <i>HIF1AN</i> , 2037-2041, TWO SITES, -108.3; <i>MACC1</i> ; <i>MAPKAPK2</i> ; <i>MECOM</i> ; <i>OCLN</i> , 3570-3572, TWO SITES, -106.2÷-108.3; <i>SLC7A11</i> , 3438-3446, THREE SITES, -106.2÷-108.3; <i>SPN</i> , 4373-4387, TWO SITES, -106.2÷-108.3; <i>TIPRL</i> , 2688-2702, EIGHT SITES, -106.2÷-108.3; <i>WDR3</i> .
Genes of breast cancer	<i>ADAT2</i> , 1950-1964, EIGHT SITES, -106.2; <i>ADCYAP1R1</i> , 3841-3853, SEVEN SITES, -106.2÷-108.3; <i>BHLHE40</i> ; <i>CBX3</i> ; <i>CDK6</i> ; <i>CISD2</i> , 1140-1146, FOUR SITES, -106.2÷-108.3; <i>EGR3</i> ; <i>FASLG</i> ; <i>FGFR3</i> , 2809, ONE SITE, -110.4; <i>FLT1</i> ; <i>HIF1AN</i> ; <i>IRSI</i> , 7318-7320, TWO SITES, -106.2÷-108.3; <i>LFNG</i> , 1270, ONE SITE, -108.3; <i>MACC1</i> ; <i>MAPKAPK2</i> ; <i>MECOM</i> ; <i>MGAT5</i> , 4307-4333, 14 SITES, -106.2÷-108.3; <i>NFAT5</i> , 8532-8548, THREE SITES, -106.2÷-108.3; <i>PEAK1</i> , 7268-7290, 12 SITES, -106.2÷-108.3; <i>PIK3RI</i> ; <i>PTP4A2</i> , 3562-3586, EIGHT SITES, -106.2÷-108.3; <i>SLC7A11</i> ; <i>SPN</i> ; <i>STAT6</i> , 94-102, FIVE SITES, -106.2÷108.3; <i>UGT8</i> , 2492-2516, THREE SITES, -106.2÷-108.3; <i>VAPB</i> , 2523-2537, EIGHT SITES, -106.2÷-108.3 27 SITES.
Genes of lung cancer	<i>ADAT2</i> ; <i>ADCYAP1R1</i> ; <i>BHLHE40</i> ; <i>CDK6</i> ; <i>DPYSL5</i> , 4857, ONE SITE, -106.2; <i>FASLG</i> ; <i>FGF9</i> ; <i>FGFR3</i> ; <i>FLT1</i> ; <i>HEMGN</i> , 1841-1849, SIX SITES, -106.2÷-108.3; <i>MACC1</i> ; <i>MAPKAPK2</i> ; <i>MECOM</i> ; <i>LILRB2</i> , 2858-2864, FOUR SITES, -106.2÷-108.3; <i>SPN</i> ; <i>STAT6</i> ; <i>UGT8</i> 17 SITES.
Genes of cardiovascular diseases	<i>ADRBK2</i> ; <i>BHLHE40</i> ; <i>CD36</i> ; <i>EGR3</i> ; <i>NDUFS2</i> , 1917-1925, five sites, -106.2÷-108.3; <i>NFAT5</i> ; <i>NOS1</i> , 5560-5568, five sites, -106.2; <i>PLA2G7</i> , 1643-1651, five sites, -106.2÷-108.3; <i>SIPR2</i> , 3189, one site, -110.4; <i>STAT6</i> .
Genes of circadian rhythm	<i>BHLHE40</i> ; <i>DBT</i> , 5929-5965, 19 sites, -106.2÷-108.3; <i>NR1D2</i> , 3337, one site, -110.4.

Note: \* – start positions of binding sites; \*\* – energy of hybridization (kJ/mole).

Typically, the more multiple binding sites available in the mRNA, the more extended is the section. mRNA of *LSM14A* and *PARN* genes having 10 and 12 binding sites, have a length of 45 nucleotides. mRNA of *BACH2*, *KCNJ10* genes containing 10 and 12 binding sites, have a length of 49 nt. mRNA of *RAPGEFL1*, *PTPN3* genes containing 18 and 21 binding sites, have a length of 57 nt and 61nt, respectively. mRNA of gene containing 38 binding sites, have a length 97nt. mRNAs of the above genes can bind more than one RISC complex containing miR-466-3p and efficiency of translation of mRNA suppression will be higher. We have developed a program of predicting miRNA binding sites with mRNAs which allows high reliability to establish these sites. At the value of  $\Delta G/\Delta G_m$  equal to 90%,

the level of  $p < 0.0001$ . For example, we were able to identify 200 genes mRNAs from 18,000 human genes which have entirely complementary binding sites for unique miR-619.

Considering the possibility of regulating that the expression of many genes are regulated by miR-466-3p, it should be expected that the concentration of miR-466-3p should not be expected to change in the norm vary widely; otherwise, excessively high or low levels of miR-466-3p would inevitably lead to the disruption of the expression of genes involved in key biological processes and would result in several pathological conditions. The type of disease will depend on the ratio of the concentrations of miR-466-3p and target mRNAs of target genes in specific cells and tissues of the body [12-18].

## References

1. Niyazova R., Berillo O., Atambayeva Sh., Pyrkova A., Alybaeva A., Ivashchenko A. miR-1322 Binding Sites in Paralogous and Orthologous Genes. // *Biomed Research International*. – 2015. – P. 1-7.
2. Ivashchenko A., Berillo O., Pyrkova A., Niyazova R., Atambayeva Sh. Binding sites of mir-1273 family on the mRNA of target genes. // *Biomed research international*. – 2014. – P. 1-8.
3. Ivashchenko A., Berillo O., Pyrkova A., Niyazova R., Atambayeva Sh. The properties of binding sites of miR-619-5p, miR-5095, miR-5096 and miR-5585-3p in the mRNAs of human genes. // *Biomed research international*. – 2014. – P. 2014.
4. Ivashchenko A., Berillo O., Pyrkova A., Niyazova R., Atambayeva Sh. MiR-3960 binding sites with mRNA of human genes. // *Bioinformation*. – 2014. – Vol. 10. – No. 7. – P. 423-427.
5. Cheng Q., Yi B., Wang A., Jiang X. Exploring and exploiting the fundamental role of microRNAs in tumor pathogenesis. // *Onco Targets Ther*. – 2013. – Vol. 6. – P. 1675-1684.
6. Hromadnikova I., Kotlabova K., Hympanova L., Krofta L. Cardiovascular and cerebrovascular disease associated microRNAs are dysregulated in placental tissues affected with gestational hypertension, preeclampsia and intrauterine growth restriction. // *Plos One*. – 2015. – Vol. 10 – No. 9. – e0138383.
7. Faruq O., Vecchione A. microRNA: Diagnostic perspective. // *Front Med*. – 2015. – 2. – P. 51.
8. Kool E.T. Hydrogen bonding, base stacking, and steric effects in DNA replication. // *Annu.Rev. Biophys.Biomol.Struct*. – 2001. – Vol. 30. – P. 1–22.
9. Leontis N.B., Stombaugh J., Westhof E. The non-Watson-Crick base pairs and their associated isostericity matrices. // *Nucleic Acids Res*. – 2002. – Vol. 30. – P. 3497–3531.
10. Ivashchenko A., Berillo O., Pyrkova A., Niyazova R., Atambayeva S. MiR-3960 binding sites with mRNA of human genes. // *Bioinformation*. – 2014. – Vol. 10. – No. 7. – P. 423-427.
11. Berillo O., Atambayeva Sh., Niyazova R., Akimniyazova A., Ivashchenko A., Pyrkova A. Features of Multiple MiR-574-5p Binding Sites and Functions of Their Target-Genes. // *Journal of Bioinformatics and Computational Biology*. – submitted for publication.
12. Druz A., Chu C., Majors B., Sanctuary R., Betenbaugh M., Shiloach J. A novel microRNA mmu-miR-466h affects apoptosis regulation in mammalian cells. // *Biotechnol Bioeng*. – 2011. – Vol. 108. – P. 1651-1661.
13. Dimmeler S., Zeiher A.M. Endothelial cell apoptosis in angiogenesis and vessel regression. // *Circ Res*. – 2000. – Vol. 87. – P. 434-439.
14. Folkman J. Angiogenesis and apoptosis. // *Semin Cancer Biol*. – 2003. – 13. – P. 159-167.
15. Druz A., Betenbaugh M., Shiloach J. Glucose depletion activates mmu-miR-466h-5p expression through oxidative stress and inhibition of histone deacetylation. // *Nucleic Acids Res*. – 2012. – Vol. 40. – P. 7291-7302.
16. Li Y., Fan X., He X., Sun H., Zou Z., Yuan H., Xu H., Wang C., Shi X. MicroRNA-466 inhibits antiviral innate immune response by targeting interferon-alpha. // *Cell Mol Immunol*. – 2012. – Vol. 9. – P. 497-502.
17. Luo Y., Liu Y., Liu M., Wei J., Zhang Y., Hou J., Huang W., Wang T., Li X., He Y., Ding F., Yuan L., Cai J., Zheng F., Yang J. Sfmt2 10th intron-hosted miR-466(a/e)-3p are important epigenetic regulators of Nfat5 signaling, osmoregulation and urine concentration in mice. // *Biochim Biophys Acta*. – 2014. – Vol. 1839. – P. 97-106.
18. Seo M., Choi J., Rae Rho Ch., Joo Ch., Lee S. MicroRNA Mir-466 inhibits lymphangiogenesis by targeting Prospero-related homeobox 1 in the alkali burn corneal injury model. // *Journal of Biomedical Science*. – 2015. – Vol. 22. – P. 3.

UDC 58.0845

Omirbekova N.Zh., Zhussupova A.I., Zhunusbayeva Zh.K.,  
Deryabina N.D., Askanbayeva B.N., Egiztayeva B.T.

Department of Molecular Biology and Genetics,  
Al-Farabi Kazakh National University, Almaty, 050038, Kazakhstan  
\*e-mail: aizhan.zhusupova@gmail.com

### ***Brachypodium distachyon* as a model plant in wheat rust research**

**Abstract:** All countries share the need to increase wheat yield and tolerance to adverse environmental factors. Rust, the most common infector of wheat, is widely dispersed on the territory of Commonwealth of Independent States (CIS). The data shows that on the territory of following countries: Kazakhstan, Kyrgyzstan, Russia, Belarus, Uzbekistan the percentage of infected wheat with rust from the total amount is approximately 20-25% annually. *Brachypodium distachyon* can be regarded as a perspective model to study various mechanisms of a rust infection.

**Key words:** rust infection, *Brachypodium distachyon*.

#### **Introduction**

Wheat was one of the first domesticated food crops and for 8,000 years has been the basic staple food of the major civilizations of Europe, West Asia and North Africa. Today, wheat is the most widely grown crop in the world and provides 20% of the daily protein and of the food calories for 4.5 billion people. It is the second most important food crop in the developing world after rice. In recent years, wheat production levels have not satisfied demand, triggering price instability and hunger riots. It is the best of the cereal foods and provides more nourishment for humans than any other food source, being a major diet component because of the wheat plant's agronomic adaptability, ease of grain storage and converting grain into flour. Wheat is also a popular source of animal feed, particularly in years where harvests are adversely affected by rain and significant quantities of the grain are made unsuitable for food use. Such low-grade grain is often used by industry to make adhesives, paper additives, and several other products and even in the production of alcohol. With a predicted world population of 9.0 billion in 2050, the demand for wheat is expected to increase by 60%.

To meet this demand, annual wheat yield increases must rise from the current level of below 1% to at least 1.6%. All countries share the need to increase wheat yield, tolerance to abiotic stresses, pathogens and pests, as well as to improve input use efficiency for a more sustainable wheat production. Improved agronomic practices and development of innovative cropping systems are also a priority aiming at rein-

forcing synergies between national and international research programmes to increase food security, nutritional value and safety whilst taking into account societal demands for sustainable agricultural production [1].

Wings of Gold racers at The State Emblem of the Republic of Kazakhstan remind sheaves of grain, gold wheat, meaning labor, abundance and material prosperity [2]. Wheat is a very important annual or biannual grass from the genus *Triticum* with the high impact on the economics of the Republic of Kazakhstan, being one of the five leading world producers on the grain market due to the high quality of the processed grain. Apart from the traditional varieties of flour, special quality flours, customized to buyer requirements are also successfully exported, going in consent with the sectoral program of agro-industrial complex development for 2013-2020 «Agribusiness – 2020» [3].

#### **Main part**

There are three types of rusts, which are infecting wheat in different ways: stem rust (*Puccinia graminis*), leaf rust (*Puccinia recondita*), and stripe rust (*Puccinia striiformis*). The symptoms are easy to detect. Firstly chlorotic flecks or brown necrotic spots appear on the leaves or stems, which further can develop into yellow strikes or patches on foliage. Another symptom of rust is brown necrotic streaks on foliage, but that occurs less rarely than the previous one. Sometimes upwardly raised orange pustules may be present on the lesions [4-6].

*Puccinia* is the fungus, which is hard to deal with. Emergence of the disease is especially sustained by wet and cool weather conditions. That means small wind or cold breeze even in sunny days can positively alter the propagation and development of that disease.

Rust, the most common infector of wheat, is widely dispersed on the territory of Commonwealth of Independent States (CIS). The data shows that on the territory of following countries: Kazakhstan, Kyrgyzstan, Russia, Belarus, Uzbekistan the percentage of infected wheat with rust from the total amount is approximately 20-25% annually.

According to the data of Kazakhstan Forbes division published at <http://www.forbes.kz> the worst condition of wheat in Kazakhstan was in 2007, when around 75% of all production was infected by rust. This year, according to experts in agricultural and economical sphere, the amount of infected wheat was about 22%, what means that one fourth of all seeding has died without any use. In 2014 the total production of wheat collection was 17 billion tons, but if to take into account the wheat infected with rust, the amount of wheat could be 20.74 billion tons that year. The data is almost the same with 2015 year results.

1 ton of wheat costs 42,000 KZT in 2015. 4 billion tons of infected wheat costs 168,000 billion tenge. That means that per year our country loses this amount of money because of the rust infection. That enormous amount of losses can be decreased by the proper investigating of the molecular mechanisms of that disease.

But the main issue is that the study of the rust disease on the wheat is very hard and complicated in the laboratory conditions. Wheat needs cool conditions of the environment; it has a slow generation cycle in comparison with other agricultural grasses. The question to find perspective and appropriate model organisms to study infectious diseases was unanswered for a long time. But the recent studies indicate that *Brachypodium distachyon* could serve as appropriate model organisms to study the molecular mechanisms of grass diseases' action [7, 8].

Nowadays the *Brachypodium distachyon* may also serve as a model organism here in Kazakhstan, because it has more advantages in comparison with studies based upon only wheat research. *Brachypodium* possesses characteristics required for an appropriate model to study cereal-pathogen interactions, including small stature, self-fertilization with the saved ability to cross-fertilize, rapid generation time, a compact genome and high transformation efficiency.

All those characteristics make *Brachypodium distachyon* very simple but effective model organism in studying the molecular mechanisms of infection. Its small stature and rapid generation time leads to the economy of territory, energy and nutrients required for optimal life establishment of a model grass. A compact genome and smaller amount of consequential repeats make the gene mapping and sequencing easier and faster, which is also important in data analysis of molecular action of infection inside the host's cell.

*Brachypodium distachyon*, like many grasses, is a host to rust pathogen described a little bit earlier in this article. That gives an another advantage of taking *Brachypodium* as a model grass, because through it all biological actions of host-cereal pathogen can be easily detected, observed and investigated much faster in comparison with studied based upon wheat [9-11].

*Brachypodium distachyon* is evolutionary very close to species like wheat, barley, oats, maize, rice, rye and sorghum. That quality of *Brachypodium* means that it can be very useful in fundamental genomics research of temperate grasses, and cereals. Those attributes also prove the statement written earlier about compact genome. Small genome of a *Brachypodium distachyon* is approximately 270 Mega base pairs. In addition only 21% of the *Brachypodium* genome consists of repetitive elements, in comparison with 26% in rice, and more than 80% in wheat (which is also a disadvantage of making a research based upon wheat molecular and genetic mechanisms). All genes are packed within five chromosomes, which make the genome very compact for a grass species. The complete genome of *Brachypodium distachyon* of inbred line Bd21 has been sequenced in Nature journal in 2010 [12].

Diploid and polyploid accessions make those perspective model organisms convenient to cultivate in a small place like laboratory. For early-flowering accessions it can take as little as three weeks from germination to flower (under an appropriate inductive photoperiod established in lad conditions). *Brachypodium distachyon*'s small size is about 15-20 cm long, which is tightly connected with rapid generation cycle of eight to twelve weeks. As a weed, it does not require specialized growing conditions, and is able to grow in temperate environmental conditions.

*Brachypodium* is considered to be a non-host to infection caused by rust. That means that *Brachypodium* has the ability to be resistant to all races, variants, and subtypes of the rust infections. Nowadays,

scientists know a few about the non-host molecular mechanisms in grass species. However, the infection of *Brachypodium* accessions with *P. striiformis* f. sp. *tritici*, *hordei* and *bromi* (wheat, barley and brome stripe rust, respectively) resulted in symptoms on different accessions ranging from the formation of small sporulating uredinia, to macroscopic lesion formation, to apparent immunity [13-15].

After the infection the microscopic analysis of stripe, stem, and leaf rusts showed no macroscopically visible lesions. But the source of these lesions identified a distribution of infection sites which contain hyphae within the grass apoplast and haustoria formation within the plant mesophyll cells. *Brachypodium* lines with macroscopically visible lesions and/or pustule development when infected by cereal rust pathogens showed extensive underlying fungal colonization of plant mesophyll cells with frequent haustoria formation at these sites.

It has also been shown that cell death is not in common within the infection sites, despite the extensive or fungal colonization. Also, *Brachypodium* callose deposition sites were proven to be identical to the callose deposition sites in wheat species during the basal immune response against these same rust pathogens. In both plant species, larger rust infection sites were proven to be able to suppress callose production in weak or old cells, supporting the theory of the presence of mechanistic overlap between the *Brachypodium* response to cereal rust infection and the wheat basal defence response. The data also shows the absence of change in salicylic acid level in *Brachypodium* leaf upon artificial infection with *Puccinia* subtypes [16-18].

Subsequent genetic analysis of *Brachypodium distachyon* rust infection has indicated that segregation between extensive and restricted wheat stripe is always inherited throughout the generations. The inheritance is controlled by a single dominant gene, which means that the positional cloning of those responsible genes for different phenotypic characteristics could be the real help in investigating the molecular mechanisms of rust infections behind non-host resistance in grass species [19-21].

All those features of *Brachypodium distachyon* makes it a perspective model to study the mechanisms of tolerance to rust infection. And it is currently being studied by our working group in terms of nitrogen and energy metabolism changes in control and test plants; results published locally and abroad (Kazakhstan, Italy, Spain, France).

## References

1. Wheat initiative: coordinating global research for wheat. Available at: [www.wheatinitiative.org](http://www.wheatinitiative.org).
2. National symbols of the Republic of Kazakhstan. Available at: [www.egov.kz/wps/portal/Content?contentPath=/egovcontent/state\\_symbols&lang=en](http://www.egov.kz/wps/portal/Content?contentPath=/egovcontent/state_symbols&lang=en)
3. Government approved Agribusiness-2020 Program (from February 12, 2013). Available at: [www.primeminister.kz/news/show/29/v-pravitelstve-prinjali-programmu-razvitija-apk-%C2%ABagrobiznes-2020%C2%BB/12-02-2013?lang=en](http://www.primeminister.kz/news/show/29/v-pravitelstve-prinjali-programmu-razvitija-apk-%C2%ABagrobiznes-2020%C2%BB/12-02-2013?lang=en)
4. Sinclair W.A., Lyon H.H. Diseases of trees and shrubs. 2nd ed. Ithaca, NY: Cornell University Press, 2005. – 659 p.
5. Peterson P.D. Stem rust of wheat: from ancient enemy to modern foe. US: APS Press, 2001. – 168 p.
6. USDA-ARS Cereal Disease Laboratory Update. Available at: [http://www.ars.usda.gov/main/site\\_main.htm?modecode=36-40-05-00](http://www.ars.usda.gov/main/site_main.htm?modecode=36-40-05-00)
7. Li C., Rudi H., Stockinger E., Cheng H., Cao M. et al. Comparative analyses reveal potential uses of *Brachypodium distachyon* as a model for cold stress responses in temperate grasses // BMC Plant Biol., 2012. – Vol. 12. – P. 65.
8. Li C., Rudi H., Stockinger J. et al. Comparative analyses reveal potential uses of *Brachypodium distachyon* as a model for cold stress responses in temperate grasses. Strong population structure characterizes weediness gene evolution in the invasive grass *Brachypodium distachyon* // Molecular Ecology, 2009. – Vol. 18. – P. 2588-2601.
9. Girin T., David L., Chardin C., Sibout R. et al. *Brachypodium*: a promising hub between model species and cereals // Journal of Experimental Botany, 2014. – Vol. 65. – No. 19. – P. 5683–5696.
10. Nirmala J., Drader T., Lawrence P.K., Yin C. et al. Concerted action of two avirulent spore effectors activates reaction to *Puccinia graminis* 1 (Rpg1)-mediated cereal stem rust resistance // Proc. Natl. Acad. Sci. USA, 2011. – Vol. 108. – P. 14676–14681.
11. Figueroa M., Castell-Miller C.V., Li F., Hulbert S.H., Bradeen J.M. Pushing the boundaries of resistance: insights from *Brachypodium*-rust interactions // Frontiers in plant science, 2015. – Vol. 6. – A. 558. – P. 1-11.
12. The International *Brachypodium* Initiative. Genome sequencing and analysis of the model grass *Brachypodium distachyon* // Nature, 2010. – Vol. 463. – No. 7282. – P. 763–768.

13. Bakker E.G., Montgomery B., Nguyen B., Eide K. et al. Strong population structure characterizes weediness gene evolution in the invasive grass *Brachypodium distachyon* // *Molecular Ecology*, 2009. – Vol. 18. – P. 2588-2601.
14. Vain P., Worland B., Thole V. et al. *Agrobacterium*-mediated transformation of the temperate grass *Brachypodium distachyon* (genotype Bd21) for T-DNA insertional mutagenesis // *Plant Biotechnology Journal*, 2008. – Vol. 6. – No. 5. – P. 236–245.
15. Lee M.Y., Yan L., Gorter F.A. et al. *Brachypodium distachyon* line Bd3-1 resistance is elicited by the barley stripe mosaic virus triple gene block 1 movement protein // *Journal of General Virology*, 2012. – Vol. 93. – P. 2729–2739.
16. Thole V., Worland B., Wright J. et al. Distribution and characterization of more than 1000 T-DNA tags in the genome of *Brachypodium distachyon* community standard line Bd21, 2010 // *Plant Biotechnology Journal*. – Vol. 8. – No. 6. – P. 734–747.
17. Huo N., Vogel J., Lazo G. et al. Structural characterization of *Brachypodium* genome and its syntenic relationship with rice and wheat, 2009 // *Plant Mol. Biol.* – Vol. 70. – No. 1-2. – P. 47–61.
18. Goddard R., Peraldi A., Ridout C., Nicholson P. Enhanced disease resistance caused by BRI1 mutation is conserved between *Brachypodium distachyon* and barley (*Hordeum vulgare*) // *Mol. Plant Microbe Interact.* – Vol. 27. – No. 10. – P. 1095–1106.
19. Hasterock R., Marasek A., Donnison I. et al. Alignment of the genomes of *Brachypodium distachyon* and temperate cereals and grasses using bacterial artificial chromosomes landing with fluorescence in situ hybridisation // *Genetics*, 2006.
20. Wolny E., Hasterock R. Comparative cytogenetic analysis of the genomes of the model grass *Brachypodium distachyon* and its close relatives // *Ann. Bot.*, 2009. – Vol. 104. – No. 5. – P. 873-881.
21. Gordon S., Priest H., des Marais D. et al. Genome diversity in *Brachypodium distachyon*: deep sequencing of highly diverse inbred lines // *Plant J.*, 2014. – Vol. 79. – No. 3. – P. 361-374.

UDC 575.633.11

Chunetova Zh.Zh., Shulembayeva K.K., Zhussupova A.I., Omarova B.

Department of Molecular Biology and Genetics,  
Al-Farabi Kazakh National University, Almaty, 050038, Kazakhstan  
\*e-mail: Chanar-79-16-06@mail.ru

### **Mutagenic activity of cadmium chloride on the genetic variability of soft wheat**

**Abstract:** The action of the chemical compound –  $CdCl_2$  on soft wheat varieties resulted in plant modifications on a number of qualitative and quantitative traits. Genetic analysis conducted on the basis of reciprocal crosses showed that the inheritance of altered traits in mutants is independent of the direction of crossing. Modification of habitus and phenotypes of mutant plants is accompanied by a violation of cell division in meiosis.

**Key words:** mutagenic activity, cadmium chloride, soft wheat varieties.

#### **Introduction**

Chemical mutagens are an effective means of formative processes in wheat breeding and receiving selection and significant deviations [1, 2]. Obtaining of mutants and using them for hybridization are required to study genetic nature of appearing changes which have great importance for the selection of effective and specific action of mutagens, and for extension and deepening of understanding the nature of the evolution of wheat. In this work we present some results of research on genetic analysis of the mutant wheat. New forms, such as dwarf mutants in wheat and barley, ultra-fast mutants in barley, resistant to fungal diseases, high-leasing and highly productive mutants might be obtained qualitatively by chemical mutagenesis [3]. These facts show that the mutants obtained by chemical mutagenesis can successfully serve as progenitors of new high-yielding varieties. However, to obtain mutants and study them – this is only the first stage of the selection work. More important is the using mutants in the hybridization to obtain positive transgressions. The hybridization makes possibility to better use mutations in wheat breeding [4-6].

#### **Materials and methods**

$M_1$ - $M_3$  mutants obtained in the process of  $CdCl_2$  4 varieties of soft wheat of local breed – Shagala, Kazakhstanskaya 3, Jenis and Lutescens 32 were used as research objects. The modified plants subsequently lay in the form of lines (A-1, A-2). During the experiment, we used the following methods: Cytogenetic, Hybridological, statistical and morphological.

Cytological studies were carried out using a microscope LOMO Mikmed-1. Genetic analysis of qualitative and quantitative traits of wheat  $F_1$  and  $F_2$  hybrids were conducted. Statistical analysis was limited to estimation of the arithmetic mean and in order to determine the reliability of the difference between the arithmetic means of quantitative traits using the Student's t test, genetic – finding a significant  $\chi^2$  value [7, 8]. Accounting of chromosomal abnormalities in MI, AI and AII of meiosis was performed on temporary acetocarmine preparations under the microscope MBI-3. The representativeness of research result provided an adequate sample size – 60-100 plants.

#### **Results and their discussion**

**Genetic analysis of mutant wheat.** Chemical mutagenesis in plant breeding is used as an effective method in order to enhance the variability of the starting material. In the world literature there is sufficient information about the creation of commercial varieties derived from experimental mutagenesis. To apply selected mutants in selection process is necessary to examine their genetic nature. For this, in genetic research are using two methods: analyzes and reciprocal crosses.

**Analyzing cross.** In order to establish the nature of any mutational change by variables usually used carrying reciprocal crosses between the original form and receiving on the basis of its mutant subsequent analysis of the hybrids  $F_1$ . In our studies  $M_2$  generation plants with modified number of quantitative and qualitative characteristics was preserved the properties displayed in  $M_1$ . To establish the homo and het-



erogygous genotype of mutant plants was carried out analyzing cross with an initial variety.

Mutant forms with signs of anthocyanin coloration of the stem, pubescent leaf surface, lengthening with spike crossed with an initial variety of Kazakhstanskaya 3. In BC<sub>1</sub> splitting signs to change and corresponds to the normal ratio of 1:1, and in F<sub>2</sub> is 3:1 ( $\chi^2 = 1.89$ ). Similar results were obtained with the mutant varieties of Shagala on the grounds of anthocyanin coloration of stem and leaf axils. BC<sub>1</sub> and F<sub>2</sub> hybrids were observed splitting on the grounds of lengthening the stem

and normal nodes in the ratio of 1:1 and 3:1, respectively, which indicates that the heterozygous nature of the mutant and monogenic inheritance of this trait.

In contrast, cleavage by productive tillering, length and density of the spike in BC<sub>1</sub> corresponded to 3:1, and an F<sub>2</sub> population of 15:1, 13:9 and 3:7, respectively. This shows that the traits of mutant lines are inherited by a polymer, and complementary mechanisms of epistatic interactions of non-allelic genes. This shows that plants reaction by chemical compounds depends on wheat genotype.

**Table 1** – Genetic analysis of F<sub>2</sub> and BC<sub>1</sub> hybrids by crossing mutants with Kazakhstanskaya 3 variety

Signs of mutants shape	The ratio of altered (modified) and normal plants					
	BC <sub>1</sub>			F <sub>2</sub>		
	<b>Line 1</b>					
The length of the spike	27:25	1:1	0.06	188:57	3:1	0.40
Beardless spike	32:29	1:1	0.04	168:48	3:1	0.89
Anthocyanins stem	10:13	1:1	0.20	126:32	3:1	1.89
Pubescence sheet	8:10	1:1	0.20	112:28	3:1	1.87
	<b>Line 3</b>					
Cranked stem	22:20	1:1	0.90	118:31	3:1	1.38
Tillering of plants	45:13	3:1	0.20	120:5	15:1	1.14
The length of the spike	45:18	3:1	0.42	223:51	13:3	0.003
Anthocyanin color of sheet leaves	19:23	1:1	0.38	97:29	3:1	0.26
The thickness of the spike	33:31	1:1	0.06	85:54	9:7	1.38

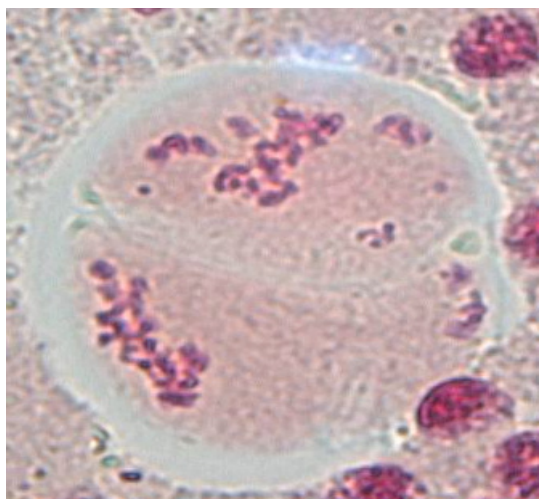
Further studies displayed arising changes in M<sub>1</sub> by the elements of productivity of Kazakhstanskaya 3 and Shagala varieties appeared in subsequent M<sub>2</sub> – M<sub>6</sub> generations. It was proved to conduct reciprocal crossing, where the modified attributes are inherited independently from direction of the crossing. Phenotypic variation of plants was accompanied by a violation of the process of meiosis.

**Cytological analysis of M<sub>2</sub> mutant plants.** Chemical mutagens because of its ability to induce a higher frequency of mutations are used in many countries around the world to create a breeding material. Chromosomal aberrations and violation of cell division during meiosis is one of the major tests for mutagenicity. Most notable in this regard is a meiotic cell division, especially in subjects like wheat, having a large number of hardly identifiable chromosomes. Moreover, violations of meiotic division are more likely to be transmitted to the next generation.

In mutant plants of M<sub>2</sub> generation percentage of damaged cells in MI meiosis equals 35, and at anaphase AI and AII – 20, which indicates a significant reduction in percentage of cells with disorders compared to M<sub>1</sub> mutant plants (64% AI and 68% – AII). Violation of this phenomenon is cytomixis – transition of contents to neighboring cells, M<sub>1</sub> amounts 20-30% of all the studied cells, while the percentage of such cells in M<sub>2</sub> decreases to 7-9%. So, the percentage of abnormalities in mutant forms of Kazakhstanskaya 3 M<sub>2</sub> equals 55%, in contrast, violation in M<sub>1</sub> – 90-95%.

Violation of meiosis in mutant plants of Kazakhstanskaya 3 variety is shown on Fig. 1-4.

Same decrease in percentage of violations is observed in mutants of Jenis, Lutescens 32 and Shagala varieties. In AI and AII some minor violations as a lagging chromosome fragments on the pole, bridge, asynchronous division. Occasionally cells with no content are observed.



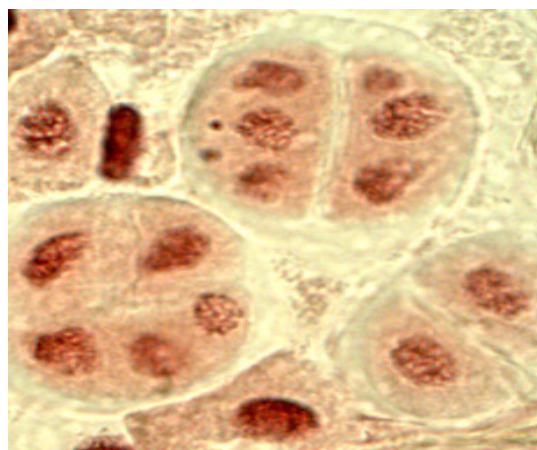
**Figure 1** – Disorientation of equator chromosomes



**Figure 2** – Fragmentation of equator chromosomes



**Figure 3** – Cytomixis – transition of cell contents into the neighboring



**Figure 4** – Pentad and hexad formation

**Cytological analysis of mutant plants M3.** To characterize meiosis in mutant lines of M3 and identification of monosomic and disomic plants in  $F_1$  hybrids with the mutant  $P_1$  1080 cells were analyzed. Results of cytological analysis of  $M_3$  mutant plants are shown on Figure 2. Proportion of cells with pyknosis in L1 line  $M_3$  mutants of Kazakhstanskaya 3 variety equals 0.29; mutant of Jenis variety – 0.10; Lutescens 32 – 0.23; line L3 of Shagala variety – 0.21 in comparison with the impaired cell  $M_1$ , respectively. Proportion of cells with univalents reaches 0.19; 0.009 and 0.16, respectively.

So, in the older generation of mutants ( $M_3$ ) of Kazakhstanskaya 3 and Shagala varieties, selected for practical selection, proportion of cells with impaired meiosis in  $M_1$  is much reduced with mutants like  $M_1$

and  $M_2$ . Violations in  $M_2$  meiosis in plants from the above varieties have the same character as  $M_1$  plants in meiosis. Typical violations in  $M_1 - M_3$  progeny mutants include: pyknosis; formation of offset spindle in metaphase I; univalents, polyvalents and asynchronous cell division in AI. This study demonstrates mutagenic effects of studied chemical compounds.

#### References

1. Luk'yanenko P.P. Selection of rust resistant varieties of winter wheat // Seed breeding. – 1968. – P. 10-18.
2. Khvostova V.V, Yachevskaya G.L. Rearrangements of chromosomes in meiosis // Cytology and genetics of meiosis. – M.: Nauka, 1975. – P. 232-263.

3. Larchenko E.A., Morgun V.V. Comparative analysis of genetic variability plant in the mutagenic treatment generative cells and maize seeds // *Cytology and Genetics*. – 2000. – Vol.34, No.4. – P. 17-19.
4. Rapoport I.A. Discovery of chemical mutagenesis // *Selected Works*. – M.: Nauka, 1993. – P. 304.
5. Salnikova T.V., Amelkina N.F. Mutagenic activity of ethylene diamine on soft wheat depending on the impact of the exposure. Post II. Violations chromosome mitotic activity of the cells // *Cytology and Genetics*. – 2000. – Vol. 34, No.4. – P. 141-147.
6. Pausheva Z.P. Retainer: composition and use. Workshop on plant cytology. – M.: Kolos, 1970. – P. 62- 67.
7. Dospheov V.A. Methods of field experience. – M.: Agropromizdat, 1985. – 351 p.
8. Plohinsky N.A. Mathematical methods in biology. – M.: Kolos, 1970. – P. 102-115.

UDC 541.64

Negim E.S.M.<sup>1\*</sup>, Nurlybayeva A.<sup>2</sup>, Irmukhametova G.S.<sup>3</sup>, Makhatova A.<sup>1</sup>,  
Basharimova A.<sup>1</sup>, Serikkali A.<sup>1</sup>, Sakhy M.<sup>2</sup>, Iskakov R.<sup>1</sup>, Mun G.A.<sup>3</sup>

<sup>1</sup>School of Chemical Engineering, Kazakh-British Technical University, 106 Walikhanov Street, Almaty, 050010, Kazakhstan

<sup>2</sup>Taraz State University named after M.H. Dulati, 60 Tole Bi Street, 080000 Taraz, Kazakhstan

<sup>3</sup>Department of Chemistry & Technology of Organic Materials,

Polymers and Natural Compounds, al Faraby Kazakh National University, 71, al-Faraby av., 050040, Almaty

\*e-mail: elashmawi5@yahoo.com

### Effect of methyl methacrylate and butyl methacrylate copolymer on the physico-mechanical properties of acryl syrup for paints

**Abstract:** The present study deals with the physico-mechanical properties of acryl syrups paint, which are made from copolymer powder and methyl methacrylate (MMA) monomer. Copolymer powders were used based on MMA and butyl methacrylate (BMA). The effect of copolymer powder to MMA- monomer ratio on the physico-mechanical properties acryl syrup mixes for paint applications was investigated. Testing included pot-life, curing time, viscosity, tensile strength, elongation, water absorption and hardness shore A. The results showed that, not only monomer composition of the copolymer but also the ratio of copolymer to MMA-monomer affected the physico-mechanical properties of acrylic films. The tensile strength, hardness, pot-life, curing time and hardness of the acrylic film increased with the increase of the MMA ratio in copolymer and decrease content of copolymer in acrylic syrup mixes. In conclusion, low copolymer content and high MMA ratio in copolymer (MMA/BMA) powders are desired to produce paint with physico-mechanical properties.

**Key words:** polymethyl methacrylate, syrups, self-curing, acrylic paint

#### Introduction

Poly(methyl methacrylate), PMMA, a kind of thermoplastic materials and self-curing for short, is an important polymer in the building industry as well as in other industries due to its excellent properties, such as transparency, lightness and safety. Typical applications are in architectural coatings, additives and polishing agents, binder, sealer, transparent neutron stopper, optical fiber, high-voltage application, and outdoor electrical application [1-5]. PMMA is classified as a hard, rigid, but brittle material, with a glass transition temperature of 105°C. PMMA has good mechanical strength, acceptable chemical resistance, and extremely good weather resistance [6]. PMMA has favorable processing properties, good thermoforming, and can be modified with pigments, flame retardant additives, UV absorbent additives, and scratch resistant coatings [7-10]. However, the physical and mechanical properties of PMMA limit its applications due to its brittleness nature [11-14]. Thus, modification of PMMA has attracted a great amount of attention from researchers all over the world, and the study of poly (methyl methacrylate) (PMMA) is a representative work in this research

field. In order to enhance its mechanical properties, scientists have developed various methods to prepare different types of PMMA through the copolymerization of MMA monomer with various types of vinyl monomers [15-17]. Self-curing PMMA are materials formulated by the mixing of two-component, one solid (powder) based on PMMA spherical beads and another liquid includes monomer and an initiator to enable the polymerization reaction to occur at room temperature and a high level of heat being generated during the exothermic reaction. In self-curing, the polymerization reaction of methacrylate monomers is initiated by the activation reaction of BPO, with an amine accelerator at room temperature, which gives free radicals for addition to monomer molecules [18]. A high level of heat being generated during the exothermic reaction [9]. Authors [19] prepared copolymer latexes based on methyl methacrylate (MMA) and butyl methacrylate (BMA) using macro-radical initiator technique. Different ratios of acrylic monomers were designed to investigate the effect of monomer compositions on physico-mechanical properties of acrylic films for paint application. The results showed that, physico-mechanical properties increased with increasing the ratio of MMA in the co-

polymer. The work was further extended to include the application of the obtained copolymer latexes to make acrylic syrups containing varying content of MMA-monomer to be self curing and modify physico-mechanical properties of paint solvent free.

## Experimental

### Materials

Methylmethacrylate (MMA) monomer (supplied by Fluka), benzoyl peroxide (BPO) (supplied

by Melbourne), N,N-dimethyl-p-toluidine (DMPT) (supplied by Fluka) and hydroquinone (HQ) (supplied by Merck) were used as purchased.

Synthesis and Characterization of Copolymer Latexes.

The preparation of copolymer latexes and the methods of analysis ( $^1\text{H}$  NMR, FT-IR, DSC, TGA and SEM) have been previously described [19]. The mix proportion of monomers in the copolymer and basic properties of synthesized copolymer are shown in Table 1.

**Table 1** – Properties of P(MMA-co-BMA) [19]

Sample No.	MMA	BMA	$T_H$	$T_{max}$	$T_k$	$T_c^a$	$T_c^b$	Appearance
			°C					
M1	10	90	325	425	450	34.15	43.30	Powder
M2	50	50				57.12	63.10	
M3	90	10				94.34	98.40	

$T$  Initial decomposition temperature.

$T^H$  Maximum rate of temperature for weight loss.

$T^{max}$  The final temperature of the decomposition.

$a^b$  Predicted using Fox equation.

$b^b$  Measured using DSC.

### Preparation of copolymer syrups

Copolymer syrup was produced by dissolving copolymer (MMA/BMA) and BPO into MMA monomer at normal temperature (25°C). Then, a liq-

uid component was produced using MMA monomer, DMPT and HQ. BPO and DMPT were added at 1.5 and 0.75 parts per hundred (pph) to syrup to act as initiator and accelerator, respectively. HQ was added in the syrup as an inhibitor. Paraffin wax was added 1% wt. of syrups. This copolymer syrup was then placed into the liquid component mixed with ratio 10/90, 15/85 and 25/75% wt/wt to maintain the mixing ratio at 100% as shown in Table 1.

**Table 2** – Formulation of copolymer syrup for acrylic paint

Group	Syrups	Copolymer (Powder, gm)	MMA (Liquid, gm)
Group 1	Syp10/M1	10	90
	Syp10/M2	10	90
	Syp10/M3	10	90
Group 2	Syp15/M1	15	85
	Syp15/M2	15	85
	Syp15/M3	15	85
Group 3	Syp25/M1	25	75
	Syp25/M2	25	75
	Syp25/M3	25	75

### Film preparation

Films were prepared by casting the acrylic syrups on leveled surfaces and allowing them to dry at room temperature for 3 hours. The films were stored in a desiccator at room temperature for further characterization and measurements.

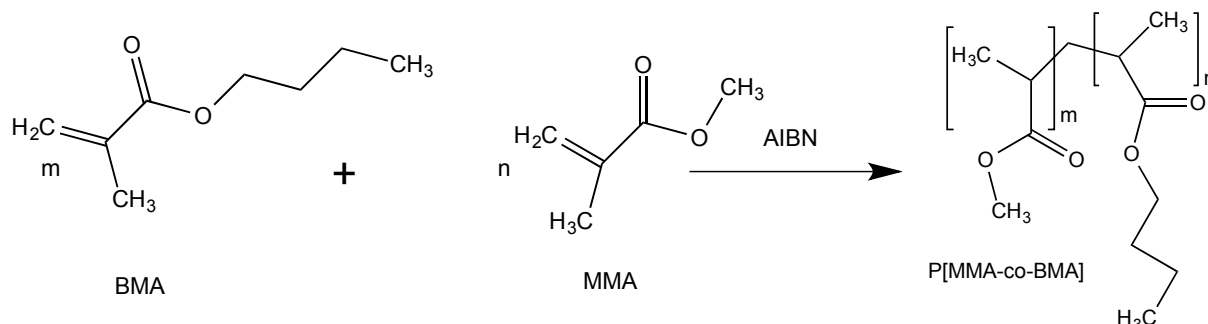
### Tests

The pot-life of fresh copolymer syrup was determined at 25 °C according to the finger-touching method prescribed in KS F 2484. The curing time of acrylic films was determined according to ASTM D5895. The viscosity ( $\eta$ ) of the dispersions was measured using a Brookfield viscometer (Model LVTDV-II) at a shear rate of 100 S<sup>-1</sup> at 25 °C. The contact angle formed between the water drops and the surface of the sample was measured using contact angle measuring system CAHN DCA-322 analyzer operated at 25 °C with water drop, and a velocity of 100  $\mu$ m/s. The drop of water was mounted on the surface to be tested with a micro-syringe and contact angle was measured from the view of water drops as observed on monitor. Results are the mean value of three measurements on different parts of the

film. The tensile properties of the acrylic syrup films were measured by using MTS 10/M tensile testing machine at a crosshead speed of 50 mm/min. An average of at least 4 measurements was taken and the 1-kN load cell was used. Shore A and D hardness was measured using an indentation hardness tester according to ASTM D2240-75. Water absorption test was according to BS 1881-122:2011.

## Results and their discussion

**Structure of copolymers.** The structure of the copolymer latexes based on methyl methacrylate (MMA) and butyl methacrylate (BMA) is shown in Scheme 1. The copolymer latexes were synthesized with different ratios (M1=10/90, M2=50/50 and M3=90/10 respectively) using azobisisobutyronitrile (AIBN) as free radical initiator. The properties of the prepared copolymer latexes have been previously reported by authors [19]. The results showed that physico-mechanical properties of the copolymer were increased by increasing the ratio of MMA in the copolymer latexes.



**Scheme 1** – General reaction for the synthesis of MMA/BMA copolymer [19]

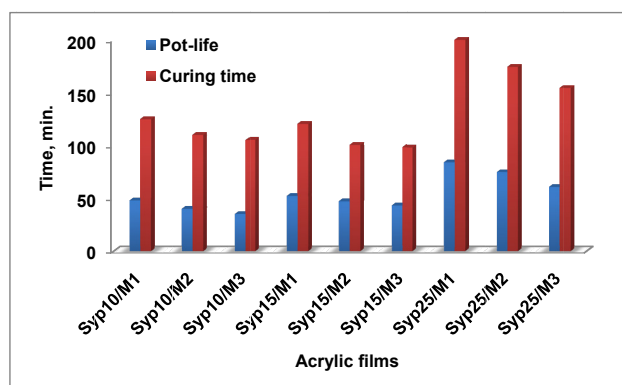
### Pot-life and curing test

Pot-life of acrylic films is the length of time in which the flow properties (such as, viscosity) of catalyzed syrup will no change within an acceptable for application. Pot-life and cure time of acrylic films (M1, M2 and M3) are measured in the lab at an ambient temperature of 25°C. Figure 1, shows a sharp decrease in pot-life and cure time of acrylic films with increasing MMA in copolymers backbone. Acrylic film (Syp25/M1) with (10% MMA) in group 3 where the content of copolymer 25% gave longest pot-life and cure time, while acrylic syrup (Syp10/M3) with (90% MMA) in group 1 where the content of copolymer 10% gave shortest pot-life and cure time. It is well that the pot-life and cure time of acrylic syrups

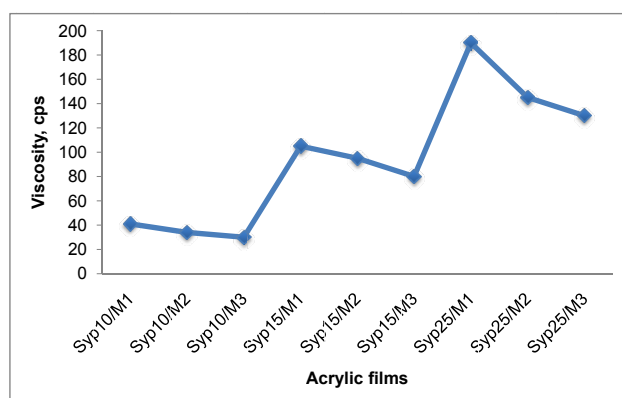
are affected by fee composition of acryl syrups such as copolymer and MMA monomer. The same behavior was reported by Jaafar and Hamizad [8] when they studied the effect of PMMA powder to liquid monomer on the properties of PMMA cement.

**Viscosity.** The effect of content of copolymer (MMA/BMA) with different composition (M1, M2 & M3) on the viscosity of syrups is shown in Figure 2. The results showed that the viscosity increased with increasing of BMA in copolymer backbone. However, the viscosity increased with increasing content of copolymer from 10% to 25%. With respect to the content of monomers and copolymer used in different composition ratios with MMA monomer to prepare paint syrups, it is evident that viscosity

values for [Syp10/M3], which contain 10% wt.% of copolymer M3 (MMA/BMA, 90/10) in group 1 is lowest one (30 cps), whereas [Syp25/M1] which contain 25% wt.% of copolymer M1 (MMA/BMA, 10/90) in group 3 is the highest one (190 cps). These results reflect differences among copolymer studied with respect to chemical structure, average molecular weight, configuration and orientation of the molecules, molecular weight distribution, polarity and chain branching. Acrylic syrups are mainly used in coatings. In acrylic, viscosity is important parameter. A suitable viscosity range is required to avoid sagging (in case of low viscosity) and practical difficulty in application (encountered with high viscosity).



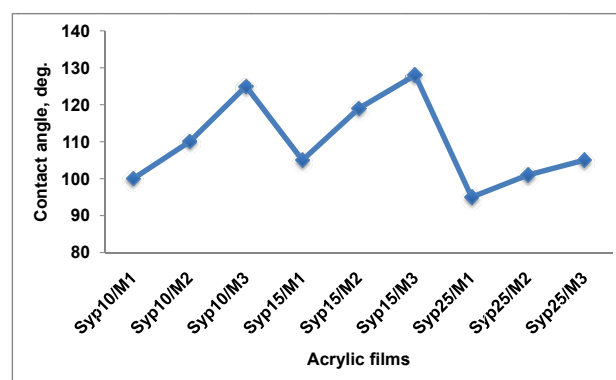
**Figure 1** – Pot-life and curing time of acrylic films containing different content of copolymers M1, M2 and M3.



**Figure 2** – Viscosity of acrylic syrups with different content of copolymer M1, M2 and M3.

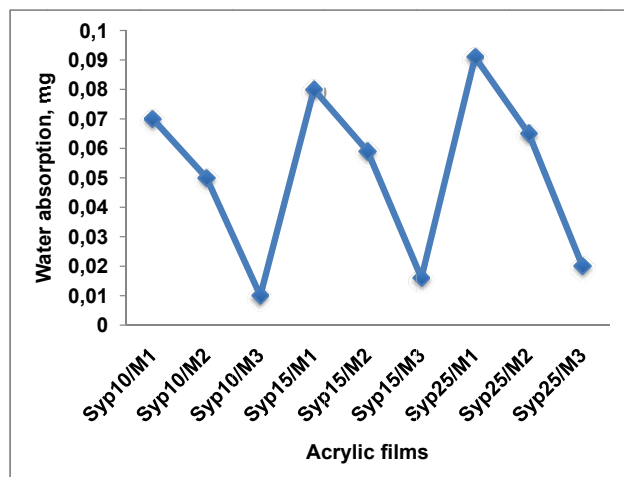
**Contact angle.** Advancing and receding contact angle measurements of the films cast from acrylic could provide more information on the hydrophilicity of dried cast films [20-23]. A better understanding of the hydrophobicity of the cast films could be ob-

tained from dynamic contact angle studies rather than from swelling studies. Figure 3 shows the measured contact angle for a drop of water on acrylic surfaces increase with increasing MMA in copolymer backbone. Syp10/M3 with 90% MMA gave the highest contact angle with 125 deg. while Syp10/M1 with 10% MMA gave contact angle of 100 deg. in-group 1. The hydrophobicity increased with the decreasing amount of copolymer in acrylic syrup. The results confirm that chain rigidity is a more significant factor in controlling the contact angle, because chain rigidity does not allow the ionic groups to come near the particle surface. Generally, if the water contact angle is smaller than  $90^\circ$ , the solid surface is considered hydrophilic and if the water contact angle is larger than  $90^\circ$ , the solid surface is considered hydrophobic.



**Figure 3** – Contact angle of acrylic films containing different content of copolymers M1, M2 and M3

**Water absorption.** Dynamic wetting tests were performed on a Camtel CDCA-100F dynamic adsorption apparatus (Camtel, UK). Each sample was cut to a size of  $1\text{ cm} \times 5\text{ cm}$  with sharp scissors. When the specimen was immersed into water for 2 months, the weight of adsorbed water was detected and recorded. The dynamic water adsorption was plotted as a function of feed composition of monomers. The results of the water adsorption tests reveal the dynamic wetting behavior of the acrylic films. The acrylic films show a very low adsorption, as shown in Figure 4. However, the water absorption of acrylic films decreased with increasing the amount of MMA in copolymer backbone in acrylic syrup. For example, the water absorption for Syp10/M3 (90% MMA) is 0.01mg and for Syp10/M1 (10% MMA) is 0.07 mg in-group 1. Also, water absorption of acrylic films in-group 1 is lower than that of group 3 as shown in Figure 4. The water absorption of Syp25/M3 (90% MMA) in-group 3 is 0.02 mg.

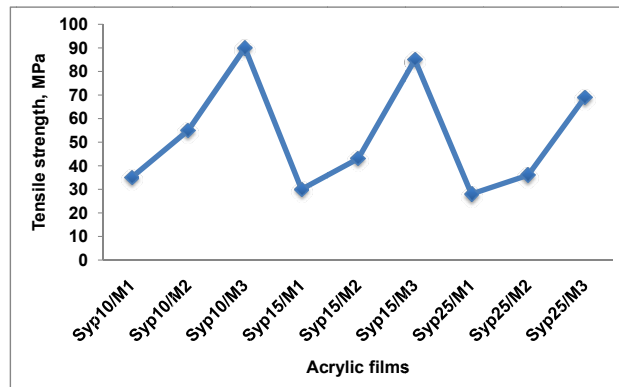


**Figure 4** – Water absorption of acrylic films containing different content of copolymers M1, M2 and M3

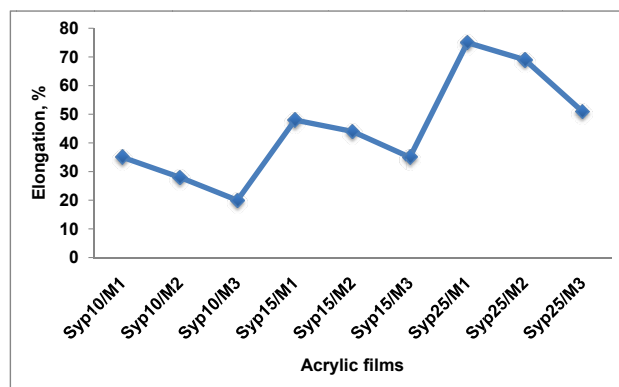
**Tensile and elongation.** Figure 5 shows that the tensile strength increased with increasing the content of MMA in copolymer backbone. For example the tensile strength of Syp10/M3 (90% MMA) is 90 MPa and this drops down to 55 and 35 MPa for the Syp10/M2 (50% MMA) and Syp10/M1 (10% MMA) containing 10% copolymer in-group 1. This is presumably due to the increased hard segment contents (MMA) in acrylic film. However, tensile strength of acrylic films decreases with increasing the content of copolymer in acrylic film. Syp25/M3 containing 25% copolymer shows substantially lower tensile strength than the Syp10/M3 containing 10% copolymer. Also, tensile strength of acrylic films affected by viscosity of acrylic syrup, whereas tensile strength decreased with increasing viscosity of acrylic syrup.

On the other hand the elongation of acrylic films decreased with increasing MMA in the copolymer backbone as shown in Figure 6. This is attributed to the increasing of flexible chain (BMA) with low  $T_g$  in the copolymer backbone. However, elongation increased with increasing the content of copolymer (MMA/BMA) in acrylic syrups. Also viscosity of acrylic syrup affected the elongation tests where the acrylic syrup with high viscosity (Syp25/M1) has longest elongation as shown in Figure 6.

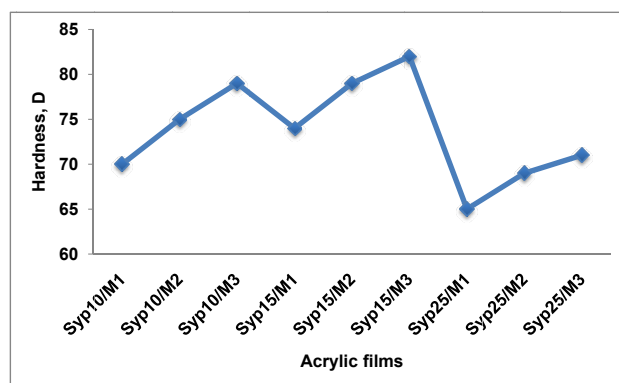
**Hardness.** The results in Figure 7 show increase in hardness shore (D) with increasing of MMA in copolymer backbone of acrylic films. However, the hardness is affected by the content of copolymer. The surface hardness for acrylic film produced by Syp10/M3 in-group 1 (10%, 90/10 MMA/BMA) was found ca. 79, while that for acrylic film produced by Syb10/M3 in-group 3 (25%, 90/10 MMA/BMA) was found ca. 71.



**Figure 5** – Tensile strength of acrylic films containing different content of copolymers M1, M2 and M3.



**Figure 6** – Elongation of acrylic films containing different content of copolymers M1, M2 and M3



**Figure 7** – Hardness of acrylic films containing different content of copolymers M1, M2 and M3

## Conclusion

In this study, acrylic syrups with an MMA solution of copolymer (MMA/BMA) as a resin and physico-mechanical properties of the syrups were



evaluated. The results obtained in this study are summarized as follows:

The pot-life, cure time, tensile, hardness shore D and water absorption of the syrup films increased with increasing MMA in copolymer backbone and decreasing the content of copolymer in syrup mixes. This is presumably due to the increased hard segment contents (MMA) in acrylic film.

The viscosity and elongation of the syrups increased with the increase BMA in the copolymer backbone and content of copolymer in syrup mixes. This attributed to the increased soft segment contents (BMA) in syrup mixes.

Monomer compositions of polymers played important role in specific characteristics of polymer films used in paint applications.

### Acknowledgements

The work was financially supported by Ministry of Science and Education of the Republic of Kazakhstan, project No. 0115PK01660.

### References

1. C. Mehmet, P. Seven, *Reac. Funct. Polym.*, 2011. – Vol. 71. – P. 395–401.
2. M.S. El-Shall, V. Abdelsayed, A.S. Khder, H. Hassan, H.M. El-Kaderi, T.E.J. Reich. *Mater. Chem.*, 2009. – Vol. 19. – P. 7625–7631.
3. J.R. Potts, S.H. Lee, T.M. Alam, J. An, M.D. Stoller, R.D. Piner, R.S. Ruoff. *Carbon*, 2011. – Vol. 49. – P. 2615–2623.
4. R.D. Priestley, C.J. Ellison, L.J. Broadbelt, J.M. Torkelson. *Science*, 2005. – Vol. 309. – P. 456–459.
5. R.P. Kusy. *J. Biomed. Mater. Res*, 1978. – Vol. 12. – P. 271–276.
6. DR. Paul, DW Fowler, JT Houston, *J. Appl Polym. Sci*, 1973. – Vol. 7. – P. 2771–2782.
7. E.P. Sang, C. Maggie, P.A. Raj. *International Journal of Dentistry*, 2009. – Vol. 2009. – P. 1-9.
8. A.S. Hamizah, J. Mariatti. *Polymer-plastics technology and engineering*, 2009. – Vol. 48. – P. 554–560.
9. N.J. Dunne, J.F. Orr. *ITBM-RBM*, 2001. – Vol. 22. – No. 2. – P. 88–97.
10. D.W. Fowler, A.H. Meyer, D.R. Paul, Low temperature curing of polymer concrete. In: *Proceedings of the second international congress on polymers in concrete*. Koriyama, Japan: College of Engineering, Nihon University, 1981. P. 421–434.
11. G. Odian. *Principles of Polymerization*. New York, 1991.
12. K.S. Murthy, K. Kishore, V.K. Mohan. *Macromolecules*, 1994. – Vol. 27. – No. 24. – P. 109-7114.
13. J.D. Peterson, S. Vyazovkin, C.A. Wight, *Journal of Physical Chemistry B*, 1999. – Vol. 103. – P. 8087-8092.
14. I. Soten, G.A. Ozin, *J.Mater.Chem.*, 1999. – Vol. 9. – No. 3. – P. 703-710.
15. P. Ghosh, S.K. Gupta, D.N. Saraf. *Chem. Eng. J.*, 1998. – Vol. 70. – P. 25-35.
16. F. Zhou, S.K. Gupta, A.K. Ray, *J. Appl. Polym. Sci.*, 2001. – Vol. 81. – P. 1951-1971.
17. P. Peyser, J. Brandrup, E.H. Immergut, Eds. *Polymer Handbook*, 3rd ed. Wiley-Interscience, New York, 1989, p. VI/219.
18. S.T. Balke, A.E. Hamielec, *J. Appl. Polym. Sci.*, 1973. – Vol. 17. – P. 905-949.
19. A. Nurlybayeva, M. Sakhy et al. *Int. J. Chem. Sci.*, 2015. – Vol. 13. – No. 2. – P. 922-934.
20. Y. Yuan, P. Lee. *Surface Science Techniques*, 2013. – Vol. 51. – P. 3-34.
21. L. Valentini et al. *Small*, 2007. – Vol. 3. – P. 1200.
22. C. Joachim, J.K. Gimzewski, A. Aviram. *Nature*, 2000. – Vol. 408. – P. 541.
23. A. Méndez-Vilas, A.B. Jódar-Reyes, M.L. González-Martín, *Small*, 5, 1366, (2009).

Baiseitov D.A.<sup>1</sup>, Gabdrashova Sh.E.<sup>1</sup>, Magazova A.N.<sup>1</sup>,  
Dalelhanuly O.<sup>1</sup>, Kudyarova Zh.B.<sup>1</sup>,  
Sassykova L.R.<sup>1</sup>, Tulepov M.I.<sup>1\*</sup>, Mansurov Z.A.<sup>1</sup>, Dalton A.B.<sup>2</sup>

<sup>1</sup>Faculty of chemistry and chemical technology, Al-Farabi Kazakh National University, Almaty, Kazakhstan

<sup>2</sup>University of Surrey, Guildford, United Kingdom

\*e-mail: tulepov@rambler.ru

## Thermogravimetric investigation and selection of catalyst of coal hydrogenation

**Abstract:** Thermo gravimetric study of coal in the presence of polymers showed that availability of high asphalt-resinous components – asphaltenes and resins benzene within the temperature of 360 – 443°C in the content was reduced. The optimum catalytics of coal hydrogenation is the compositions on the basis of Pd / C, at which there was the greatest absorption of hydrogen and Co / C, where the hydrogenation rate was maximum.

**Key words:** coal, polymers, hydrogenation, paste-head, Balkhash concentrate catalysts.

### Introduction

The efficiency and effectiveness of performance of coal hydrogenation process at an industrial environment is carried out with great difficulties. Except the importance of features and structure of the original coal, a macro kinetic choice of pressure's modes, temperature and catalysts also has a great value.

The aim of majority processes of coal's chemical recycling (with the exception of the production of carbon materials) is its conversion into low molecular organic products, with a quite homogeneous composition. The conversion of coal into the more organic compounds can be achieved under the heat treatment and exposure to different reagents [1, 2]. During the heating process the weak aliphatic chains, which bind condensed aromatic structures, are usually disrupted primarily. The disruption of carbon-oxygen bonds has a decisive contribution during the process of depolymerization of brown coal.

Management of the reactions of disruption of certain bonds can be done by selective introduction of metal catalysts into the functional groups of the coal substance. For example, the temperature of aliphatic bond's disruption, which connects two aromatic fragments, reduces if a divalent metal cation replaces the protons of two neighbour phenolic groups.

The main disadvantages of known techniques of chemical recycling of coal compared with the technologies of oil refining and petrochemical are a relatively low productivity and stringent conditions for their implementation (high temperature and pres-

sure). To eliminate these shortcomings in the coal recycling, there is a wide spread usage of catalysts and new catalytic processes, which allows to obtain variety products from coal with a fuel and chemical features [3-8].

### Experimental part

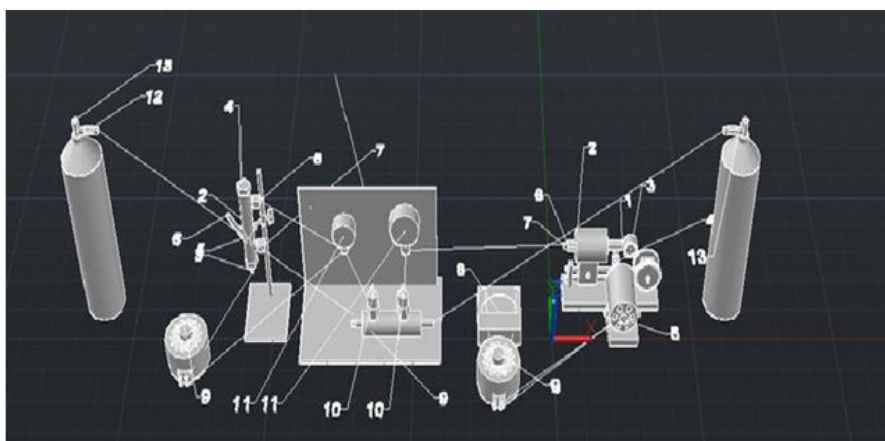
The experiment was conducted as following: 5 g of a mixture of dry brown coal from Karazhirskeyi field was subjected to mechanical activation with a particle size of less than 0.1 mm, then a polyethylene with a particle size less than 0.5 mm, which was taken in an amount of from 10 to 70 wt.% by weight of a mixture of coal – polyethylene, were placed in a steel autoclave rotary with a volume of 0.5 l. The substances as Pd, Co, Mo and Fe were added as catalysts.

The autoclave was closed and the hydrogen was supplied until achieving a pressure of 5.0 MPa. The autoclave was heated to 430°C with continuous stirring, then it was kept at this temperature during 60 minutes, while the pressure in the autoclave was 6.0 MPa. After that, the autoclave was cooled and the gaseous products were separated. Then, the fraction, which was boiling up to 200°C, was separated from autoclave, and it was freed out in a nitrogen trap. The solid product was separated and filtered.

Thermogravimetric studies were performed under the following experimental conditions: weight of the sample – (0.3 ± 0.03 g); analytical grinding; ceramic crucible with a lid, height of which is 15 mm and diameter 5 mm. Processing of the derivatograms in-

cluded analysis of thermogram. The weight loss of the sample at a given temperature was determined according to the thermogravimetric curve. The rate of mass loss was determined in accordance with a

differential thermogravimetry, temperature highs endo – or exo – effects – according to a differential thermogravimetric adsorption in line with standard procedures.



1 – reactor with a rotating autoclave, 2 – oven, 3 – manometer measuring the pressure at the outlet  
4 – tap to collect gases, 5 – stationary reactor, 6 – bush for measuring the temperature in the stationary reactor, 7 – thermocouple for temperature control in a rotating reactor,  
8 – manometers for temperature control, 9 – LATRS, 10 – taps for establishing pressure in the reactor,  
11 – manometer for controlling the pressure in the reactors, 12 – reducers to control the gas flow,  
13 – cylinders of compressed argon and helium gases.

**Figure 1** – Installation for hydrogenation in a stationary reactor and in a rotating autoclave

## Results and their discussion

Thermogravimetric analysis was performed for the samples of original materials: solid polymeric products and coal material. A measurable weight loss curves (TG curves), and mass loss rate (DTG curves) were calculated on the basis of 1 g of the original sample and manifested as the temperature dependence, the nature of which is illustrated by the given thermograms (Figure 2.3). On the basis of DTG curves, the temperature ( $T_{max}$ ) was determined in correspondence to the maximum rate of weight loss. In this paper, the weight loss is identical to the output of volatile products and the rate of mass loss is equivalent to the rate of release of volatile products during the heating.

When grinding coal from Karazhir field, there were identified some general patterns, which are well observed by differential thermogravimetric curves after mechanical processing of coal in the mill.

Thermogravimetric curves (Figure 2.4) have a one minimum indicating to dehydration at the temperatures 109–116°C.

During the mechanical impact on coal, along with a change in the total amount of soluble fractions, their composition and structure are also changes, compared with the fractions of the original coal.

The following stages of the transformation of coal from «Karazhir» field, after mechanical activation in the presence of a catalyst based on Fe and hydrogen-donor solvent tetralin have been established by the method of gravimetric study: 1) Dehydration at temperatures 109°C; 2) thermal decomposition of a macro molecular structure of coal with formation of the radical fragments of 272–385°C; 3) recombination of these radicals with formation of high molecular products, saturation of radicals as a result of hydrogenation reactions by molecular hydrogen or by a hydrogen of hydrogen-donor solvent with formation of a low molecular products at the temperature range of 559–619°C.

Thermogravimetric study of coal in the presence of polymers (Figure 4) showed that the presence of high asphalt-resinous components – asphaltenes and benzene resins at the range 360–443°C was reduced in their content.

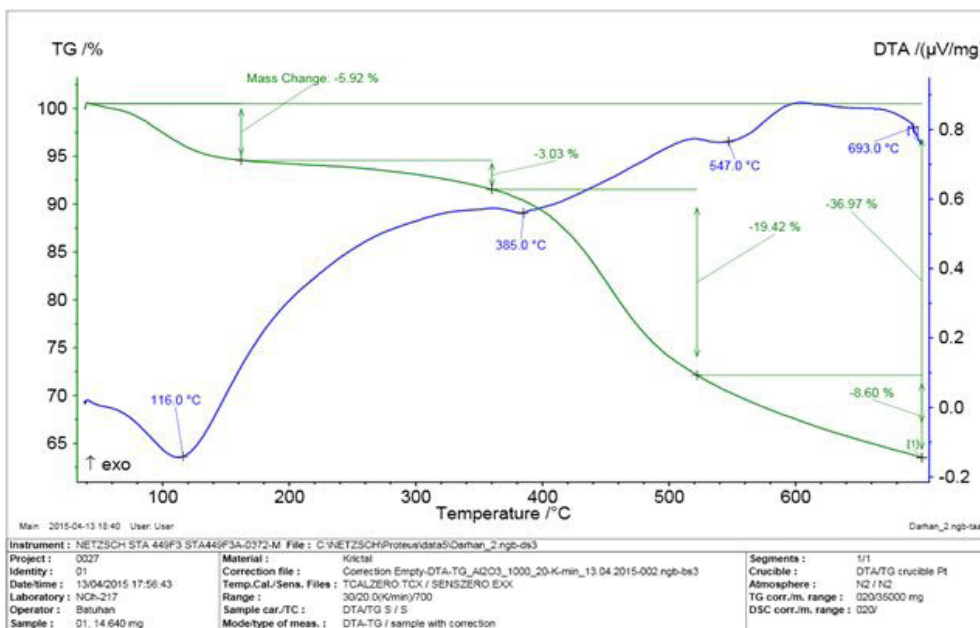


Figure 2 – Thermogravimetric study of the original coal

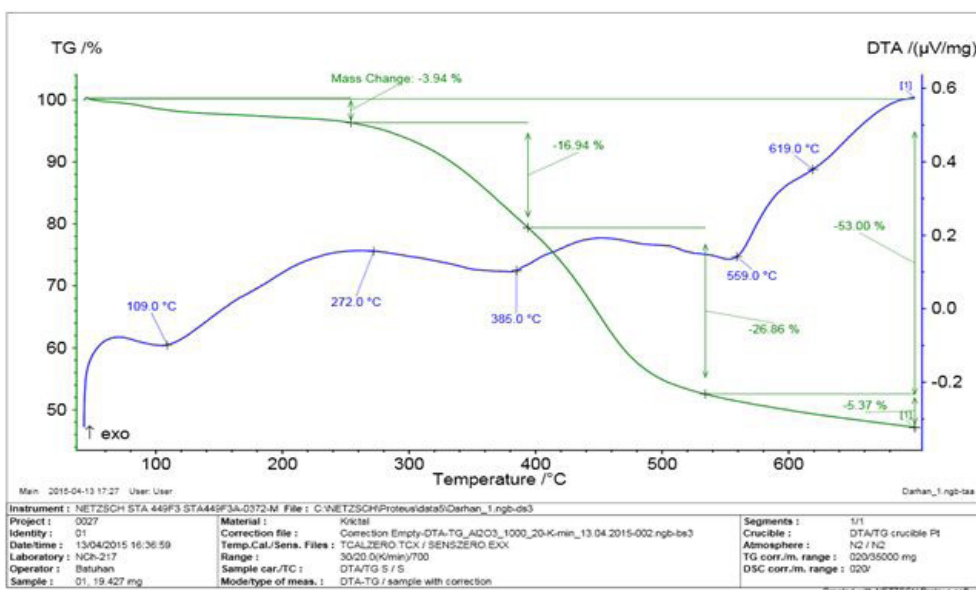


Figure 3 – Thermogravimetric studies of coal conversion after mechanical activation in the presence of a catalyst BC

Role of the components with lower molecular weight – benzene resins and oils was increased as a result of thermal effects in the bitumen. The pres-

ence of light petroleum-ether resins and aromatic hydrocarbons within the range of 443–527°C was increased in the content of the oil fraction.

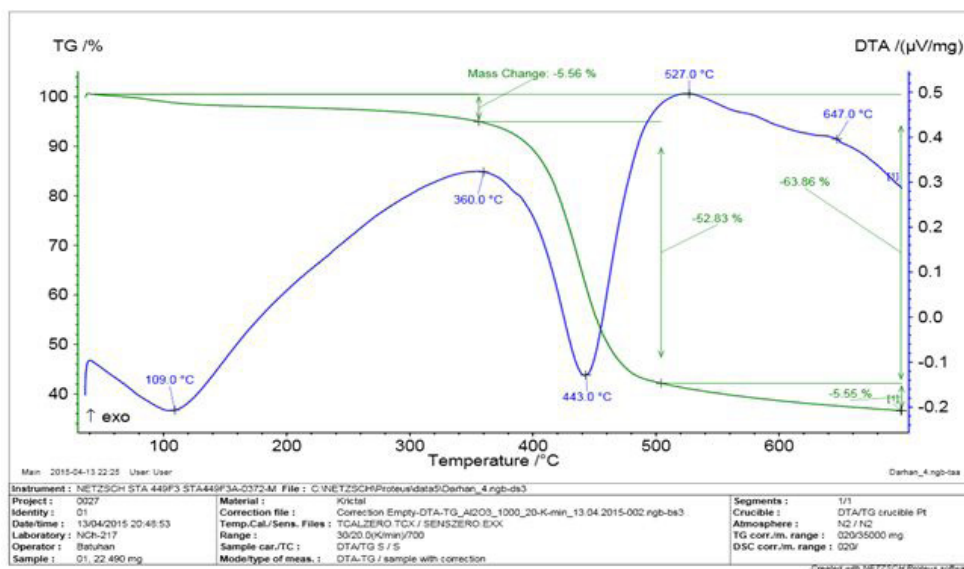


Figure 4 – Thermogravimetric studies of coal and polymers conversion

Thus, it was found that the iron catalysts promoted thermal decomposition of organic mass of coal.

Series of experiments was performed with the aim to select the optimum composition of the catalyst.  $Al_2O_3$  and carbon were used as the carriers, while Pd, Co, Mo and Fe were used as an active phase. The percentage of metal in all of the catalyst was 5%. The experiment was conducted at a temperature of 325°C and a pressure of 5 MPa.

During the hydrogenation of the original material at all catalysts, there is a direct relationship between the hydrogen absorption and duration of the experiment. The maximum result was observed at the catalyst containing Pd and was  $V_{H_2} = 27.4$  mmol (Figure 5).

In terms of swallowed hydrogen, catalysts are arranged in the following order:

Pd/C (27.4 mmol) > Co/C (19.6 mmol) > Mo/C (12.6 mmol) > Fe/C (5.3 mmol)

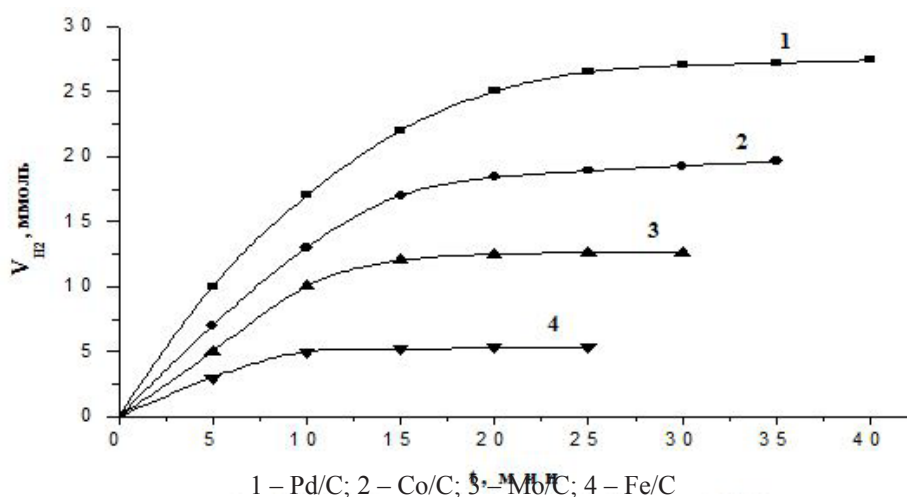


Figure 5 – The dependence of the absorption of hydrogen from the duration of the experiment at different catalysts with 5% metal content

Characteristically, with the duration of the experiment the catalysts arrange in the same sequence. In contrast to hydrogen absorption, the maximum rate of hydrogenation is observed on Co-containing catalyst and is 47.2 mmol/min\*g CT (Figure 6).

Figure 6 shows that the maximum hydrogenation speed of the first three catalysts are observed on the 4th minute of hydrogenation, after that

the rate is sharply fell and in the range of 15–40 min is almost unchanged. On the catalyst of Fe/C hydrogenation takes place at the lowest rate, the maximum of which is observed at the 2-nd minute of hydrogenation and it is 18.7 mmol/min\*g CT, which is ~ 2.5 times lower than the maximum speed observed on the most active Co-containing catalyst.

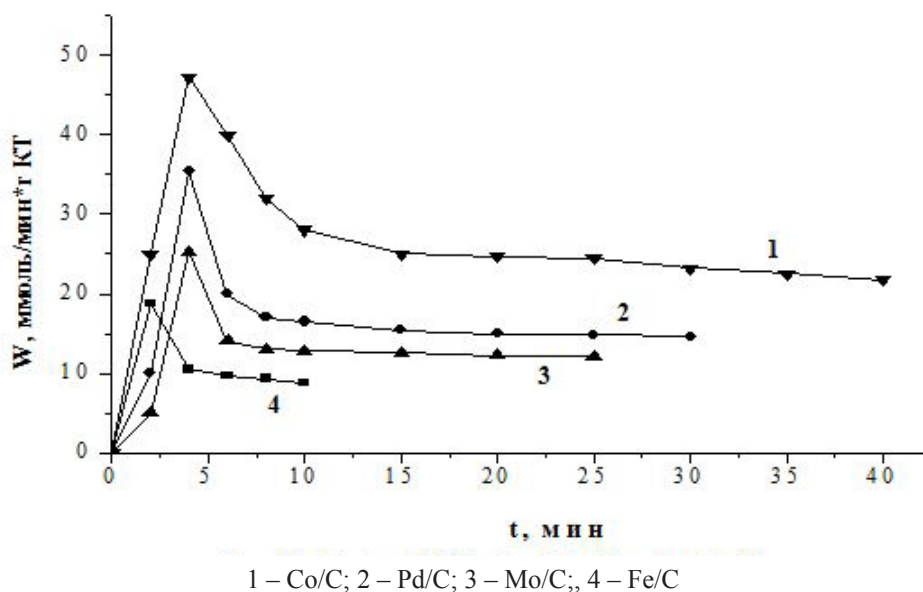


Figure 6 – The dependence of the rate of hydrogen uptake from the experiment time on the different catalysts

## Conclusion

Thus, based on the results of experiments, the highest activity still have catalysts on the basis of Pd/C, at which there was the greatest absorption of hydrogen and Co/C, in which the hydrogenation rate was the highest.

## References

1. Kuznetsov B.N. Catalysis of chemical reactions of coal and biomass. – Novosibirsk: Nauka. Sib. Office, 1990. – 302 p.
2. Liu Z.Y., Zondlo J.W., Stiller A.H., Dadyburjor D.B. Coal Tire Coliquefaction Using an Iron Sulfide Catalyst Impregnated in Situ in the Coal // *Energy and Fuels*, 1995. – Vol. 9. – P. 673-679.
3. Abotsi G.M., Bota K.B., Saha G., Mayes S. Effects of Surface Active Agents on Molybdenum Adsorption onto Coal for Liquefaction // *Prepr. Pap.-Am. Chem. Soc., Div. Fuel Chem.*, 1996. – Vol. 41. – P. 984-987.

4. Liu Z., Yang J., Zondlo J.W., Stiller A.H., Dadyburjor. D.B. *In situ* impregnated iron-based catalysts for direct coal liquefaction // *Fuel*, 1996. – Vol.75. – P. 51-57.

5. Jandosov J., Mansurov Z.A., Tulepov M.I., Bisenbaev M.A., Ismagilov Z.R., Shikina N.V., Ismagilov I.Z., Andrievskaya I.P. Syntesis of microporous –mesoporous carbons from rice husk via  $H_3PO_4$ - Activation // *Periodical of Advanced Materials Research*, 2013. – Vol. 602-604. – P. 85-89 (Thomson Reuters impact factor 1).

6. Kudaibergenov Kenes, Ongarbayev Yerdos, Mansurov Zulkhair, Tulepov Marat, Tileuberdi Yerbol. Rice Husk Ash for Oil Spill Cleanup // *Applied Mechanics and Materials*, 2014. – Vol. 446-447. – P. 1508-1511.

7. Kudaibergenov Kenes, Ongarbayev Yerdos, Tulepov Marat, Mansurov Zulkhair. Scanning Electron Microscopic Studies of Carbonized Rice Husk And Apricot Stone // *Advanced Materials Research*, 2014. – Vol. 893. – P. 478 – 481.

UDC 556.114

Romanova S.M., Akanova G.Z.\*

Al-Farabi Kazakh National University, Almaty, Kazakhstan

\*e-mail: gulsara\_48@mail.ru

### Removal of mineral salts (including bicarbonate calcium and magnesium) from Ulken Almaty and Kishi Almaty rivers

**Abstract:** For evaluated some components of hydrochemical balance watercourses necessary to carry out the calculation flow of chemicals, which is very important not only for biological productivity, but also studied intensity of erosion and accumulation processes occurring in the basin. It was learned of long-term dynamics of this process can also deeper understanding the nature of the influence of those or other lithological and anthropogenic factors in the basin on the formation of chemical composition and quality of the river water. The article presents data on the flow of dissolved mineral substances, including calcium and magnesium carbonates, rivers Ulken Almaty, Kishi Almaty in comparison to other rivers of northern slope of Ili Alatau (Shilik, Turgen, Esik, Esentai) over many years. It was established that during the period from 2009 to 2010 years water of Ulken Almaty upstream 5,486 tons of mineral salts, and in the downstream – 7,135 tons, and the share of calcium bicarbonate (calculated of calcium carbonate) have an average of 68% of all salts. Kishi Almaty river in the upstream 4,776 tons (including calcium bicarbonate – 4,080 tonnes) and downstream – 29,520 tons (including 18,745 tons of calcium bicarbonate).

**Key words:** calcium carbonate equilibrium, removal mineral salts, ion flow, water flow, water consumption

#### Introduction

Removal of calcium and magnesium carbonate salts is part of the remove of mineral salts. To calculate the removal of carbonate salts necessary to investigate the carbonate calcium equilibrium in the river waters. The results of systematic hydrological observation and monitoring of water quality of the rivers of northern slope of the Ile Alatau possible to calculate flow minerals from the territory of the river basins in Kapshagai reservoir. Calculation chemical substances of flow is great importance not only for the assessment of a number of components of the chemical balance and biological productivity of basins, but also for the knowledge intensity of erosion and accumulation processes occurring in the basin. In this regard, the study of long-term dynamics of this process makes it possible to deeper understanding the nature of the influence of those or other lithological and anthropogenic factors in the basin on the formation of the chemical composition and quality of the river water.

L.V. Brazhnikova, B.A. Beremzhanov and M.A. Ibragimova to investigate the data on the ion flow for rivers all Balkash basin for 1936-1949 y. [1, 2] and 1961-1968 years. [3]. A.N. Nevskaya calculated ion flow of 17 rivers arid areas of Kazakhstan and it is established that during the peak of the flood goes up to 80% of the ion flow [4].

Ion flow of rivers of northern slope of the Ili Alatau after 1968 was not calculated. In this regard, we have calculated the flow of mineral salts, nutrients and organic matter, microelements for rivers Shilik, Turgen, Ulken Almaty, Kishi Almaty and Esentai for 2000 – 2003 years [5] and compared with the data for the period 2009-2010.

#### Experimental part

To calculate the ion flow of these rivers used results of the chemical analysis of monthly water samples authors and Kazhydromet data on the chemical composition and water flow of the rivers from 1997 to 2002. (Table 1). The ion flow is calculated by the standard technique [6, 7].

Methods of determining the components of carbonate and calcium balance is detailed in the manual [8]. The calculation of the components of the calcium carbonate equilibrium produced by the method and recommendations O.A. Alekin and N.P. Morichev [9], S.M. Romanova [10] without the formation of ion pairs and complexes.

According to the recommendations of L.V. Brazhnikov, A.S. Demchenko [11] and O.A. Alekin [12] definition of unstable components of water (pH, permanganate oxidation performed immediately after sampling, and such as P, Fe, Si in laboratory after canning appropriate reagents. Identification of all the

components of the chemical composition of water was carried out by conventional methods in hydrological practice [11-15] (Table 1). Verification of these methods have shown that the error rate does not exceed the values of their accuracy.

Water flow in the river was measured by a surface float. To measure water flow above and below the main hydrometric alignment equidistant break two additional alignment so as to move the length of the floats

between the upper and lower alignment was at least 20 seconds. This duration is due to the fact that the timing with a stopwatch in determining the duration of the course of the floats can be mistakes due to rounding to whole seconds and due to some inaccuracies determine when passing through the float line alignment. Floats throw only stem of the river, where there is the highest rate of the river. Of all running floats (5-10) selected three float with the least duration of the course.

**Table 1** – Methods for determination of the components of the chemical composition of water

Component	Method	The sensitivity of the method	Accuracy of the method
pH	Colorimetric	0,05 unit pH	±0.5-0.8%
Ca <sup>2+</sup> , Mg <sup>2+</sup>	Complexometric indicators murexide with chrome and black GS-ET	0,5 mg/l	±0.5%
Na <sup>+</sup> +K <sup>+</sup>	Calculated from the difference between the sum of cations and anions in the 1 / z (C) mol / l		
HCO <sub>3</sub> <sup>-</sup> , CO <sub>3</sub> <sup>2-</sup>	Volumetric, direct titration	10 mg/l	±1-5%
SO <sub>4</sub> <sup>2-</sup>	Gravimetric	10 mg/l	±0.5%
Cl <sup>-</sup>	Volumetric, argentometric	10 mg/l	±0.5-0.8%
NH <sub>4</sub> <sup>+</sup>	Photometric reagent Nessler	0.002 mg/l	±4-5%
NO <sub>2</sub>	Photometric with Griess reagent	0.5 µg/l	±3-5%
NO <sub>3</sub>	Photometric, the revolt-leniem metal cadmium nitrate to nitrite	0,010 mg/l	±5%
The mineral phosphorus	Photometric with ammonium molybdate and ascorbic acid	0.005 mg/l	±1.5-5.5%
Silicon	Photometric with ammonium molybdate	0.5 mg/l	±2%
Iron	Photometric with sulfosalicylic acid	0.02 mg/l	±8%
Oxidation permanganate	By Kubel	0.5 mg/l	±4-5%
Manganese	Photometric with formaldoxime	5 µg/l	±2%
Oxygen	Iodometric according to Winkler	0.05 mg/l	±0.3-0.5%

## Results and their discussion

It is known that the absolute values of ion flow depends from water availability on the year. In 2000, river Shilik had the highest ionic flow among the rivers of northern slope of the Ile Alatau, which amounted to 161,540 tons (water flow is 440.8 km<sup>3</sup>), and in 2001, 109,591 tons (water flow is 375 km<sup>3</sup>). In 2002, the annual value of the ion flow increased to 196,726 tons, and water flow to 645 km<sup>3</sup>, i.e. 1.8 times more than in 2001.

The same can be noted for river Turgen. In 2000, the flow of mineral salts there was 31, 379 tons (water flow 113 km<sup>3</sup>), and in 2002, 56, 561 tons. The rivers Ulken Almaty, Kishi Almaty, Esentai examined data on upstream and downstream. The calculation showed that the ion flow of Ulken Almaty in 2000,

on upstream was 3, 395 tons, and on downstream was 21, 118 tons, and with the flow increased by 6.2 times. In the following 2001 and 2002 the increase ion flow is reduced by half.

Ion flow of solutes river Ulken Almaty for the period from 1997 to 2002, ranges 920.3-17 959.9 tons, the minimum values correspond to the lowest values of the water flow.

Ion flow river Kishi Almaty for 2001 is 1.5-2 times greater than r.Ulken Almaty, although the water flow is less (Table 2).

Ion flow r.Esentai with the flow increases. For example, in 2002, at a point al-Farabi avenue ion flow is 5631 tons, and at a point Ryskulov avenue, i.e. downstream with the flow increases to 2230 and 7861 tons, correspondingly.



**Table 2** – Changes in the annual ion flow ( $R_p$ ), depending on the water flow ( $R_w$ ) for some of the rivers Ili Alatau

r. Kishi Almaty – Almaty (2.0 km above the city)			r. Kishi Almaty – Almaty (0.5 km below the reset fur factory)			r. Kishi Almaty – Almaty (4.0 km below the city)			r. Kishi Almaty – Almaty (0.5 km below the reset radio center)		
Year	$R_w$ , km <sup>3</sup>	$R_p$ , t	Year	$R_w$ , km <sup>3</sup>	$R_p$ , t	Year	$R_w$ , km <sup>3</sup>	$R_p$ , t	Year	$R_w$ , km <sup>3</sup>	$R_p$ , t
2000	16.7	3378.0	1998	1.98	524,7	1998	11.7	4,5440	1998	22.7	10,3717
2001	14.8	6124.5	2000	23.26	9207,1	2000	39.3	17,1460	2001	41.9	25,8630
						2001	33.7	13,9540			
r. Ulken Almaty – Almaty 9.1km above the city			r. Ulken Almaty – Almaty (0.5 km below the city)			r. Ulken Almaty – Almaty 0.5 km below the reset water flow			r. Ulken Almaty -Ustya 12 km above the estuary		
Year	$R_w$ , km <sup>3</sup>	$R_p$ , t	Year	$R_w$ , km <sup>3</sup>	$R_p$ , t	Year	$R_w$ , km <sup>3</sup>	$R_p$ , t	Year	$R_w$ , km <sup>3</sup>	$R_p$ , t
1997	8,5	1839,1	1997	20.3	3503,0	1997	17.9	3525,5	1997	28.0	14238,1
1998	4,8	920,3	1998	5.2	2207,5	1998	5.8	1979,2	1998	7.9	3807,8
2000	11,4	3395,5	2000	45.9	14555,1	2000	102.1	31027,5	2000	55.3	21718,7
2001	16,2	3537,8	2001	38.9	9514,9	2001	49.5	12222,8	2001	2.6	1336,3
2002	26,0	6107,7	2002	43.3	10609,6	2002	71.6	17959,9			
r. Esentai – Almaty al-Farabi avenue						r. Esentai – Almaty – Ryskulov avenue					
Year		$R_w$ , km <sup>3</sup>	$R_p$ , t		Year		$R_w$ , km <sup>3</sup>	$R_p$ , t			
2000		10.9	2463		2000		11.0	2617,0			
2001		17	4360		2001		18.7	5144,0			
2002		21.6	5631		2002		29.0	7861			

The authors calculated flow of mineral salts rivers Ulken Almaty, Turgen and Kaskelen for 2003 and 2009-2010 (Table 3). As you can see, the flow of mineral salts of r.Turgen only for June and July 2003 is 13, 900 tons. Ion flow of river Kaskelen over the same period more than (17,531 tons.) river Turgen (13 900 tons), although water flow less (Table 3). If, in June 2003, the most submitted  $\text{HCO}_3^-$  (1435 tons) and  $\text{Ca}^{2+}$  (383 tons), in July predominant ions become  $\text{SO}_4^{2-}$  (5800 tons), and  $\text{Na}^+$  (3105 tons). Flow of river Kaskelen formed by flowing tributaries, in particular river Ulken Almaty. Removal of mineral salts river Ulken Almaty in June and July 2003 is 2 300 tons. with the prevalence of  $\text{HCO}_3^-$  and  $\text{Ca}^{2+}$  ions. For this study the rivers with increasing annual water or season an increase the ion flow (eg, r.Ulken Almaty correlation coefficient is – 0,89-0,95).

During the period from March 2009 to July 2010 (16 months) the water of river Ulken Almaty river upstream 5,486 tons of mineral salts, and in the downstream – 7135 tons, share of calcium bicarbonate (calculated of calcium carbonate) have an average of 68% of all salts. Kishi Almaty river in the upstream

(Medeu) for the period from March to November 2009 removed 3,039 tons of substances, including calcium bicarbonate – 2,833 tons, and from January to May 2010, 1,737 and 1,247 tons respectively, with an average of during this period 82% of all minerals.

In the downstream of the river Kishi Almaty for 10 months of 2009, 18,952 tons of salt removes, and the share of calcium bicarbonate accounting for 63%, and for 6 months of 2010, 10,568 tonnes and 64%, respectively. The data in Table 2 that the Kishi Almaty river flowing through the city Almaty, enriched in minerals by 24.7 thousand tons, in other words, removal of salts increases by more than 6 times in the downstream than compared with upstream. It should be noted that the columbia area of river Kishi Almaty more (1,240 km<sup>2</sup>) 2.7 times compared to the river Ulken Almaty (461 km<sup>2</sup>), but the average of the 2009-2010 consumption of water at the outlet of the mountain river Ulken Almaty (1.26 m<sup>3</sup>/s), river Kishi Almaty (1.38 m<sup>3</sup>/s) and in the mouth portions are little differ 1.75 m<sup>3</sup>/s to 1.86 m<sup>3</sup>/s, respectively. This explains the higher salt removal river Kishi Almaty compared with river Ulken Almaty.

**Table 3** – Removal of mineral salts some rivers of Ili Alatau

No. point (station)		Date of sampling	Consumption, m <sup>3</sup> /s	R <sub>w</sub> , 1*10 <sup>9</sup>	Mineralization, mg/l	R <sub>p</sub> , ton
r. Turgen	13	10.06.03	14.4	37.3	122.0	4551
	27	17.07.03	23.4	62.7	134.0	8402
	39	27.07.03	21.5	57.6	178.0	10253
r. Kaskelen	18	10.06.03	6.72	17.4	149.0	2593
	32	18.07.03	18.4	49.3	303.0	14938
r. Ulken Almaty	5	10.06.03	0.57	1.47	174.0	256
	36	17.07.03	4.89	13.1	156.0	2044
r. Ulken Almaty, the upstream (3.5 km above the district Orbita)	48	31.03.09	0.973	2.31	155.8	360,52
	140	05.07.09	2.258	5.37	169.8	911,83
	166	02.08.09	1.723	4.10	150.8	617,98
	196	13.09.09	1.413	3.66	141.4	517,81
	248	22.11.09	0.421	1.09	178.9	195,18
	272	07.01.10	0.546	1.30	162.1	210,57
	309	28.02.10	0.390	0.94	204.2	192,76
	336	27.03.10	0.445	1.06	193.3	204,51
	380	24.05.10	0.303	0.72	208.1	150,04
r. Ulken Almaty (downstream, Boraldai)	399	14.07.10	4.150	9.87	159.5	1574,27
	144	05.07.09	3.710	8.82	159.7	1409,19
	160	01.08.09	2.339	5.56	156.9	872,83
	200	13.09.09	1.239	3.21	170.4	547,15
	223	25.10.09	0.859	2.04	207.7	424,33
	278	08.01.10	0.443	1.05	241.2	254,22
	316	28.02.10	0.468	1.13	329.4	372,89
	342	28.03.10	1.950	4.64	245.3	1137,70
	371	22.05.10	0.578	1.37	402.4	553,30
r. Kishi Almaty (downstream, Medeu)	406	14.07.10	4.170	9.92	157.7	1564,07
	49	31.03.09	0.347	0.83	193.3	159,47
	128	13.06.09	0.109	0.28	283.9	80,34
	138	05.07.09	2.303	5.48	123.3	675,31
	165	02.08.09	5.850	13.9	117.1	1629,33
	195	13.09.09	1.381	3.58	138.1	494,40
	247	22.11.09	1.170	3.03	159.1	482,55
	271	07.01.10	0.439	1.04	160.5	167,56
	321	08.03.10	0.228	0.54	259.1	140,43
	335	02.04.10	1.092	2.83	198.9	562,89
379	24.05.10	0.908	2.16	177.8	384,04	

Continuation of table 3

No. point (station)	Date of sampling	Consumption, m <sup>3</sup> /s	R <sub>w</sub> , l*10 <sup>9</sup>	Mineralization, mg/l	R <sub>p</sub> , ton	
r. Kishi Almaty (downstream, Pokrovka, source Almerék)	18	22.02.09	1.354	3.28	736.8	2413,76
	61	12.04.09	3.044	7.89	634.9	5009,36
	111	27.05.09	2.874	6.83	494.3	3378,54
	121	13.06.09	1.404	3.64	504.0	1834,06
	152	05.07.09	1.737	4.13	503.8	2081,20
	167	02.08.09	1.030	2.45	550.6	1348,97
	203	13.09.09	1.423	3.69	438.8	1618,29
	230	25.10.09	0.960	2.28	555.2	1267,52
	296	30.01.10	0.985	2.34	685.3	1605,66
	345	28.03.10	2.942	7.00	499.5	3495,00
	372	22.05.10	3.303	7.86	501.0	3935,86
	387	27.06.10	1.300	3.37	454.4	531,33

### Conclusion

1. A study of water flow of the rivers Ulken Almaty and Kishi Almaty showed that the greatest flow of water masses in the summer. So, for the river Ulken Almaty summer in the upper portion of the water flow reaches  $5.37 \cdot 10^9 - 9.87 \cdot 10^9$  l, while the lower alignment –  $8.82 \cdot 10^9 - 9.92 \cdot 10^9$  l at respective maximum water flow, 2.26-4.15 m<sup>3</sup> / s and 3.71-4.17 m<sup>3</sup> / s. The lowest water flow in the autumn – winter period. So, for the river Ulken Almaty in the upper portion of flow decreases to  $1.09 \cdot 10^9 - 1.30 \cdot 10^9$  l, while the lower alignment –  $1.05 \cdot 10^9 - 1.13 \cdot 10^9$  l at the appropriate minimum water flow 0.42-0.45 m<sup>3</sup> / s and 0.44-0.47 m<sup>3</sup> / s.

2. For river Kishi Almaty a similar pattern in the distribution of water flow. Thus, in the upper portion of the maximum water flow in summer reaches  $13.9 \cdot 10^9$  l, while the lower alignment –  $7.89 \cdot 10^9$  l at respective maximum water flow rate of 5.85 m<sup>3</sup>/s and 3.04 m<sup>3</sup>/s. The lowest water flow of the river in the autumn and winter period. So, for the river Kishi Almaty in the upper portion of stock is reduced to  $1.04 \cdot 10^9$  l (and in early spring before  $0.54 \cdot 10^9$  l), while the lower alignment –  $2.28 \cdot 10^9$  l at the appropriate minimum water flow of 0.44 m<sup>3</sup>/s and 0.96 m<sup>3</sup>/s.

3. The calculation of the removal of mineral salts North Slope rivers Ili Alatau allowed to establish the following. During this period the water river Ulken Almaty in the upstream 5,486 tons of mineral salts, and downstream – 7,135 tons, and the share of calci-

um bicarbonate (calculated calcium carbonate) have an average of 68% of all salts. River Kishi Almaty in the upstream removed 4,776 tons substances (including calcium bicarbonate – 4,080 tons) and downstream – 29,520 tons (including 18,745 tons of bicarbonate).

### References

1. Alekin O.A., Brazhnikova L.V. Flow solutes from the territory of the USSR. – M.: Nauka, 1964. – 215 p.
2. Brazhnikova L.V. Ion flow rivers of USSR. – Irkutsk, 1961. – 250 p.
3. Ibragimova M.A. Physico-chemical characterization of the river basin of Balkhash lake. Dissertation work. – Almaty, 1969. – 245 p.
4. Nevskaya A.I. Hydrochemical characteristics of surface slow in dry regions of Kazakhstan. Bulletin of the Kazakh SSR. – 1956. – No 9. – 43-52 p.
5. Dostai Z.D., Romanova S.M., Kunshygar D.Z. Hydrological state of rivers of Northern Slope of the Ili Alatau // Hydrometeorology and ecology, 2004. – No. 1. – P. 144-153.
6. Nikanorov A.M. **Hydrochemistry**. – L.: Hydrometeoizdat, 1989. – 351 p.
7. Alekin O.A., Brazhnikova L.V. Methods to calculate ion flow // Hydrochemical materials, 1963. – Vol. 35. – 149 p.
8. Alekin O.A., Moricheva N.P. Calculation of carbonate equilibrium. Modern methods of analysis of natural waters. – M.: A.S. USSR, 1962. – 110 p.

9. Moricheva N.P. Calcium carbonate equilibrium in water of river Volga. Dissertation work. – Novocherkask, 1955. – 232 p.
10. Romanova S.M., Kunanbaeva G.S. Carbonate calcium equilibrium in natural waters. The methodical manual for master students on a special course «Chemistry of natural waters and salts of Kazakhstan». – Almaty: Kazakh University, 2002. – 32 p.
11. Brazhnikova L.V., Tkachenko A.S. Research and forecasting contamination of rivers Hydrochemical materials. – Almaty, 1977. – Vol. 67. – 114 p.
12. Alekin O.A. Handbook for chemical analysis of surface waters. – Almaty, 1973. – 269 p.
13. Reznikov A.A., Mulikovskaya E.P. Methods of analysis of natural waters. – M.: Nedra, 1970. – 488 p.
14. Romanova S.M. Practical work of hydrochemistry. – Almaty: Kazakh University, 2011, – 82 p.
15. Unified methods of water analysis / Edited by Lure Y.Y. – M.: Chemistry. 1971. – 375 p.

UDK 54-414

Serikpayeva S.B. \*, Erzhanova N.S., Iminova R.S., Zhumagaliyeva Sh.N.,  
Beysebekov M.K., Abilov Zh.A.

Al-Farabi Kazakh National University, Kazakhstan, Almaty

\*e-mail: sany2994@mail.ru

## Possibilities of composite materials use on the basis of polivinilpirrolidon and bentonite clay as sorbents of heavy metals ions

**Abstract:** The chemically crosslinked gels based on bentonite clay of the Manyrak deposit (East Kazakhstan region) and nonionic polymer polyvinylpyrrolidone were synthesized with using the process of intercalation of the monomer in the aqueous suspension of bentonite. Swelling degree, sorption capacity of the obtained polymer-clay composites to metal cation ions are evaluated. It is shown that with increasing the concentrations of bentonite clay in gels the sorption capacity to metal ions increases significantly.

**Key words:** bentonite clay, gel polymer-clay composites, sorption.

### Introduction

Interest to polymer-clay composite materials, and also to researches of reactions of a complex formation with their participation is caused by that such complexes, along with valuable properties of components have improved thermal, mechanical and sorption properties. Polymer-clay compositions on the basis of natural and synthetic polymers are available carriers of medicinal substances and sorbents [1]. One of ways of polymer-clay compositions obtaining is radical intercalation polymerization «*in situ*» of monomer on a surface of clay silicates [2]. As a result, are formed more uniform material with uniform distribution of a mineral in all volume of a polymeric matrix. A continuous phase in composites can be synthetic polymers, and as a filler the bentonite clays (BC), with a predominant content of the mineral montmorillonite [3]. It is known that Kazakhstan is rich in deposits of this valuable mineral. Therefore, in the present study offers new perspectives for the using of composite materials based on non-ionic polymer – polyvinylpyrrolidone (PVP) and BC of deposit Manyrak as environmentally friendly and cost-effective sorbents of heavy metal ions.

### Experimental part

Composite gels of PVP-BC were synthesized by «*in situ*» intercalation radical polymerization of an aqueous monomer solution with incorporated purified bentonite clay particles. N,N-methylene-bisacrylamide (MBAA) was used as the crosslinking

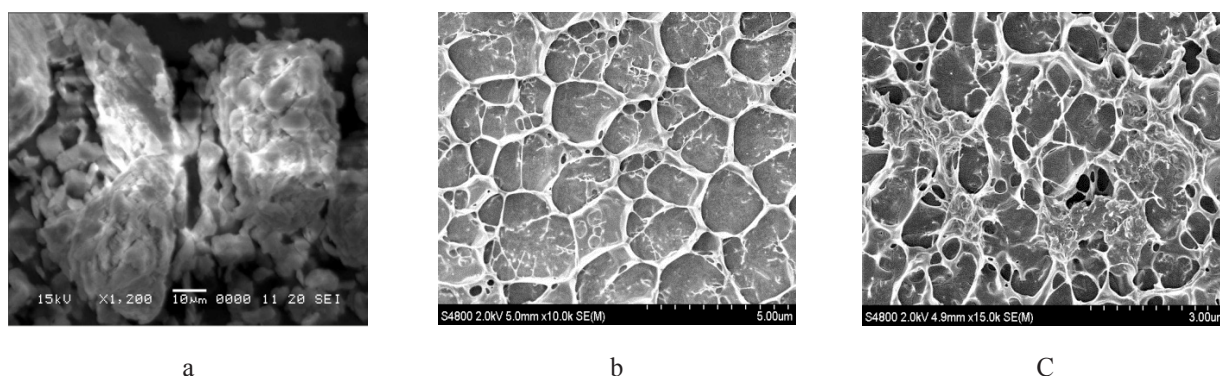
agent without further purification, and 2,2-azo-bis-isobutyronitrile (AIBN) was used as initiator which has undergone several times recrystallization. Conditions of carrying out synthesis and the characteristic of initial components of composite gels are described in early works [4]. The morphology of bentonite clay, reference and composite gel samples were examined by high-resolution scanning and cryo-scanning electron microscopy (SEM, cryo-SEM) by using the scanning electron microscope S-4800 from Hitachi (Japan). The respective samples were rapidly frozen in melting nitrogen and fractured in a cryo chamber at -145°C. After etching for 45s at -98 °C, the samples were sputtered with a thin platinum layer. The degree of swelling of gels and bentonite clay was investigated by method of equilibrium swelling. Amount of sorption ions of metals by obtained composites was determined by atomic adsorption ASS Shimadzu 6200 microscope.

### Results and their discussion

It is known that indisputable the conditions of carrying out polymerization affect on physical and chemical properties of polymer-clay compositions. As a result of carrying out series of experiences and research of an exit of gel-fraction and the swelling ability, the optimum ratio monomer-solvent, equal to the content of water 70, and monomer – 30 vol.% is established with the different maintenance of a mineral complex. In early works [5, 6] data polymer-clay compositions were offered as the carrier of medicinal substance of a rikhlokain with the maintenance of BC

of 1-3 mas.% monomer volume, and in this work we consider possibility of application of these compositions as sorbents of metal ions, and for improvement the sorption properties we changed the maintenance of concentration of BC of 1-4 mas.% of the total volume, which in turn should have a beneficial influence on the quantitative values of sorption. By results of the previous works [5, 6] it was also established that increase of concentration of crosslinking agent and BC promotes increase in an exit of gel-fraction, the ash content and densities of the gels.

The scanning microscopy is used for research of morphology of a surface of composite gels [7]. Apparently from figure 1, bentonite clay (a) has flaked layered structure. Figure 1 (b) shows the formation of polymeric matrix as a result gel formation of PVP homogels, and polymer-clay compositions of PVP-BC with represent varying degrees intercalated structure due to the penetration of the monomer into the inter-layer space of the clay and uniform distribution of the clay particles in the polymer matrix. The result is the formation of homogeneous compositions.



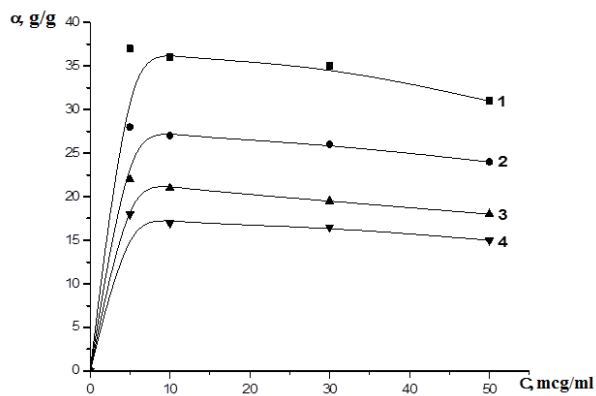
**Figure 1** – Cryo-SEM snapshots of BC (a), cryo-SEM snapshots of PVP homogels (b), and composite gels of PVP-BC (b).

By results of the previous works [5, 6] at research of the swelling capacity, morphology and structure it is established that compositions of PVP-BC combine properties of initial components and are characterized by biocompatibility and homogeneity. It was revealed that with increasing content of the crosslinking agent, concentration of BC and in the presence of electrolyte degree of swelling of the PVP-BC composite gels considerably decreases. Increase in temperature and pH environment leads to reduction of volume of composite gel that testifies about incentive susceptibility of gels. These characteristics of clay compositions of polymer can be explained by the non-Coulomb nature of interaction, formation of through hydrogen bonds and hydrophobic interactions, and also greatly influenced by negatively charged particles of BC.

Polymer-clay materials, due to high sorption and complexing ability, are excellent sorbents of cations of metals. Therefore one of the most important branches of possibility of application of clay polymeric composites can note the purification of industrial sewage of heavy metals [8]. In this connection and to evaluate the sorption ability of the obtained polymer compos-

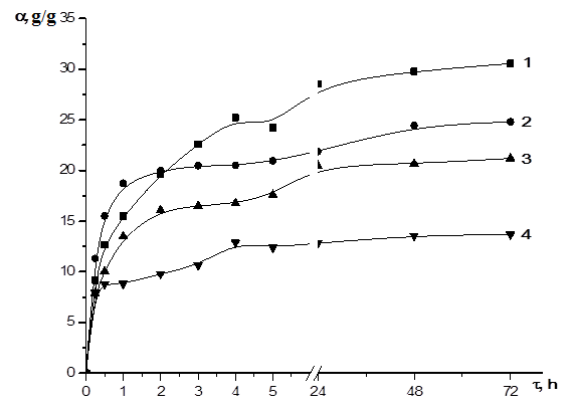
ites was studied sorption  $Pb^{2+}$ ,  $Zn^{2+}$ ,  $Cd^{2+}$  by gels. Studies were carried out by atomic adsorption spectroscopy using the spectrometer AAS Shimadzu 6200. For clarification of the nature of interaction of ions of metals with composites the swelling ability of gels in solutions of metals was studied. Swelling ability of gels in solutions of metals was studied for clearing up of the nature of interaction of ions of metals with composites. The results of studies of the effect of concentration solution of metals on the swelling behavior of the gels (Figure 2, for example, a solution of  $Pb^{2+}$ ), found that increasing of the concentration of  $Me^{2+}$  ions in the solution decreases the volume of composite gels.

With increasing content of bentonite clay swelling capacity of the gels naturally decreases, as can be seen from the data in Figure 3, which shows the swelling kinetics of the composite gels in solution  $Cd^{2+}$  (30 mcg/ml) containing bentonite clay 1, 2 and 4% by weight. Probably, the gradual contraction of the gel in a solution of the metal occurs due to the ionic strength of the last, however, is compacted mesh with the content of bentonite, which further prevents to increase in the net.



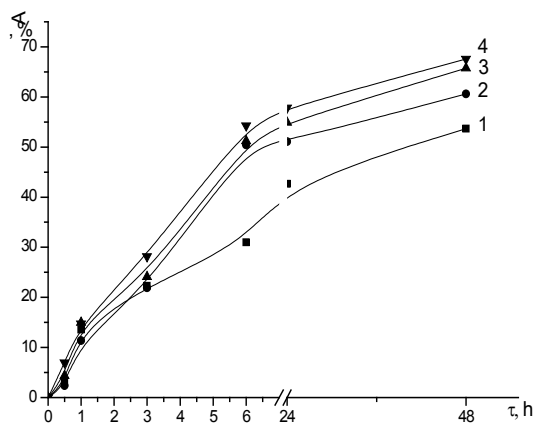
$t=25^{\circ}\text{C}$ ; PVP-1; PVP-BC: BC,  
1% - 2; BC, 2% - 3; BC, 4% - 4;  
[AIBN]=0,5 mol.%; [MBAA]=1 mol.%

**Figure 2** – The dependence of the degree of swelling of gels on the concentration of  $\text{Pb}^{2+}$



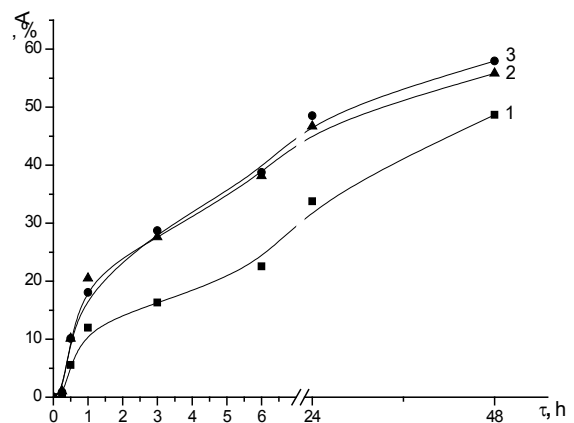
$t=25^{\circ}\text{C}$ ;  $[\text{Cd}^{2+}] = 30 \text{ mcg/ml}$ ; PVP-1; PVP-BC: BC,  
1% - 2; BC, 2% - 3; BC, 4% - 4;  
[AIBN]=0,5 mol.%; [MBAA]=1 mol.%

**Figure 3** – Kinetics of gels swelling in the sample solution  $\text{Cd}^{2+}$



$t=25^{\circ}\text{C}$ ;  $[\text{Cd}^{2+}] = 10 \text{ mcg/ml}$ ;  
PVP-1; PVP-BC: BC, 1% - 2; BC, 2% - 3; BC,  
4% - 4; [AIBN]=0,5 mol.%; [MBAA]=1 mol.%

**Figure 4** – Kinetics of sorption  $\text{Cd}^{2+}$  on the gels PVP-BC



$t=25^{\circ}\text{C}$ ; 1- $[\text{Pb}^{2+}]$ , 2- $[\text{Zn}^{2+}]$ , 3- $[\text{Cd}^{2+}]$   
[AIBN]=0,5 mol.%; [MBAA]=1 mol.%

**Figure 5** – The kinetics of sorption of metal ions on the gel PVP-BC (BC, 1%) of the combined solutions

As a result of the analysis of sorption of cations of metals the obtained composite gels are revealed some regularities. So, the limit values are set the sorption during the day. And with the increase in the content of bentonite clay composites there is a significant increase in the amount of adsorption of metal ions, that testifies to a primary role of clay in sorption of cations of metal (Figure 4). In general, it is possible such interactions of metal ions with composite gels as a coordination bond and electrostatic binding between the lone pairs of the polymer, the active centers of

bentonite clay and free orbitals of the metal lattice. Increasing the concentration of  $\text{Me}^{2+}$  in the solution leads to a decrease in the sorption, for example the value of the sorption of  $\text{Cd}^{2+}$  ions on gels PVP-BC 1% per day in a solution of 10 mcg/ml up to 57%, 30 and 50 mcg/ml 45 and 42%, respectively.

Also, for research of selectivity of composite gels was prepared combined solution of heavy metals. The results showed that polymer-clay gels can adsorb simultaneously some metals complex solution. Figure 5 shows the adsorption of ions of metals in com-

position of PVP-BC (BC, 1%) in complex solution. Numerical values of sorption of ions of metals from complex solution it is much less, than in solutions of ions of metals separately. It is connected with that metals compete among themselves, so in 24 hours the composition of PVP-BC (BC, 1%) absorbs of lead 31%, of zinc 42%, of cadmium 48%.

Thus, chemically cross-linked homogeneous, water-swallowable polymer-clay compositions based on BC of deposit Manyrak (East Kazakhstan region) and nonionic polymer PVP are obtained through the formation of complex by hydrogen bonds and hydrophobic interactions. It was estimated the sorption capacity of chemically cross-linked polymer-clay composite gels PVP-BC in relation to heavy metal cations. Swelling, sorption properties and morphology of the gels was established. With increase in the content of bentonite clay in gels their swelling ability naturally decreases, and the number of sorption of ions of metal significantly increases. It is shown that with increasing of concentration of  $Me^{2+}$  sorption ability of composite gels decreases. Results of further research of composite gels on the basis of PVP and BC gives the chance of perspective use as sorbents of cations of heavy metals.

## References

1. Ergozhin E.E., Akimbayeva of A.M. Organomineral sorbents and multifunctional system based on natural aluminosilicate and carbon-mineral raw materials. – Almaty: Print-S., 2007. – 373 p.
2. Chvalun S.N., Novokshonova L.A., Box A.P., Brevnov P.N. Polymer-silicate nanocomposites: physical and chemical aspects of synthesis by polymerization *of in situ* // I Grew. chemical. (Zh. Ros. chemical about-va of D. I. Mendeleyev). – 2008. – t. LII. – No. 5. – P. 52-57.
3. Sakipova Z.B., Dilbarhanov R.D., Tulegenova A.U. Bentonite clay in medicinal forms technology // Pharmacy Kazakhstan. – 2009. – No. 7. – P. 57-61.
4. Arykova G.B., Eshatova A.S., Beysebekov M.M., Iminova R.S., Zhumagaliyeva Sh. N., Beysebekov M. K. Synthesis of composite gels on the basis of polyvinylpyrrolidone and bentonite clay // Materials II-nd international. Kaz.-Ros. Conference on chemistry and chemical technology. – Karaganda, 2012. – P. 72-75.
5. Serikpayeva S.B., Eshatova A.S., Beysebekov M.M., Iminova R.S., Zhumagaliyeva Sh. N., Beysebekov M. K., Abilov Zh.A. Preparation and study on composite media polyvinylpyrrolidone and bentonite clay // Proceeding of the international symposium «Modern chelenges of higher education and science in the feld of chemistry and chemical engineering». – Almaty, 2013. – P. 64-66.
6. Serikpayeva S.B., Eshatova A.S., Beysebekov M.M., Iminova R.S., Zhumagaliyeva Sh. N., Beysebekov M. K., Abilov Zh.A. Study sorbtion of rihlo-kaine on composition gels based polyvinylpyrrolidone and bentonite clay // Science of Kazakhstan. – 2014. – No. 2. – P. 7-11.
7. Mikitayev A.K., Kaladzhyan A.A., Lednev O.B., Mikitayev M.A. Nanocomposite materials based on organoclay // the Electronic magazine «It Is Investigated in Russia». – 2004. – P. 912-921.
8. Somn V.A., Kondratyuk E.V., Kurtukova L.V., Komarova L.F. Water purification prospects from ions of heavy metals by means of natural materials // Sb. works XI Mezhd. NPK «Water supply and water disposal: quality and efficiency». – Kemerovo, JSC KVK Expo-Sibir. – 2008. – P.135-139.



UDC 582.951.4.002.68

Shakeshev M.T.<sup>1</sup>, Korulkin D.Yu.<sup>2</sup>, Nauryzbaev M.K.<sup>2</sup>

<sup>1</sup>Al-Farabi Kazakh National University, Almaty, Kazakhstan

<sup>2</sup>«Center of physico-chemical methods of research and analysis», Almaty, Kazakhstan

\*e-mail: Dmitriy.Korulkin@kaznu.kz

## Tannin quantification in industrial waste of tobacco production and selection of optimal extraction parameters

**Abstract:** Optimum technological parameters of extraction for the sum of tannins from tobacco dust (*Nicotiana tabacum* L) waste of tobacco production were established. The basic process parameters to obtain the highest yield of tannins from raw materials such as selection of optimum extractant ratio of raw material to solvent, extraction time, temperature and mode, selection of the optimal precipitator for tannins and the optimal ratio of extract to precipitator. A process technological scheme of tannins extraction from tobacco dust waste was suggested.

**Key words:** tobacco dust (*Nicotiana tabacum* L.), tobacco extraction, tannins, technological block diagram of tannins extraction

### Introduction

Although tannin is frequently cited as an example of a plant defensive chemical [1, 2] experimental documentation of a defensive role for tannin is limited. Clear demonstration of a defensive function for tannin depends on accurate quantitation of tannin. When adequate analytic methods are available, it will become possible to determine whether there is any correlation between tannin content and patterns of herbivory. The accuracy with which a chemical component in a biological matrix, such as tannin in tobacco dust, can be determined depending on several factors. The tobacco dust of interest must be collected and preserved so that the component is not altered or destroyed. The component must be extracted from tobacco in high yield. The method of assaying the component must be free of interferences from other materials present in the extract. However, there is no consensus on the best method for preserving tobacco or the most efficient solvents for extracting tannins [1, 2]. The purpose of this study was to compare and to quantitate the extractability of tannin with various solvents as well as developing technological scheme for extraction of tannins.

### Experimental

Selection of the optimal technological scheme of producing substance from medicinal plants is based on complete exhaustion. This object is achieved by selecting a suitable extracting agent, optimum ratio between extracting agent and plant raw materials

as well as the extraction duration, temperature and mode.

**Selection of the optimal extractant.** Selecting the optimal solvent had the following objective: to choose a solvent that extracts the greatest quantity of tannins from the tobacco waste dust. The following solvents were used: Ethanol 80% water, 2-Butanol, 50% dioxane, dioxane, ethyl acetate, ethanol 50%, ethanol 30%, ethanol 70%, dimethyl. The results are shown in Table 1.

**Determination of the optimum ratio between raw material and the solvent (80% ethanol).** Obviously, keeping a constant amount of the plant material and increasing the amount of the extractant in the extraction process will lead to higher extraction yield. However, increasing the amount of extractant will also reduce the concentration of biologically active substances in the extract, thus addition of the extractant cannot be infinite.

Therefore, in determining the optimal amount of extractant selected, the next ratio of raw material to extractant were used 1:5, 1:7, 1:9 and 1:10. Controlled variables of the extraction process are: the mass of raw material (1 g) and extraction time (3 hours). Results are presented as a histogram (Figure 1).

**Methodology of tannins yield determination.** The exact portion of the dry extract (1-2g) or liquid substance(3-5g) is placed into 100 ml flask, then 30 ml of purified water and 30 ml of a 10% solution of copper acetate (II) added, heated on a boiling water bath for 30-40 minutes to complete precipitation of tannins. Cooled, filtered through an accurately

weighed filter. The filter cake was washed with purified water until a negative reaction to the copper ferrocyanide solution and dried to constant weight at a temperature 100-105°C.

Filter with the precipitate burned; ash was wetted with concentrated nitric acid and was calcined at the same temperature to constant weight.

The content of tannins in the sample was determined by the difference between the weight of tannate copper after drying filter with precipitate and the weight of copper oxide after calcination.

**Determining the optimum extraction temperature.** For the next step it was necessary to consider the effect of temperature on the extraction process of extracting the maximum amount of tannin from the investigated tobacco dust waste. For this purpose 6 samples of 1g. were filled with 10 ml. 80% ethanol. The first sample was left at room temperature for 24 hours and rest had been heated for 1 hour. Second heated at 40°C, and the third – at 50°C, and the fourth – at 60°C, the fifth – at 70°C, and a sixth – at the reflux at 80°C. Then the quantitative content of tannins was determined. Results are presented as a histogram (Figure 2).

**Determining the optimal extraction time.** For this 5 samples of 1g. were filled with 80% ethanol. The first sample was heated on a water bath at reflux at 80°C for 1 hour, the second – for 2 hours, the third for 3 hours, the fourth for 4 hours and the fifth for 5 hours. Then the tannins content was quantified. Results are presented as a histogram (Figure 3).

**Determining the optimal mode of extraction.** An important indicator for an exhaustive set of extraction of BAS medicinal plants is the number of extractions. Raw material maintains a portion of extractant on its surface and between pieces because of its absorbent retention ability within the cells. In order to determine the multiplicity of extraction 4 samples of 1g were filled with 10 ml 80% ethanol. The first and third sample was left at room temperature for 24 hours. Then all four samples heated at 80°C in two modes: samples number 1 and 2 were continuously heated for 4 hours; the solvent of samples 3 and 4 was decanted every hour and a new portion of ethanol was added. Then the tannins content was quantified. Results are presented as a histogram (Figure 4).

**Selection of the optimal precipitant of tannins.** For this purpose four samples of extract obtained from the previous steps were poured with equal volume of saturated solutions of various salts: sample 1 – lead acetate, sample 2 – barium chloride, sample 3 – calcium chloride, sample 4 – ferrous sulfate. Then samples were left in the refrigerator for 2 hours after

which the tannins content was quantified. Results are presented as a histogram (Figure 5).

**Determination of the optimum ratio of the extract to precipitant.** Equal amounts of the extract obtained in previous steps were poured with different amounts of lead acetate: first extract – 20% of the amount of the precipitant (v/v), the second extract – 40% (v/v), third extract – 60% (v/v), fourth extract – 80 % (v/v) and the fifth extract with equal volume of precipitant. Samples were left in the refrigerator for 2 hours. Then the tannins content was quantified. All experiments were performed in parallel. Results are presented as a histogram (Figure 6).

## Results and their discussion

**Selection of the optimal extractant.** Based on calculations made the optimum solvent which extracts the greatest number of hydrolysable tannins is 80% ethanol.

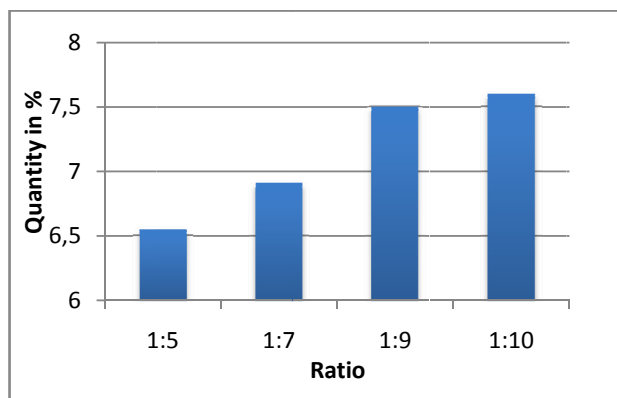
**Table 1** – Selection of the optimum solvent

Mass (g)	Solvent	Tannins yield (%)
0.997	Ethanol 80%	6.5491
0.934	Dimethyl	0.8901
0.922	Ethanol 70%	0.6387
0.945	Ethanol 30%	0.4032
0.968	Ethanol 50%	0.3220
0.933	Ethyl acetate	0.1856
0.965	Dioxane	0.1077
0.961	50% dioxane	0.0937
0.941	2-Butanol	0.0368
0.934	Water	0.0185

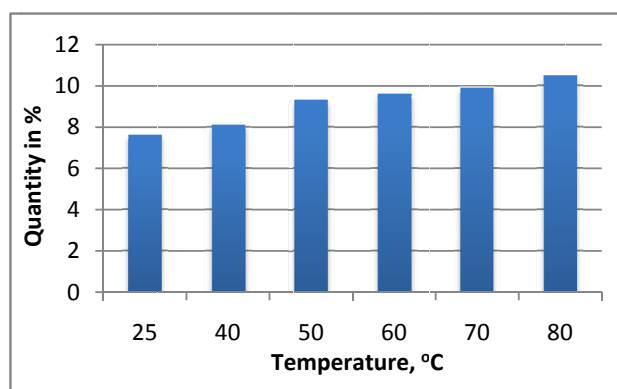
**Determination of the optimum ratio between raw material and the solvent (80% ethanol).** According to data it is clear that using the selected solvent for extracting the most amount of tannins is possible when the ratio of raw materials to solvent is 1:10, whereas the change in this ratio upwards or downwards significantly reduces the yield.

**Determining the optimum extraction temperature.** As can be seen from the figure, the optimum extraction temperature is 80°C. At higher temperatures there is a volatilization of the solvent.

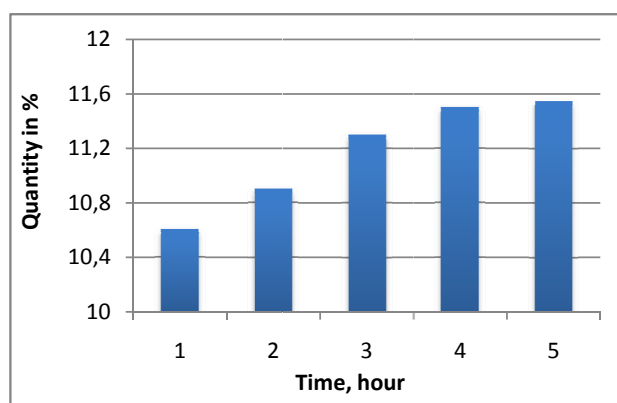
**Determining the optimal extraction time.** According to tannins yield with different extraction time it can be concluded that the optimum extraction time is 4 hours.



**Figure 1** – Dependence of the tannins yield on the ratio of raw material to solvent



**Figure 2** – Dependence of the tannins yield on the extraction temperature

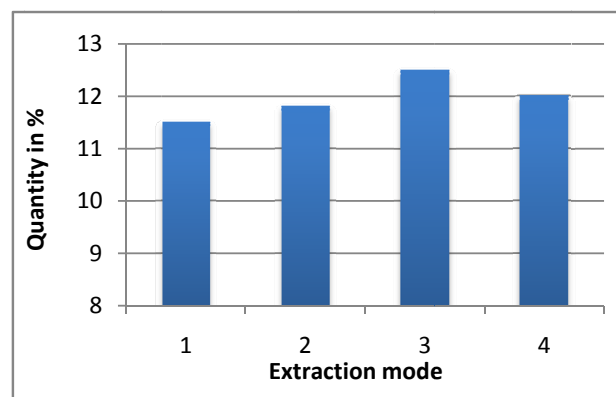


**Figure 3** – Dependence of the tannins yield on the extraction time

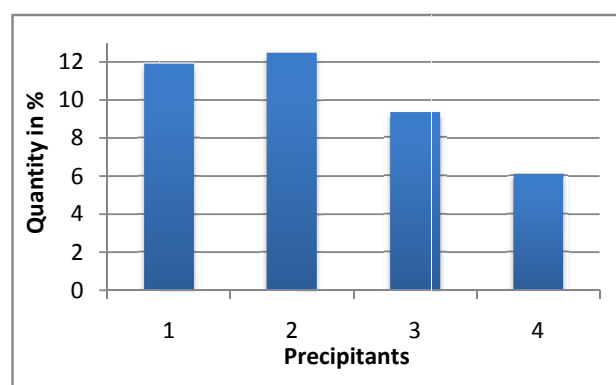
***Determining the optimal mode of extraction.***

Based on the obtained data it can be concluded that the optimal extraction mode is a mode in which the raw material is continuously extracted for 4 hours without infusion.

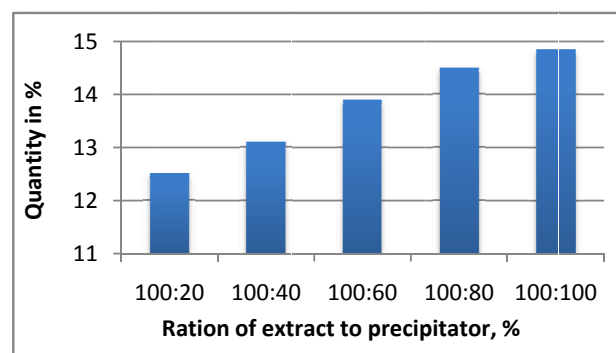
***Selection of the optimal precipitant of tannins.***  
According to obtained data the best tannin precipitant is lead acetate (II).



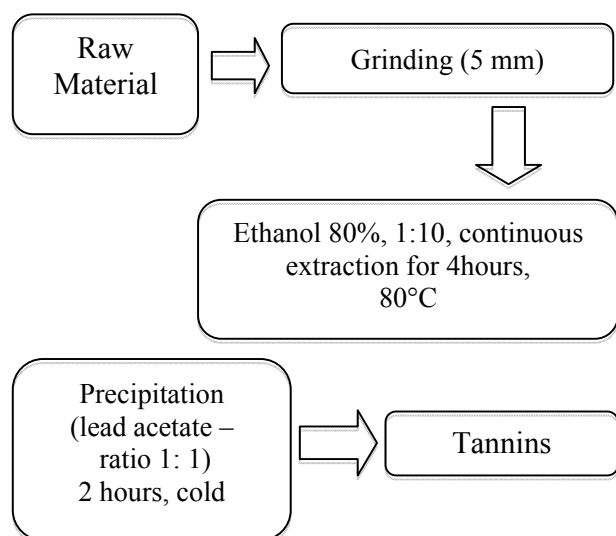
**Figure 4** – Dependence of the tannins yield on the extraction mode (1-4x1h without infusion; 2-4x1h with infusion; 3-1x4h without infusion; 4-1x4h with infusion)



**Figure 5** – Selection of the optimal precipitant of tannins from extract (1- barium chloride; 2- lead acetate II; 3- calcium chloride; 4- iron sulfate II)



**Figure 6** – Dependence of the tannins yield on the ratio of extract to precipitator.



**Figure 7** – Technological scheme of polysaccharides extraction from tobacco dust (*Nicotiana tabacum* L).

**Determination of the optimum ratio of the extract to precipitator.** Based on the data displayed in Figure 6 it is obvious that the optimal ratio of extract to precipitator is 1:1.

**Technological scheme of extraction of tannins.** Based on the analysis of the data we have found that the optimum parameters are:

1. Extraction of raw material with 80% ethyl alcohol
2. The ratio of raw material to solvent is 1:10
3. The extraction temperature 80°C
4. Extraction time is 4 hours
5. Extraction mode is continuous heating without a daily infusion for 4 hours.

Thus, the optimal technology scheme of tannins extraction is represented in block diagram in Figure 7.

## Conclusion

In order to detect biological activity of a substance derived from tobacco dust waste of tobacco production qualitative and quantitative characteristics of the raw material were determined. Optimization of the technological parameters of extraction of tannins was carried out. Based on the data obtained the technological scheme of tannins extraction was developed. The determination of biological activity of substances will be established in the next work.

## References

1. Swain T. Tannins and lignins, pp. 657-682, in G.A. Rosenthal and D.H. Janzen (eds.). *Herbivores: their interaction with secondary plant metabolites*. Academic Press, New York, 1979.
2. Hagerman E. Extraction of tannin from fresh and preserved leaves // *J. Chem. Ecol.*, 1988. – Vol. 14 – No. 2 – P. 453–461.
3. Mercurio M.D., Smith P.A. Tannin quantification in red grapes and wine: Comparison of polysaccharide- and protein-based tannin precipitation techniques and their ability to model wine astringency // *J. Agric. Food Chem.*, 2008. – Vol. 56. – No. 14. – P. 5528–5537.
4. Naurato N., Wong P., Lu Y., Wroblewski K., Bennick A. Interaction of tannin with human salivary histatins // *J. Agric. Food Chem.*, 1999 – Vol. 47. – No. 6. – P. 2229–2234.
5. Lloyd D.J. Tannin Chemistry // *Nature*, 1934. – Vol. 134. – No. 3390. – P. 611–614.
6. Schofield P., Mbugua D.M., Pell A.N. Analysis of condensed tannins: a review // *Animal Feed Science and Technology*, 2001. – Vol. 91. – No. 1–2. – P. 21–40.
7. Scalbert. Antimicrobial properties of tannins // *Phytochemistry*, 1991. – Vol. 30. – No. 12. – P. 3875–3883.

Burdelov L.A.<sup>3</sup>, Eszhanov A.B.<sup>1</sup>, Hughes N.<sup>2</sup>, Nurtazin S.T.<sup>1</sup>,  
Herwig Leirs<sup>2</sup>, Baibagysov A.M.<sup>1\*</sup>

<sup>1</sup>Al-Farabi Kazakh National University, Almaty, Kazakhstan

<sup>2</sup>University of Antwerp, Belgium

<sup>3</sup>M. Aykimbaev Kazakh Scientific Center for Quarantine and Zoonotic Diseases, Almaty Kazakhstan

\*e-mail: azim.baibagysov@gmail.com

### **Preliminary prospects of assessment using telemetry in the study of gerbils' mobility in natural plague focus**

**Abstract:** The article shows that a relatively quick obtaining direct and most importantly absolutely accurate data on individual movements of marked individuals, based on field research in 2012-2014 makes telemetry a very promising direction in mobility study of the potential plague hosts in natural focus of this infection. It is concluded that methods of telemetry are likely applicable not only for rodents but also for any other small mammals, for which catch methods on alive animals are practiced.

**Key words:** great gerbil, radio beacon, movements and GPS-data logger.

#### **Introduction**

The role of the great gerbil (*Rhombomys opimus* Licht.) as a main host of *Yersinia pestis* infectious agent has long been recognized as a key to the present time in Central Asian desert natural plague foci, including the Southern Balkhash region, where our observations were conducted [1-3]. Great gerbil is a landscape forming species due to mass character, active burrowing activity, family and colonial lifestyle with complex burrows, for which a name colonies was fixed in literature. Favourable conditions for the interspecies exchange with ectoparasites, especially by fleas are created because of rich fauna of ectoparasites in its burrows and visit them almost by all animals that are potential hosts of the plague infection [3].

Four types of mobility is isolated from great gerbils: 1) prospecting of surrounding area and its neighbouring burrows with a duration of up to several days; 2) migration to nearest burrows – colonies; 3) migration within the ecological population; 4) vagrancy, eviction outside of the territory, which is annually used by ecological population [4]. Great gerbils can go for a long distance from their colonies and they are even able to negotiate water obstacles during the migration [5, 6]. Thereby they are expanding their range, which has a great epizootic value. In spite of predominantly settled group life [7], great gerbil are able to pass a considerable distance (up to 12 km within 7-8 months; maximum – 17 km for 1 month according to observations of tagged animals) [8]. For

example, the expansion of its range in Western Kazakhstan passed with speed to 4-5 km, sometimes up to 13 km per year [9]. Even then, a settled portion of the population is in constant movement because the great gerbils' family rarely satisfied with one burrow and uses from 2-3 to 11-12 colonies [10, 11]. At the same time accepted that the bulk of gerbils' movements occur within only 100-500 m [7].

Thereby, one of limiting factors for the emergence and fading of epizootics is a great gerbil's mobility [12]. Despite the fact that over the past decade, hundreds or even thousands of papers on Biology and epidemiological role of this species published, but precisely this aspect of great gerbil's life still little known. In particular, there is a very little information about the character of great gerbil's migration activity. There are almost no quantitative characteristics of great gerbil movements, including a distance, which it is able to move. There is no data on their time spent on the surface and underground of colonies, frequency and regularity running on neighbouring colonies, and so on. The main reason for this lies in the great complexity of direct gerbils' mobility observations by labelling. That is why the great bulk of data that published in the literature obtained predominantly by various indirect methods (prolonged visual observations on fixed routes and sites, constantly operating line of catch tools, long roundup of inhabited and uninhabited colonies and so on). Whereby the data for this section of great gerbil ecology is initially conditional and insufficiently accurate in many ways.

In connection with the outlined, the relevance of bringing modern technologies becomes apparent to get answers for questions posed above. The first such attempt took place in the southern Balkhash region very recently [13]. However, it is clearly appeared unsuccessful because the technology of works in essence, was little different from conventional labelling and instead of cutting off fingers used chips with electronic tags. It complies with bioethics, but there are no advantages in terms of getting factual data, because in this case, as in ordinary labelling, there are needs for multiple recapture marked individuals, but a return of labels usually takes a small place. Meanwhile the telemetry techniques can allow obtaining far more accurate data on gerbils' migratory activity. The main purpose of this work was to test this possibility.

### Materials and methods

Works were carried out in the Southern Balkhash on Bakanas ancient delta plain and plain Akdala for the period 2012-2014. There had originally been tested the possibility of using a pretty massive GPS-loggers (10-15% of an adult great gerbil body weight) and worked out ways more comfortable for animals their attachment in April 2012 (Figures 1 and 2). At the same time there was verified the effectiveness of radio direction finding of tagged animals that were in burrows.

The basic works were started only after obtaining positive results. 151 great gerbils, 30 midday jirds (*Meriones meridianus*), 1 lybian jird (*M. libycus*) and 1 tamarisk jird (*M. tamariscinus*) were caught in 2013. 42 great gerbils were caught in 2014, on 30 of them were fixed radio beacons and on 12 – GPS-loggers. However, full analyses of obtained data beyond the scope of this work, because their technical processing is not yet completed due to the fact that demands a lot of time. In this is not difficult to see by the illustration below. Here we give only fragmentary information, which as a rule do not keep within settled representations and indicate a particular value of telemetry techniques to study gerbils' mobility as potential hosts of plague infection in nature.

To catch the animals were used traditional zoological methods that are widely used for such purposes. Zaitsev traps were used to catch great gerbils – 5 traps on the colony. Sherman traps were used to catch jirds. They were deployed in 10 rows, with an interval of 10 m between traps, forming a kind of «network». It allowed revealing the spatial structure of tagged animals and boundaries of their individual plots during recapture.

GPS-loggers (TechnoSmart Company, Italy) due to their massiveness have been fixed only on great gerbil. VHF-radio beacon (Very High Frequencies, Advanced Telemetry Solutions, USA), with a frequency of 30-300 MHz signal whose weight does not exceed 5% of animal body weight was fastened with nylon tape on midday jirds and small great gerbils. Each radio beacon had individual frequency by which the animal was then taped, with noting the coordinates of its location as well. Radio receiver with antenna manufactured by *Title Scientific (Australis 26k Tracking receiver)* has been used for detecting beacon signal.



**Figure 1** – Great gerbil with a GPS-logger  
(photo taken by A.B. Eszhanov)



**Figure 2** – The same gerbil, which appeared on the surface after 20 minutes following the release  
(photo taken by L.A. Burdelov)

After attaching the GPS-logger or beacon animals were placed in a cage and kept there for some time to check their reactions to collar with the device. The device is removed from the animal in case of misbehaviour. Animals with normal reaction were released at the site of capture. Then, in order to minimize stress and avoid unnatural behaviour, animals were not disturbed during 5 days.

For signal presence and location of the animal twice a day, morning and evening has checked by the antenna each individual of great gerbil with beacon. In the case where a signal from a particular animal is missing, the search is extended covering more and more territory. As for jirds, due to their twilight-night activity, monitoring was conducted from sunset and till late night with an interval of 2 hours during the period approximately from 20 pm to 02 am. Moreover, there has been tested labelling technique on midday jirds by using different colours fluorescent powders. Animals were placed in a bag or a plastic bag and then powder was coated onto the animal using a small brush. Animals' movements had been tracked with UV light lamp at the night by fluorescent particles of the powder, which were left on the ground. However, this method appeared practically ineffective due to the rapid powder fall from gerbils because of its total small amount and obviously low power of the ultraviolet lamp. Therefore, it was excluded from further consideration.

### Results and their discussion

Field trials on direction finding location of animals with radio beacons by using a portable antenna showed that the signal reception is very strongly influenced by terrain relief features. Thus, the signal reception range in some cases amounted to 700 meters, with the proviso that a man with antenna is located in an elevated. On the plain, the signal can be caught at a distance of 300 meters. Signal reception significantly deteriorated in areas with dense shrubs and in open terrain, the antenna sensitivity is again increased. The signal from the ground, when animals were in burrows, recorded at a depth of 1 m. During tracking on a radio signal it was able to establish that labelled female great gerbil with number 1080 covered a distance of 1.2 km in two days from the initial place of capture to the point of her latest discovery. This animal, leaving its burrow occupied empty, and apparently, had settled there for a long time, because the signal proceeded until the end of observations from the same burrow. And traces of the active life is becoming increasingly visible on the surface of the

colony – there were cleared inlets, appeared trails and feed tables, number of excrement increased as well. It is also remarkable that the maximum movements range in this case is fixed at the female, but according to the literature, females of great gerbils have a lower migratory activity due to its clearly expressed territorial behaviour. Other individual covered a distance of 850 m during the day. Despite the fact that the biggest distance of movement was recorded at the female (roguish type activity), males of gerbils during the breeding season compared with females, still generally have a greater migration activity. It was possible via VHF-radio beacon to establish that the male of midday gerbil (*Meriones meridianus*) per night covered a distance of 600 meters, by moving short dashes with frequent stops from the burrow to burrow. Animal shows clear signs of search activity because the animal practically did not eat on its way and encountering empty burrows after a short their examination continued its movement.

However, the use of GPS-loggers promises the most interesting results. This method may force reconsideration existing views on speed and range of great gerbils' migrations. To verify this it is sufficient to look carefully to Figures 3 and 4. Now we have immediately to doubt on the phenomena plaguing views on the overall low mobility great gerbils in common conditions of, in particular the range missiles of their local movements within 100-500 m.

Unfortunately, there are certain serious obstacles to massive use of GPS-loggers, such as: – their insufficient miniature size and high cost (used model costs about € 1000, and the smaller device is more expensive);

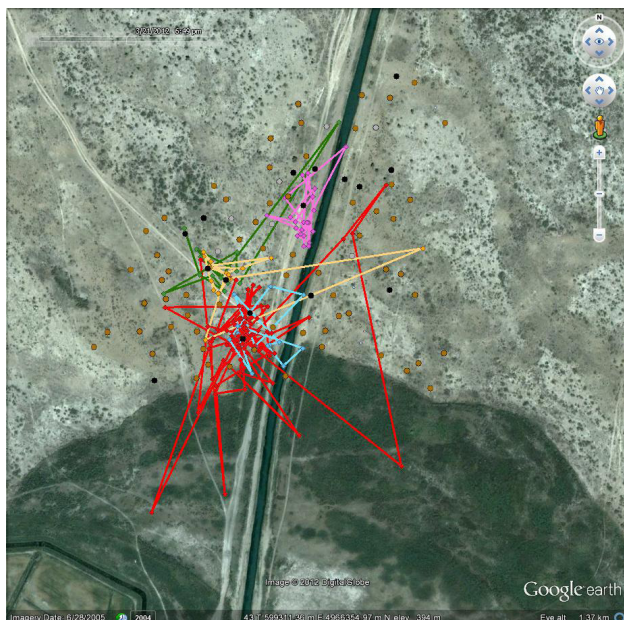
– small battery life, possibility of obtaining erroneous data during the period when marked individuals on surface of the ground in a state of prolonged immobility

– inability to fix rodents movements under the ground and, of course, obligatory animals recaptures to return the device and read information from them.

At the same, time the advantages that reveal this method to study the mobility of rodents in general and hosts of the plague in particular, are so obvious that more than justify efforts to overcome these difficulties. Furthermore, although in use of GPS-loggers, as in ordinary tagging recapture is required; they are performed only within 2-3 days after the beginning of each new observations cycle within one field visit. This greatly facilitates the return of expensive devices and their reuse.

The transition from use of GPS-loggers to use GPS-trackers is very tempting, which can indepen-

dently transfer accumulated information to satellite. However, it is clear that the main obstacle for this will be an even greater energy expenditure, which generates all the same necessity to recaptures of animals for resumption the charge of batteries.

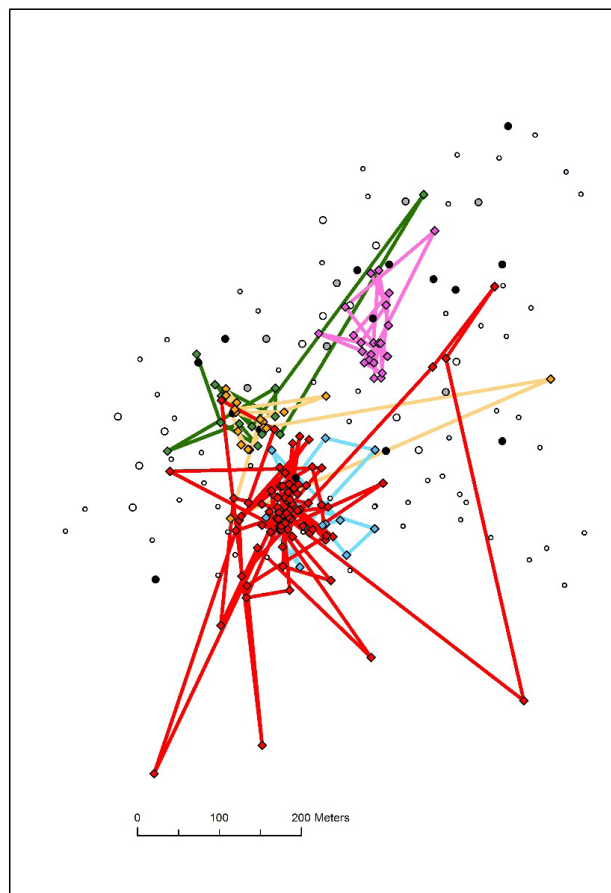


**Figure 3** – Movements of five great gerbils in one-cycle observations (usually 2-3 days due to limited battery life) in real space

## Conclusion

Based on our research it can be concluded that:

1. Despite on encountered difficulties of using telemetric techniques to a relatively fast obtain straight and, most importantly, absolutely accurate data on individual movements of marked individuals make a telemetry very promising direction in mobility study of potential hosts of the plague in the natural foci of this infection;
2. Our experience shows that telemetry methods are applicable is likely not only to rodents but also to any other small mammals, for which capture methods live animals are practiced;
3. Using a radio telemetry to study migrations, its character and range at small desert mammals such as gerbils, showed their high informative value and based on which this method can be recommend for more widespread use.



**Figure 4** – The same movements of five great gerbils in scheme, allowing to assess their real distance

## References

1. Burdelov A.S., Petrov V.S., Hruscelevskiy V.P. Mesto bolshoi peschanki v biocenozah pustin SSSR. Materiali VII nauchnoi konferencii protivochumnih uchrezhdeniy Srednei Azii i Kazakhstana. – Almaty, 1971. – P. 283-285.
2. Dubrovskiy U.A., Bokshtein F.M. Sravnitel'naya rol' nor peschanok i drugih grizunov v formirovanii podzemnoi chasti biocenozov pustin // Ekologiya i medicinskoe znachenie peschanok fauni SSSR. – M., 1981. – P. 191-197.
3. Atshabar B.B., Burdelov L.A., Sadovskaya V.P. e.a. Atlas rasprostraneniya osobo opasnih infekcyi v Respublike Kazakhstan. – Almaty, 2012. – 232 p.
4. Umatov A.M. Vliyanie osvoiniya zemel na rasselenie bolshih peschanok v golodnoi stepi. Gryzuni. Materiali VI Vsesoiuznogo soveshaniya. – M., 1983. – P. 568-569.



5. Saraev F.A. Bolshaiya peschanka v pravoberezhnoi poime reki Ural. Mater.nauch.konf. Ekologicheskie aspekti epizootologii i epidemiologii chumi i drugih osobo opasnih infekcii. – Almaty, 1996. – P. 144-145.
6. Saraev F.A. Odin iz vozmojnih sposobov preodoleniya bolshimi peschankami reki Ural. Mater.nauch.konf. Ekologicheskie aspekti epizootologii i epidemiologii chumi i drugih osobo opasnih infekcii. – Almaty, 1996. – P. 145-146.
7. Naumov N.P., Lobachev V.S. Struktura poseleniya i podvizhnost bolshih peschanok. Mater. IV nauch.konf. po prirod.ochagvos.i profil.chumi., 1965. – P. 178-181.
8. Lobachev V.S. Opit izhucheniya prirodnogo ochaga chumi v Priaralskih Karakumah: Avtoref. diss. ... cand. biol. nauk. 1975. – 22 p.
9. Okulova N.M., Bidashko F.G., Grazhdanov A.K. O skorosti izmeneniya granic i krujeva areala u grizunov. Sovremennie problem zoo- and filogeografii mlekopitaiushih. Mat.konf., 2009. – 63 p.
10. Lobachev V.S. Osobennosti ispolzovaniya nor-kolonii bolshimi peschankami. Bull. Mosk. o-va ispit. prir., otd. biol., 1967. – Vol. 72. – No. 1. – P. 21-28.
11. Burdelov L.A., Burdelov A.S., Bondar' E.P. et al. Ispolzovanie nor Bolshoi peschankoi – *Rhombomys opimus* (Rodentia, Cricetidae) i epizootologicheskoe izuchenie neobitaemih kolonii v Sredneaziatskom ochage chumi // Zool. j. – 1984. – V. LXIII. – Vol. 12. – P. 1848-1858.
12. Rudenchik U.V., Soldatkin I.S. Sezonnii izmeneniya podvijnosti bolshih peschanok i rasprostraneniya epizootyi chumi v Severnih Kyzylkumah // Problemi osobo opasnih infekcyi, 1969. – Vol. 1. – P. 34-39.
13. Davis S., Klassovskiy N., Ageyev V. et al. Plague metapopulation dynamics in a natural reservoir: the burrow system as the unit of study // Epidemiol. Infect., 2006. – Vol. 7. – P. 1-9.

UDC 547.913

Baiseitova A.M.<sup>1</sup>, Aisa H.<sup>2,3</sup>, Jenis J.<sup>1\*</sup><sup>1</sup>Faculty of Chemistry and Chemical Technology, Al-Farabi Kazakh National University, Almaty, Kazakhstan<sup>2</sup>Xinjiang Technical Institutes of Physics and Chemistry, Central Asian of Drug Discovery and Development,<sup>3</sup>Xinjiang Key Laboratory of Plant Resources and Natural Product Chemistry, XTIPC CAS, R. P. China.

\*e-mail: aizhabaiseitova@gmail.com

**Chemical constituents of *Dracocephalum nutans***

**Abstract.** In this study we investigate the chemical constituent in aerial parts of *Dracocephalum nutans*. The moisture content (6.13%), total ash (2.18%), extractives (35.25%) and quantitative and qualitative analysis of biologically active constituents of aerial parts of *Dracocephalum nutans* were determined. In The Institute of Combustion Problems using the method of multi-element atomic emission spectral analysis in the ash of *Dracocephalum nutans* were found 11 macro-micro elements, main of them was K(794.5750 µg/ml), Ca (440.63 µg/ml), Fe (4.5005 µg/ml), Zn (1.6911 µg/ml). The volatile oil constituents were extracted from the aerial parts of *Dracocephalum nutans* by water steam distillation were analyzed by GC-MS method. More than forty compounds were separated. Their relative contents were determined by area normalization in which 45 volatiles were identified. The major volatile oils of 1H-Cycloprop[e]azulen-7-ol, decahydro-1,1,7-trimethyl-4-methylene (14.23%), Caryophyllene oxide (11.30%), 1,6-Octadien-3-ol, 3,7-dimethyl (7.69%), (-)-myrtenyl acetate (5.67%), Naphthalene, 1,2,3,4,4A,5,6,8A-octahydro-7-methyl-4-methylene (5.29%), (-)-spathulenol (4.76%), Benzene, 1-methoxy-4-(1-propenyl) (4.73%), 4-ah-cycloprop[e]azulen-4A-ol, decahydro-1,1,4,7-tetra[ethenyl] (4.65%), Germacrene D (4.42%), (E)-3(10)-caren-4-ol (4.23%), Bicyclo[7.2.0]undec-4-ene, 4,11,11-trimethyl-8-methulene (3.67%),  $\alpha$ -Caryophyllene (3.60%), 12-oxabicyclo[9.1.0]dodeca-3,7-diene, 1,5,5,8-tetramethyl (2.13%).

**Key words:** *Dracocephalum nutans*; chemical constituent, Altay region; quantitative and qualitative analysis, Volatile oils; GC-MS

**Introduction**

*Dracocephalum L.* (dragonhead) is a genus of about 60 to 70 species of flowering plants in the family Lamiaceae, native to temperate regions of the Northern Hemisphere distributed in alpine and steppe regions of Asia [1–2]. The main distribution centre is assumedly the alpine steppes of the Pamir Altai and Tian-Shan [2]. The genus *Dracocephalum L.* is represented by 45 species in Eurasia, 22 species grow in mountains of Kazakhstan. Among them *D. goloskokovii*, *D. pavlovii*, *D. karataviense* are endemic rare in the Kazakhstan [3]. *Dracocephalum L.* extracts and oil are used in the pharmaceutical, cosmetic, food and flavouring industries. *Dracocephalum L.* essential oil extracts has antibacterial, antimicrobial, and antioxidant activities [4].

Essential elements are not only present in the body, playing important roles in the processes of the organism, but can be derived from the outside world, can then be used to insufficient life processes in organs and cells. Due to the rich presence of certain elements in the various medicinal plants, such plants are widely

used in traditional medicine as herbs and drugs [5].

Essential oils are volatile compounds derived from primarily from non-wood plant parts such as leaves, flowers and fruit. Essential oils have a pleasant aroma, because of what is used in cosmetics, detergent and food products [6]. Plants use essential oils for protection against insects, because of which the extracted essential oils have been used in agriculture as pesticides [7]. The important characteristic of the essential oils is their healing ability, so their pharmacology and medicine used for the treatment and prevention of various, both internal and external diseases and deficiencies.

In this study has been made the investigation the chemical constituents from Kazakh traditional medicinal plant of *Dracocephalum nutans* [8] grown in Altay region of Kazakhstan for the first time.

**Materials and methods**

Plant material: *Dracocephalum nutans* was collected in Altay region of east Kazakhstan, in 2014 and identified by Prof. Shen Guan Min from the Xin-

jiang Institute of Ecology and Geography, Chinese Academy of Sciences.

The moisture content, total ash, extractives and quantitative and qualitative contents of biologically

active constituents of aerial parts of *Dracocephalum nutans* were determined according to methods reported in the State Pharmacopeia XI edition techniques.

**Table 1** – Qualitative and quantitative screening of the powdered aerial parts of *Dracocephalum nutans*

Contents, %						
Moisture contents	Total ash	Extractives (80% C <sub>2</sub> H <sub>5</sub> OH)	Organic acids	Flavonoids	Saponins	Polysaccharides
6.13	2.18	35.25	0.39	0.11	2.29	1.17

In The Institute of Combustion Problems using the method of multielement atomic emission spectral

analysis in the ash of *Dracocephalum nutans* were analyzed elemental constituents.

**Table 2** – Compozition of macro–micro elements

Element	Cu	Zn	Cd	Pb	Fe	Ni	Mn	K	Na	Mg	Ca
µg/ml	0.6098	1.6911	0.0374	0.4522	4.5005	0.0149	1.3556	794.5750	4.5919	107.73	440.63

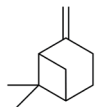
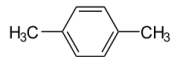
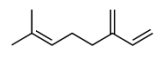
The oils were isolated by water–distillation for 4 hrs and then dried over anhydrous sodium sulphate.

GC–MS analysis: the aerial part of *Dracocephalum nutans* were analyzed by Electron Impact Ionization (EI) method on Perkin–Elemer Autosystem XL – TurboMass (Gas Chromatograph coupled to Mass Spectrometer) fused silica capillary column (30m x 2.5mm; 0.25 µm film thickness), coated with PE–5 ms were utilized. The carrier gas was helium (99.999%). The column temperature was programmed from 60°C (held for 5 min) at 2°C/min to 180°C at 3.5°C/min to 290°C.

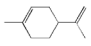
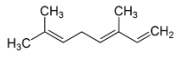
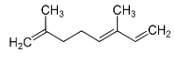
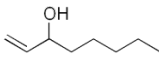

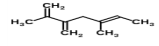
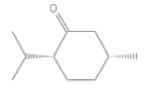

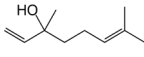
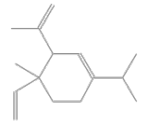
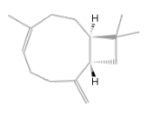
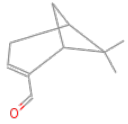
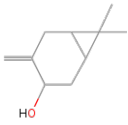
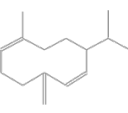
The latter temperature maintained for 40 min (acquisition parameters full scan; scan range 40–350 amu). The injector temperature was 310°C. Injection with a 0.1 µl detector ion source (EI–70eV). Samples were injected by splitting with the split ratio 1:60.

Identification of the compounds: Identification of compounds was done by comparing the NIST and Wiley library data of the peaks and mass spectra of the peaks with those reported in literature. Percentage composition was computed from GC peak areas on PE–5 ms column without applying correction factors.

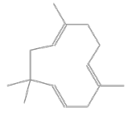
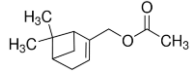
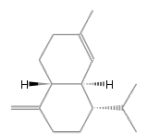
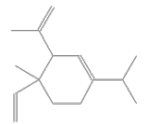
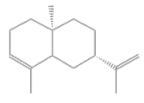
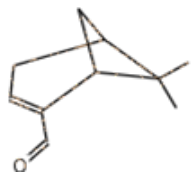
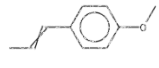
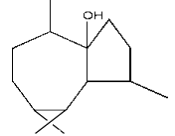
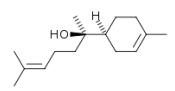
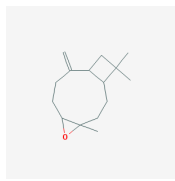
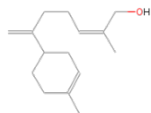
**Table 3** – The volatile constituents of aerial parts of *Dracocephalum nutans*

Peak No.	Constituents	t <sub>R</sub> (min)	Molecular Formula	Structure	MW	Content (%)
1	β–Pinene	21.14	C <sub>10</sub> H <sub>16</sub>		136	0.28
2	p–Xylene	23.51	C <sub>8</sub> H <sub>10</sub>		106	0.16
3	β– Myrcene	24.72	C <sub>10</sub> H <sub>16</sub>		136	0.35

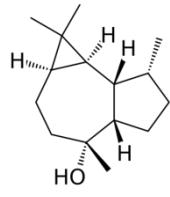
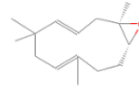
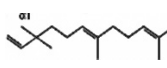
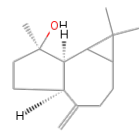
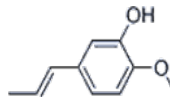
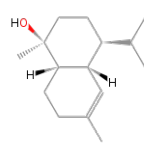
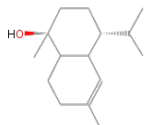
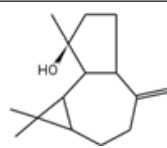
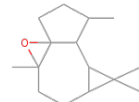
Continuation of table 3

Peak No.	Constituents	$t_R$ (min)	Molecular Formula	Structure	MW	Content (%)
4	Limonene	27.62	C <sub>10</sub> H <sub>16</sub>		136	0.30
5	1,3,6-Octatriene E,3,7-dimethyl -(E)-	30.25	C <sub>10</sub> H <sub>16</sub>		136	0.13
6	1,3,7-Octatriene,3,7-dimethyl-	31.75	C <sub>10</sub> H <sub>16</sub>		136	0.22
7	1-Octen-3-ol	48.95	C <sub>8</sub> H <sub>16</sub> O		128	0.48
8	Bicyclo[4.1.0]heptane,7-(1-methylethylidene)-	52.67	C <sub>10</sub> H <sub>16</sub>		136	0.35
9	1,5-Heptadiene, 2,5-dimethyl -3-methylene-	52.67	C <sub>10</sub> H <sub>16</sub>		136	0.35
10	Cyclonhexanone,5-methyl-2-(1-methylenhyl)-,cis	53.80	C <sub>10</sub> H <sub>18</sub> O		154	0.67
11	Cyclobutane[1,2,3,4] dicyclopentene, decahydro-32	56.52	C <sub>15</sub> H <sub>24</sub>		204	1.18
12	1,6-Octadien-3-ol,3,7-dimethyl-	58.12	C <sub>10</sub> H <sub>18</sub> O		154	7.69
13	Cyclohexane, 1-ethenyl-1-methyl-2,4-bis(1-methylethenyl)-,	63.21	C <sub>15</sub> H <sub>24</sub>		204	1.63
14	Bicyclo[7.2.0]undec-4-ene,4,11,11-trimethyl-8-methulene-	64.16	C <sub>15</sub> H <sub>24</sub>		204	3.67
15	Bicyclo[3.1.1]hept-2-ene-2carboxaldehyde, 6,6-dimethyl	66.08	C <sub>10</sub> H <sub>14</sub> O		150	0.87
16	(E)-3(10)-caren-4-ol	67.85	C <sub>10</sub> H <sub>16</sub> O		152	4.23
17	GermacreneD	67.42	C <sub>15</sub> H <sub>24</sub>		204	4.42

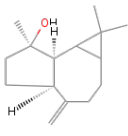
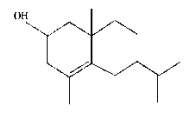
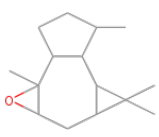
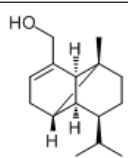
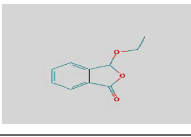
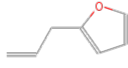
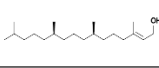
Continuation of Table 3

Peak No.	Constituents	$t_R$ (min)	Molecular Formula	Structure	MW	Content (%)
18	$\alpha$ -Caryophyllene	69.99	C <sub>15</sub> H <sub>24</sub>		204	3.60
19	(-)-myrtenylacetate	71.00	C <sub>12</sub> H <sub>18</sub> O <sub>2</sub>		194	5.67
20	Naphthalene,1,2,3,4,4A,5,6,8A-octahydro-7-methyl-4-methylene	73.31	C <sub>15</sub> H <sub>24</sub>		204	5.29
21	Cyclohexene, 4-ethenyl-4-methyl-3-(1-methylethenyl)-1-(1-methylethyl)-	74.77	C <sub>15</sub> H <sub>24</sub>		204	0.56
22	Naphthalene,1,2,3,4,4A,5,6,8A-octahydro-7-methyl-4-methylene-1-methylethenyl)-(1- $\alpha$ ,A, $\beta$ )	76.41	C <sub>15</sub> H <sub>24</sub>		204	0.40
23	Bicyclo[3.1.1]hept-2-ene-2-methanol, 6,6-dimethyl-	78.87	C <sub>10</sub> H <sub>16</sub> O		152	1.48
24	Benzene,1-methoxy-4-(1-propenyl)-	82.06	C <sub>10</sub> H <sub>12</sub> O		148	4.73
25	4H-cycloprop [e]azulen-4A-ol,decahydro-1,1,4,7-tetra-[ethenyl]-	90.30	C <sub>15</sub> H <sub>26</sub> O		222	4.65
26	$\alpha$ -Bisabolol	94.02	C <sub>15</sub> H <sub>26</sub> O		222	1.31
27	Caryophyllene oxide	95.03	C <sub>15</sub> H <sub>24</sub> O		220	11.30
28	Lanceol, cis	96.66	C <sub>27</sub> H <sub>42</sub> O <sub>3</sub>		414	0.41

Continuation of Table 3

Peak No.	Constituents	$t_R$ (min)	Molecular Formula	Structure	MW	Content (%)
29	Ledol	97.50	C <sub>15</sub> H <sub>26</sub> O		222	0.57
30	12-oxabicyclo [9.1.0]dodeca-3,7-diene,1,5,5,8-tetramethyl	98.75	C <sub>15</sub> H <sub>24</sub> O		220	2.13
31	1,6,10-dodecatrien -3-ol,3,7,11-trimethyl -	100.66	C <sub>15</sub> H <sub>26</sub> O		222	0.19
32	(-)-spathulenol	103.97	C <sub>15</sub> H <sub>24</sub> O		220	4.76
33	Phenol,2-methoxy-4-(1-propenyl)-	106.45	C <sub>10</sub> H <sub>12</sub> O <sub>2</sub>		164	0.71
34	Tau-Muurolol	107.88	C <sub>15</sub> H <sub>26</sub> O		222	0.36
35	α-Cadinol	111.05	C <sub>15</sub> H <sub>26</sub> O		222	0.81
36	1H-CYCLOPROP[E]AZULEN-7-OL, DECAHYDRO-1,1,7-TRIMETHYL-4-METHYLENE-	112.81	C <sub>15</sub> H <sub>24</sub> O		220	14.23
37	Ledene oxide - (II)	119.18	C <sub>15</sub> H <sub>24</sub> O		220	0.32

Continuation of Table 3

Peak No.	Constituents	$t_R$ (min)	Molecular Formula	Structure	MW	Content (%)
38	Spathulenol	119.86	C <sub>15</sub> H <sub>24</sub> O		220	0.43
39	6-isopropenyl -4,8A-dimethyl -1,2,3,5,6,7,8,8A-octahydro -naphthalen -2-ol	120.42	C <sub>15</sub> H <sub>24</sub> O		220	1.03
40	ISOAROMADENDRENE EPOXIDE	123.97	C <sub>15</sub> H <sub>24</sub> O		220	0.23
41	Tricyclo[4.4.0.02,7]dec-3-ene-3-methanol,1-methyl-8-(1-methylethyl)-	130.02	C <sub>15</sub> H <sub>24</sub> O		220	0.34
42	1(3H)-Isobenzofuranone,3-ethoxy	130.93	C <sub>10</sub> H <sub>10</sub> O <sub>3</sub>		178	1.72
43	Furan,2-(2-propenyl)-	132.08	C <sub>7</sub> H <sub>8</sub> O		108	0.37
44	Phytol	134.26	C <sub>20</sub> H <sub>40</sub> O		296	1.20

## Results and their discussion

The moisture content (6.13%), total ash (2.18%), extractives (35.25%) and quantitative and qualitative contents of biologically active constituents of aerial parts of *D. nutans* were determined. Total ash content is important in determining the mineral composition of the plant, due to the fact that they are basically the inorganic part of the plant. Moisture contents is also an important factor characterizing stability and also due to the fact that thanks to the water in the plant can be various microorganisms.

In The Institute of Combustion Problems using the method of multielement atomic emission spectral analysis in the ash of *D. nutans* were found 11 macro-micro elements, main of them was K (794.5750 µg/ml), Ca (440.63 µg/ml), Fe (4.5005 µg/ml), Zn (1.6911 µg/ml). Trace elements have a significant

role in the fight against various human diseases and diseases observed in the study of the elements in relation to the indigenous medicinal plants. At the same time, major and trace elements play an important role in the construction and restoration of health and disease conditions of the human body. Progress has occurred in the field of medical sciences during the last few years [9].

Volatile oils from the aerial parts of *D. nutans* were analyzed by GC-MS.

Forty four compounds were separated. Their relative contents were determined by area normalization. The yield from whole herbs of *D. nutans* was found to be 3.21%. Table 1 report the composition of the volatiles of the aerial parts of *D. nutans*. The components have been identified in the volatiles of *Dracocephalum nutans* which the major constituents are 1H - Cycloprop[e]azulen - 7 - ol, decahydro - 1, 1,

7 – trimethyl – 4 – methylene –, (14.23%), Caryophyllene oxide (11.30%), 1, 6 – Octadien – 3 – ol, 3, 7 – dimethyl – (7.69%), (–) – myrtenyl acetate (5.67%), Naphthalene, 1, 2, 3, 4, 4A, 5, 6, 8A – octahydro – 7 – methyl – 4 – methylene (5.29%), (–) – spathulenol (4.76%), Benzene, 1 – methoxy – 4 – (1 – propenyl) – (4.73%), 4 ah – cycloprop[e]azulen – 4A – ol, decahydro – 1, 1, 4, 7 – tetra – [ethenyl] – (4.65%), Germacrene D (4.42%), (E) – 3(10) – caren – 4 – ol (4.23%), Bicyclo [7.2.0] undec – 4 – ene, 4, 11, 11 – trimethyl – 8 – methylene – (3.67%),  $\alpha$  – Caryophyllene (3.60%), 12 – oxabicyclo [9.1.0] dodeca – 3, 7 – diene, 1, 5, 5, 8 – tetramethyl (2.13%).

According to the report 1H – Cycloprop[e]azulen – 7 – ol, decahydro – 1, 1, 7 – trimethyl – 4 – methylene (14.23%) is antifungal, insecticidal and larvicidal, agent [10]. And second major volatile constituent caryophyllene oxide (11.30%) showed analgesic and antiinflammatory activates [11]. 1,6 – Octadien – 3 – ol, 3, 7 – dimethyl – (7.69%) also called as linalool is used as a scent in 60–80% of perfumed hygiene products and cleaning agents including soaps, detergents, shampoos, and lotions [12–13].

Findings suggest that linalool reverses the histopathological hallmarks of AD and restores cognitive and emotional functions via an anti-inflammatory effect. Thus, linalool may be an AD prevention candidate for preclinical studies [14].

## Conclusion

The moisture content (6.13%), total ash (2.18%), extractives (35.25%) and quantitative and qualitative analysis of biologically active constituents of aerial parts of *D. nutans* were determined. In The Institute of Combustion Problems using the method of multi-element atomic emission spectral analysis in the ash of *D. nutans* were found 11 macro–micro elements, main of them was K(794.5750  $\mu\text{g/ml}$ ), Ca (440.63  $\mu\text{g/ml}$ ), Fe (4.5005  $\mu\text{g/ml}$ ), Zn (1.6911  $\mu\text{g/ml}$ ).

The volatile oils constitutes were extracted from the aerial parts of *Dracocephalum nutans* by water steam distillation which analyzed by GC–MS method. More than forty compounds were separated. Their relative contents were determined by area normalization in which 45 volatiles were identified. Active principles of the Kazakh traditional medicinal plant (*Dracocephalum nutans*) that responsible for the activity were determined. While the major volatile constituents are 1H – cycloprop[e]azulen – 7 – ol, decahydro – 1, 1, 7 – trimethyl – 4 – methylene (14.23%), caryophyllene oxide (11.30%), 1, 6 – octadien – 3 – ol, 3, 7 – dimethyl – (7.69%) which possessing an-

tifungal, insecticidal, larvicidal anti-inflammatory, and analgesic activities separately.

## Acknowledgement

This research was supported by the Chinese Academy of Sciences Visiting Fellowship for Researchers from Developing Countries (Grant No. 2013FFGB0003).

## References

1. Li N.Y., Jian G.X., Cheng H.H., Tong W. The phenolic compounds from *Dracocephalum moldavica* L.// *Biochemical Systematics and Ecology*. – 2014. – 54. – P. 19-22.
2. P. Lazarevic, M. Lazarevic, Z. Krivosej, V. Stevanovic. On the distribution of *Dracocephalum ruyschiana* (Lamiaceae) in the Balkan Peninsula// *Phytologia Balcanica*. – 2009. – 15 (2). – P. 175-179, Sofia.
3. «Kazakhstan» National Encyclopedia // *Kazakh Encyclopedia reduction*, 1998.
4. S. Yousefzadeh, S. A. M. Modarres–Sanavy, F. Sefidkon, A. Asgarzadeh, A. Ghalavand, K. Sadat–Asilan. Effects of Azocompost and urea on the herbage yield and contents and compositions of essential oils from two genotypes of dragonhead (*Dracocephalum moldavica* L.) in two regions of Iran// *Food Chemistry*. – 2013. – 138 (2013). – P. 1407-1413
5. Jay Prakash Rajan, Kshetrimayum Birla Singh, Sanjiv Kumar, Raj Kumar Mishra. Trace elements content in the selected medicinal plants traditionally used for curing skin diseases by the natives of Mizoram, India// *Asian Pac J Trop Med*. – 2014. –7(Suppl 1): – P. 410-414
6. Yong–Lak Park, Jun–Hyung Tak. Chapter 6 – Essential oils for arthropod pest management in agricultural production systems// *Essential Oils in Food Preservation, Flavor and Safety*. – 2016. – P. 61-70.
7. Sanjib Bhattacharya. Chapter 3 – Cultivation of essential oils // *Essential oils in food preservation, flavor and safety*. – 2016. – P. 19-29.
8. Xu X., Konirbay B., Jenis J., etal. *The Kazakh Materia Medica*, The Ethnic Press: Beijing, 2009. – P. 357.
9. Shahin Aziz, Koushik Saha, Nasim Sultana, Husna Parvin Nur, Md. Aminul Ahsan, Shamim Ahmed, Md. Kamal Hossain. Comparative studies of elemental composition in leaves and flowers of *Catharanthus roseus* growing in Bangladesh // *Asian Pac J Trop Biomed*. – 2015. – 10(1016). – P.1-5.
10. A. Akpuaka, M.M. Ekwenchi, D.A. Dashak, A. Dildar. Biological activities of characterized iso-



lates of n-hexane extract of *Azadirachta indica* A. Juss (Neem) leaves // *Nature and Science*, 2013. –11(5). – P. 141-147.

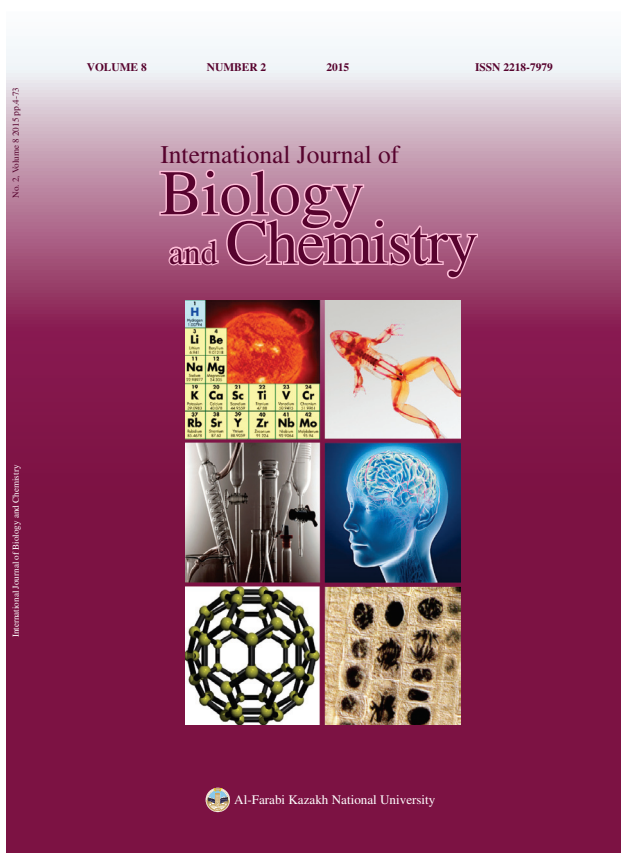
11. M.J. Chavan, P.S. Wakte, D.B. Shinde. Analgesic and anti-inflammatory activity of Caryophyllene oxide from *Annonasquamosa* L. bark // *Phyto-medicine*. – 2010. – 17(2). – P. 149-151.

12. Brared Christensson J., Forsström P., Wen- nberg A.M., Karlberg A.T., Matura M. Air oxidation increases skin irritation from fragrance terpenes//

*Contact Dermatitis*. – 2009. – 60. – P. 32-40.

13. BraredChristensson J., Matura M., Backtorp C, Borje A., Nilsson J.L.G, Karlberg A.T. Hydroperoxides form specific antigens in contact allergy // *Contact Dermatitis*. – 2006. – 55(4). – P. 230-7.

14. Angélica Maria Sabogal-Guáqueta, Edison Osorio, Gloria Patricia Cardona-Gómez. Linalool reverses neuropathological and behavioral impairments in old triple transgenic Alzheimer's mice // *Neuropharmacology*. – 2016. – 102. – P. 111-120.



## International Journal of Biology and Chemistry

The Journal publishes experimental and theoretical findings in the field of Biology, Chemistry, Chemical and Biotechnology. Among the subjects are modern issues of organic synthesis technology; scientific basis for production of biologically active preparations; modern issues of raw materials processing technologies; production of new materials and technologies; study of chemical and physical properties and structures of oil and coal; bioremediation; theoretical and practical issues of hydrocarbons processing; modern achievements in the field of biomedicine, molecular biology, genetics, nanotechnology and etc.

The journal has an international focus; it publishes articles of foreign authors from the USA, Israel, Germany, the UK, Austria, France, Egypt, Pakistan, Ireland, Russian Federation and other countries and is published in English.

Creation of the special International Journal of Biology and Chemistry is of great importance for our University, since a vast number of scientists are willing to publish their papers, what as a consequence will help to widen the geography of future collaborations. We will be glad to publish papers of scientists from all the continents.

«International Journal of Biology and Chemistry» is registered at the Ministry of Culture and Information of the Republic of Kazakhstan. The journal registration certificate No. 10140-Zh is of 21.05.2009.

The journal website <http://ijbch.kaznu.kz> provides free access to full-text articles published since 2010.